CRCLEME

Cooperative Research Centre for
Landscape Evolution & Mineral Exploration

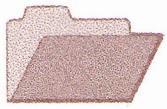

OPEN FILE
REPORT
SERIES

CSIRO
EXPLORATION
AND MINING

AMIRA

Australian Mineral Industries Research Association Limited ACN 004 448 266

REGOLITH-LANDFORM DEVELOPMENT AND SITING AND BONDING OF ELEMENTS IN REGOLITH UNITS, MT GIBSON DISTRICT, WESTERN AUSTRALIA

R.R Anand, H.M. Churchward and R.E. Smith

CRC LEME OPEN FILE REPORT 61

November 1998

(CSIRO Division of Exploration Geoscience Report 165R, 1991.
Second impression 1998)

AMIRA
Australian Mineral Industries Research Association Limited ACN 004 448 266

CRCLEME
Cooperative Research Centre for Landscape Evolution & Mineral Exploration

CSIRO
EXPLORATION AND MINING

REGOLITH-LANDFORM DEVELOPMENT AND SITING AND BONDING OF ELEMENTS IN REGOLITH UNITS, MT GIBSON DISTRICT, WESTERN AUSTRALIA

R.R Anand, H.M. Churchward and R.E. Smith

CRC LEME OPEN FILE REPORT 61

November 1998

(CSIRO Division of Exploration Geoscience Report 165R, 1991.
Second impression 1998)

CRC LEME is an unincorporated joint venture between The Australian National University, University of Canberra, Australian Geological Survey Organisation and CSIRO Exploration and Mining
Headquarters: CRC LEME c/o CSIRO Exploration and Mining, Private Bag, PO Wembley, Western Australia, 6014

RESEARCH ARISING FROM CSIRO/AMIRA REGOLITH GEOCHEMISTRY PROJECTS 1987-1993

In 1987, CSIRO commenced a series of multi-client research projects in regolith geology and geochemistry which were sponsored by companies in the Australian mining industry, through the Australian Mineral Industries Research Association Limited (AMIRA). The initial research program, "Exploration for concealed gold deposits, Yilgarn Block, Western Australia" (1987-1993) had the aim of developing improved geological, geochemical and geophysical methods for mineral exploration that would facilitate the location of blind, buried or deeply weathered gold deposits. The program included the following projects:

P240: Laterite geochemistry for detecting concealed mineral deposits (1987-1991). Leader: Dr R.E. Smith.
Its scope was development of methods for sampling and interpretation of multi-element laterite geochemistry data and application of multi-element techniques to gold and polymetallic mineral exploration in weathered terrain. The project emphasised viewing laterite geochemical dispersion patterns in their regolith-landform context at local and district scales. It was supported by 30 companies.

P241: Gold and associated elements in the regolith - dispersion processes and implications for exploration (1987-1991). Leader: Dr C.R.M. Butt.
The project investigated the distribution of ore and indicator elements in the regolith. It included studies of the mineralogical and geochemical characteristics of weathered ore deposits and wall rocks, and the chemical controls on element dispersion and concentration during regolith evolution. This was to increase the effectiveness of geochemical exploration in weathered terrain through improved understanding of weathering processes. It was supported by 26 companies.

These projects represented "an opportunity for the mineral industry to participate in a multi-disciplinary program of geoscience research aimed at developing new geological, geochemical and geophysical methods for exploration in deeply weathered Archaean terrains". This initiative recognised the unique opportunities, created by exploration and open-cut mining, to conduct detailed studies of the weathered zone, with particular emphasis on the near-surface expression of gold mineralisation. The skills of existing and specially recruited research staff from the Floreat Park and North Ryde laboratories (of the then Divisions of Minerals and Geochemistry, and Mineral Physics and Mineralogy, subsequently Exploration Geoscience and later Exploration and Mining) were integrated to form a task force with expertise in geology, mineralogy, geochemistry and geophysics. Several staff participated in more than one project. Following completion of the original projects, two continuation projects were developed.

P240A: Geochemical exploration in complex lateritic environments of the Yilgarn Craton, Western Australia (1991-1993). Leaders: Drs R.E. Smith and R.R. Anand.
The approach of viewing geochemical dispersion within a well-controlled and well-understood regolith-landform and bedrock framework at detailed and district scales continued. In this extension, focus was particularly on areas of transported cover and on more complex lateritic environments typified by the Kalgoorlie regional study. This was supported by 17 companies.

P241A: Gold and associated elements in the regolith - dispersion processes and implications for exploration. Leader: Dr. C.R.M. Butt.
The significance of gold mobilisation under present-day conditions, particularly the important relationship with pedogenic carbonate, was investigated further. In addition, attention was focussed on the recognition of primary lithologies from their weathered equivalents. This project was supported by 14 companies.

Although the confidentiality periods of the research reports have expired, the last in December 1994, they have not been made public until now. Publishing the reports through the CRC LEME Report Series is seen as an appropriate means of doing this. By making available the results of the research and the authors' interpretations, it is hoped that the reports will provide source data for future research and be useful for teaching. CRC LEME acknowledges the Australian Mineral Industries Research Association and CSIRO Division of Exploration and Mining for authorisation to publish these reports. It is intended that publication of the reports will be a substantial additional factor in transferring technology to aid the Australian Mineral Industry.

This report (CRC LEME Open File Report 61) is a Second impression (second printing) of CSIRO, Division of Exploration Geoscience Restricted Report 165R, first issued in 1991, which formed part of the CSIRO/AMIRA Project P240.

Copies of this publication can be obtained from:
The Publication Officer, c/- CRC LEME, CSIRO Exploration and Mining, PMB, Wembley, WA 6014, Australia. Information on other publications in this series may be obtained from the above or from http://leme.anu.edu.au/

Cataloguing-in-Publication:
Anand, R.R.
Regolith-landform development and siting and bonding of elements in regolith units, Mt Gibson District, Western Australia
ISBN 0 642 28298 6
1. Laterite 2. Geochemistry - Western Australia.
I. Churchward, H.M. II. Smith, Raymond Ernest III. Title
CRC LEME Open File Report 61.
ISSN 1329-4768

EXECUTIVE SUMMARY

Regolith-landform Relationships
The complex regolith of the Mt. Gibson district is explained in terms of the distribution of: (a) regimes where the essentially-complete laterite profile is preserved, commonly forming broad crests and upper gentle slopes, (b) regimes of erosion of the laterite profile to the level of saprolite/saprock/bedrock resulting in terrain characterized by low to medium hills, and (c) regimes characterized by depositional accumulations of detritus provided by the erosion of the laterite profile, commonly burying the complete and partly-truncated lateritic weathering profile in the lower slopes and valley floors. In the latter, sediments reach 30 m in thickness and residual laterite up to 6 m thick was observed to occur under the sediments.

The regolith units were mapped over a 17-km x 10-km area, the regolith stratigraphy established, and the regolith units were characterized. A regolith-landform model for the Mt. Gibson district describes relationships in terms of erosion and burial of complete and partly-truncated profiles. Lateritization and post-lateritization processes responsible for the formation of a variety of regolith types are discussed.

Midway North Area
The pattern of regolith at Midway North which characterizes the district relates closely to the erosional and depositional modification of the deeply-weathered mantle. A total of 25 samples representing various regolith units were characterized petrologically, mineralogically, and geochemically. Systematic mineralogical and geochemical differences occur between transported and residual regolith units. For example, the colluvial units (soils and hardpanized colluvium) contain higher amounts of kaolinite and quartz relative to the underlying residual regolith units. Hematite increases upwards in the residual weathering profile. The Al content in goethite also tends to increase towards the top of the residual profile.

Lateritic residuum is enriched in Cu, Pb, Zn, As, W, Ag, and Au which are associated with hematite and goethite. The calcareous clays overlying acid, plastic clays largely consist of dolomite, kaolinite with small amounts of hematite, calcite, halite, and palygorskite. These clays have low contents of chalcophile elements, but contain significant amounts of Au. However, the amounts of Au are very low in clays relative to the lateritic residuum. The upper saprolite is depleted compared to the lower saprolite in Au and chalcophile elements. Acid, red plastic clays developed from the weathering of underlying saprolite are also low in Au.

Carbonates
Scanning electron microscopic studies of calcareous soils and nodular calcretes from the Mt. Gibson Au deposits reveal a fossilized community of soil micro-organisms dominated by filamentous structures preserved in fine detail by calcite. The calcite forming the filaments has a variety of crystal habits. Calcified filaments observed in samples of nodular calcrete suggest that biological activity could have played a significant role in the formation of the carbonates in the regolith.

Siting and Bonding of Elements and Dispersion Processes
The bulk samples of soils, lateritic residuum, hardpanized colluvium (red-brown hardpan), and calcareous soils were separated into various morphological groups, such as magnetic vs. non-magnetic nodules/clasts, matrix vs. clasts, calcareous fragments vs. ferruginous clasts, and cores vs. cutans. The petrological, mineralogical, and geochemical characteristics of these materials were established. Non-magnetic lateritic nodules/clasts are the dominant fraction of both soils and lateritic residuum. The magnetic and non-magnetic nodules/clasts have different internal fabrics. The cores of magnetic nodules/clasts are black and massive, whereas those of non-magnetic nodules/clasts are yellowish brown and porous. Hematite is a dominant mineral in both magnetic and non-magnetic lateritic nodules/clasts. The non-magnetic lateritic nodules/clasts contain higher amounts of goethite and kaolinite relative to the magnetic lateritic nodules/clasts, while maghemite is present in the magnetic nodules/clasts. The cutans of nodules and pisoliths are dominated by goethite. Goethite in the lateritic residuum is highly Al-substituted (17 mole %).

Iron, Cr, V, Pb, As, W, Sb, Bi, and Zn are enriched in magnetic lateritic nodules/clasts relative to the non-magnetic lateritic nodules/clasts. By contrast, Al, Si, Cu, Ag, Au, and Ni are relatively more abundant in non-magnetic lateritic nodules/clasts. Cores of both groups of nodules/clasts contain higher amounts of Au than cutans.

The matrix of hardpanized colluvium (red-brown hardpan) consists of kaolinite, quartz, and amorphous silica. The mean values of Au and Ag for the matrix of hardpan are higher than, or very similar to, those for lateritic nodules.

Carbonate fractions separated from nodular calcrete are anomalous in Au. The magnitude of the anomaly is, however, smaller than that of lateritic nodules and pisoliths.

The possible associations of Au, Pb, Zn, As, Cu, Ni, Cr, and V with various secondary mineral species are discussed. Chromium, V, Ga, Pb, As, and Sb are strongly associated with hematite. Goethite and kaolinite appear to have strong affinities for Cu, Ni, Ag, and Au. Hydromorphic dispersion appears to be the major dispersion process that extended the geochemical halo in the upper part of the regolith.

CONTENTS

1.0 PROJECT LEADER'S PREFACE

R.E. Smith
30 August 1991

Fundamental building blocks of the CSIRO/AMIRA Laterite Geochemistry Project are four substantial multidisciplinary geochemical orientation studies: Mt. Gibson, Bottle Creek, Lawlers, and Boddington. In each case geochemical dispersion arising from concealed Au deposits is studied by establishing an understanding of the regolith-landform and bedrock relationships, not only of the immediate ore environments, but also of the district within which the deposits lie. In this way a regolith-landform framework of reference is established for each orientation study area within which each sample or collection of samples and information arising from them are tightly controlled.

The Mt. Gibson district characterizes the complex lateritic sand plain terrain of the semi-arid Perenjori/Nigham region where an essentially-complete undulating lateritic peneplain, though extensively preserved, is undergoing dismantling by erosion. Burial of complete and partly-truncated laterite profiles by erosional detritus, has taken place on many of the slopes and in the low lying areas. These are important dynamic processes which are continuing.

The Mt. Gibson orientation study is being presented in several substantial reports as components of the research are completed. The regolith-landform relationships for the area local to the main lateritic gold areas, the S, C and N Pits, together with initial geochemical dispersion patterns, were presented in Report 20R (Anand, *et al.*, March 1989). The present report extends those findings, and places the more detailed study in the district-scale regolith-landform context. It also investigates the regolith setting of the Midway North area within which lies the Hornet Zone bedrock gold deposit.

Mining development at Midway North lies 1 km to the north of the area covered in Report 20R and the present report provides an important link in regolith stratigraphy and geochemistry between the two areas.

A theme within the Laterite Geochemistry Project on the siting and bonding of elements of interest leads to a knowledge of dispersion processes and improvements in exploration methods. Contributions to these topics from the Mt. Gibson research are presented in this report, as is an investigation of carbonates in the regolith. A separate report, currently being finished, will cover the geochemistry of systematically-collected samples of lateritic materials forming the Mt. Gibson orientation data sets.

2.0 INTRODUCTION

The overall objectives of the Mt. Gibson study are to establih a well-controlled regolith-landform framework and within which, to carry out a geochemical orientation study about the concealed Au deposits. A report has already been issued discussing the regolith relationships and geochemical dispersion patterns in laterite at the S, C, and N Pits (Anand *et al.*, March 1989). That report included the surface distribution of regolith units, regolith stratigraphy, characterization of units, and regolith-landform model for the mine environments. The present report covers the following components:

- District scale regolith-landform framework;
- Regolith, mineralogy, and geochemistry of regolith units present in the Midway North Pit;
- Investigation of the siting and bonding of Au and chalcophile elements in transported and residual regolith at the S, C, and N Pits;
- Dispersion processes; and
- Origin of carbonates in the regolith.

3.0 GENERAL SETTING

3.1 Location and Access

The Mt. Gibson Gold Project, a joint venture between Forsayth (Gibson) Ltd and Reynolds Australia Mines Pty Ltd, is located (117°45'E 29°45'S) some 300 km northeast of Perth and some 200 km from the west coast (Fig. 1). The mine site is 100 km NE along the Great Northern Highway from Dalwallinu and then 10 km east via a formed gravel road.

3.2 Climate

The area has a semi-arid to arid hot Mediterranean climate with a 250-mm average annual rainfall, most of which falls during the cooler months of May to August. However, there is a significant component of summer rainfall from erratic thunderstorms.

3.3 Vegetation

The area is mantled by thicket communities (Beard, 1976) of various acacia species (particularly *Acacia resinomarginea*). Eucalypt woodlands, largely of salmon gum *(Eucalyptus salmonaphloria)*, York gum *(Eucalyptus loxophleba)*, and mallee *(Eucalyptus oleosa)*, while some native pine *(Callitris columellaris)* occur on the finer textured soils along valleys and in local erosional tracts. *Acacia resinomarginea* is prominent amongst the sand-plain communities in both upland and lowland situations.

3.4 Geomorphology

In studying the pattern of the regolith in weathered terrain, it is important to consider the physiography, not merely because it is part of the physical setting, but because it is relevant to the patterns of stripping of the weathered regolith. The area chosen for the district scale reconnaissance study at Mt. Gibson is typical of large parts of the weathered surface of the Great Plateau, a major physiographic feature in the western quarter of the continent (Jutson, 1950). The landforms are in keeping with those described by Bettenay and Mulcahy (1972) for the upper parts of the major regional drainage systems, so that the general features comprise broad, saline valley floors flanked by extensive, gently-undulating, often sandy, tracts. Occasional belts of hills, usually associated with greenstone sequences, are emergent above the general plateau surface.

This area has an elevation of from 310 to 360 m above mean sea level (asl) and is located on a broad divide between the extensive playas of Lakes Moore and Monger, both of which occur at about 300 m asl. The broadly-convex local divides that form most of the skyline are at 340 to 360 m asl and these are flanked by long gentle slopes which grade at 1 in 50 (2%) on the upper slopes to 1 in 200 overall (0.5%), leading to the local Lake Karpa drainage sump at 310 m asl (Fig. 2). Emergent above the general plateau skyline are a few prominent crests and monadnocks, flanked by steep irregular slopes just beyond the NE limit of the area. The most prominent are Mt. Gibson (480 m) and Mount Singleton (620 m).

Whilst the valleys of this area could be seen as the prime focus of stripping of the deep mantle, there is no clear trend of progressively-increasing erosion with valley size. Thus, for instance, in granitic terrain pockets of more effective stripping appear to have no consistently-ordered pattern, so that some of the more extensive outcrops of granite are far from the direct influence of relief such as on the main drainage divides in the NW corner of the area. It is suggested that the depth of weathering of granites, which is known to vary considerably, could have a significant effect on the stripping.

Stripping of the weathered mantle from greenstone terrains can result in the development of shallow, broad, gently-sloping concavities in upland areas. They are flanked by low breakaways whose smooth crests are capped by smooth gentle backslopes that trend away from the erosional tract and are seen as remnants of the ancient weathered landsurface. A situation such as this occurs just west of the N pits.

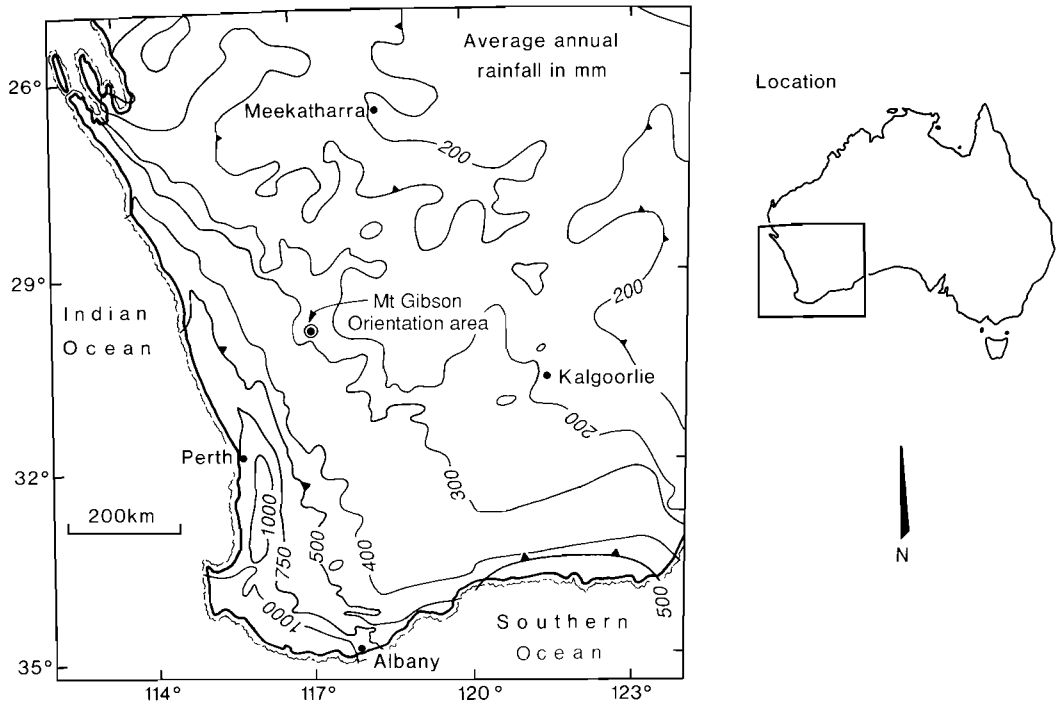

Fig 1. Location of the Mt. Gibson orientation study area placed within the rainfall gradient for the south-west part of the continent.

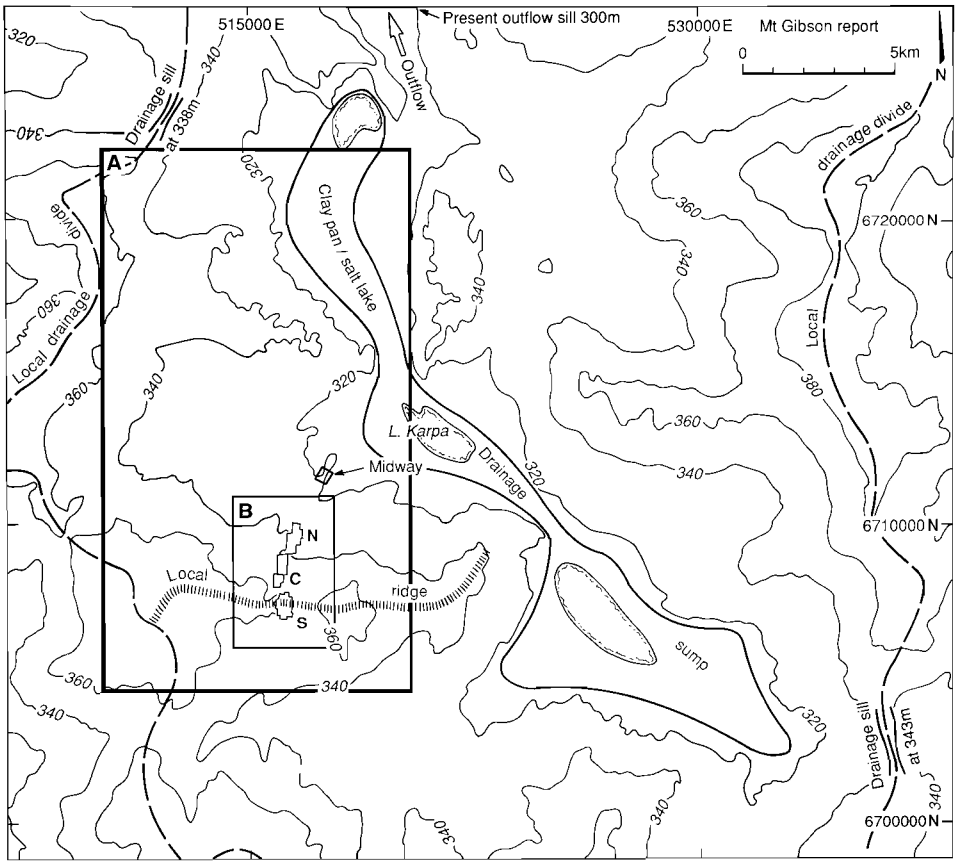

Fig. 2. Map showing the topographic setting of the Mt. Gibson gold mining area (the S, C, N, Pits and Midway) and the surrounding district. The rectangle A shows the area covered by this report. The rectangle B shows the area covered by an earlier report (Anand *et al.*, March 1989) within which siting and bonding of elements in regolith units was carried out.

In the northern part of the study area, an erosional zone includes a hill stripped of its weathered mantle, whose summit is elevated above the gently-graded backslopes of adjacent laterite-capped remnants. The latter are often not continuous, but are represented by a number of low cuesta-like rises with drainage from the erosional tracts feeding out onto adjacent broad valley floors.

In addition to these more effectively-stripped areas, crests in relatively-stable areas are gently stripped exposing the upper parts of the lateritic residuum. The detritus so generated is the source of the colluvium that mantles the adjacent slopes. These deposits are non-calcareous and are extensively hardpanized. They represent a gentle modification of the weathered land surface, and weathered materials dominate the colluvial mantle.

The S to N mine pits are arrayed along the upper flanks of a broad NS oriented crest (Fig. 2). This crest, just west of the pits, is occupied by broad shallow, erosional tracts that are flanked by low breakaways. The mine pits have been established in the EW trending backslope of these breakaways.

3.5 Geological Setting and Mineralization

The Mt. Gibson district forms part of the southern Murchison Province within the cratonic Archaean Yilgarn Block of Western Australia. Arcuate N to NW trending belts of thick synclinorial sequences of Archaean supracrustal rocks, comprising the Murchison Supergroup, are preserved within a gneissic terrain intruded by Archaean granitoids. Within the belts, the lithologic successions can be divided into associations of either mafic, volcanic, or sedimentary affiliation as recognized by Hallberg (1976) following Muhling and Low (1973). Four such lithologic associations were established by regional 1:250,000 scale mapping of the YALGOO, KIRKALOCKA, NINGHAN and PERENJORI sheets (Muhling and Low, 1977; Lipple *et al.*, 1983; Baxter *et al.*, 1983; and Baxter and Lipple, 1985). The sequence of these lithological associations is repeated from belt to belt with an apparent consistency of stratigraphic order.

Steeply-dipping hematite-quartz veins (1-10 cm thick) hosted by saprolitic tuffaceous metasediments were exposed in the S2, C1, C3, and N2 Pits after partial stripping of the lateritic cover and were found to contain values up to 31 g/t Au. Although the size and frequency of known occurrences of these veins in the mine area appear to be inadequate to account for the Au content of the regolith, a number of small prospects (Tobias' Find, Orion, Mt. Gibson Well, Leake's Find) on the western fringe of the auriferous laterite, attest to a broader distribution of shear-controlled vein systems in the unmapped sub-surface.

The S, C, N, and Midway North Pits are sited within the Retaliation-Yandhanoo Fold Belt (Lipple *et al.*, 1983) and this comprises a basal sequence of mafic volcanic rocks with substantial epiclastic sedimentary and felsic volcanic components in the middle and upper parts of the sequence, all metamorphosed to low greenschist and low amphibolite facies.

Mapping and re-interpretation of the Mt. Gibson mine area (Watkins and Hickman, 1988a,b) identified the basal part of the Retaliation sequence as comprising tholeiitic basalts and derivative amphibolite and mafic schists, some high-Mg basalt overlain by volcaniclastic sediments, felsic lavas/tuffs, minor mafic volcanic rocks, and some banded iron formations. This sequence probably equates with the Gabanintha and Windaning Formations of Watkins and Hickman (1988b) and is separated, to the east, by a strike-slip fault from undifferentiated mafic volcanics. This supracrustal sequence forms a synformal enclave within gneissic Archaean granitoids.

At the Mt. Gibson mine, the primary Au mineralization appears to be developed in quartz veins along shears in a 400 to 500-m thick sequence of very poorly-exposed interlayered volcaniclastic and epiclastic metasediments, felsic and mafic volcanic rocks, cherts and "quartz-eye" porphyries, and in the massive to weakly-foliated amphibolite forming the structural footwall (Fig. 3). The enclosing granitoids have a gneissic to pegmatoidal character and outcrop to the E, S, and W of the mine site. Greenstones (amphibolites) are exposed as rubble on upland areas to the west (Tobias' Find and west of N1 Pit) and to the E of the mine site.

The supracrustal sequence and the granitoids are intruded by ENE-trending dolerite dykes.

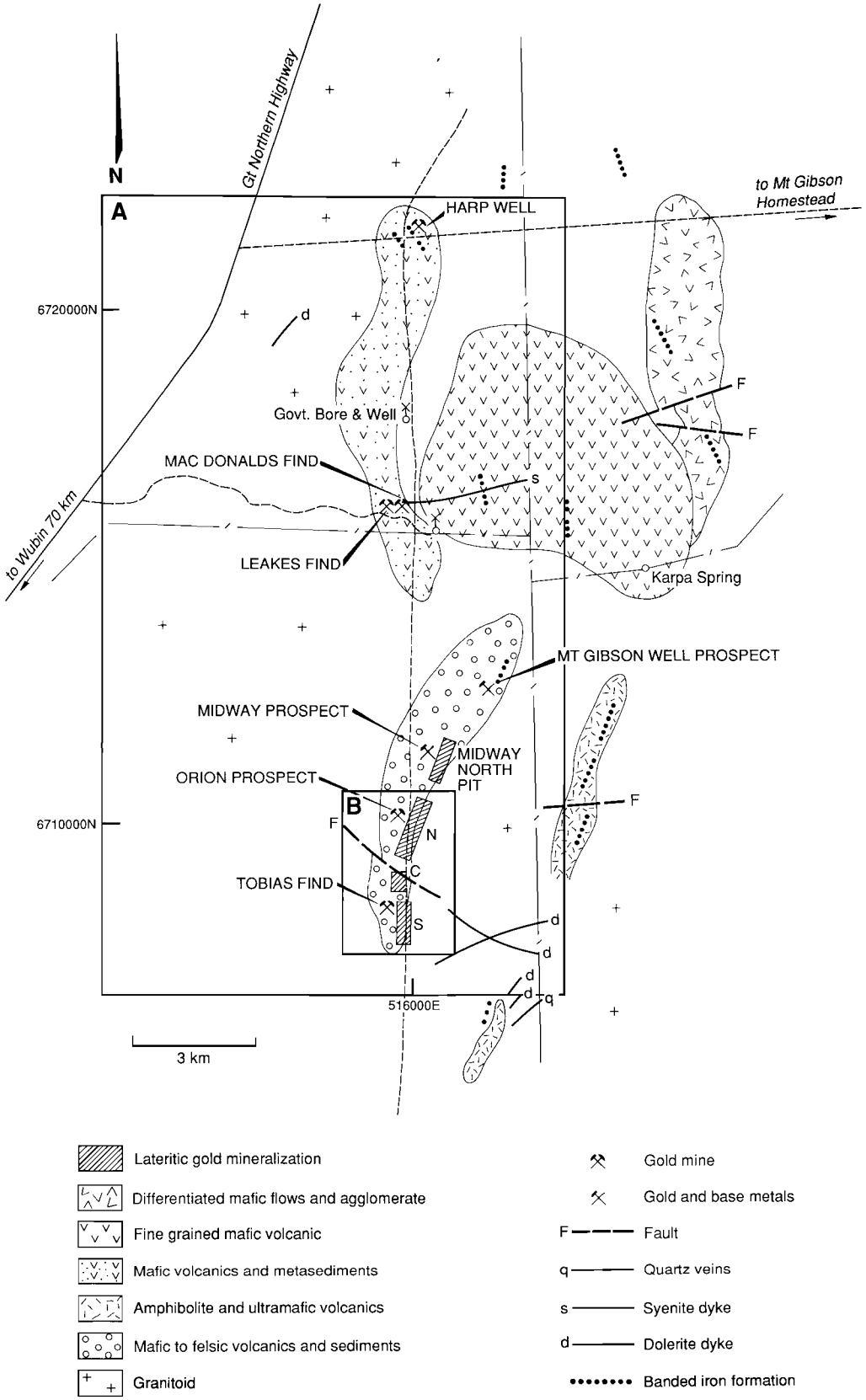

Fig. 3. Geology of the Mt. Gibson area (after El-Ansary and Sale, 1990)

4.0 REGOLITH-LANDFORM RELATIONSHIPS IN THE MT. GIBSON DISTRICT

4.1 The Surface Distribution of Regolith Units

Figure 4 shows the surface distribution of regolith-landform units for the Mt. Gibson district. This map resulted from the interpretation of 1:50,000 black and white aerial photography (Run 10/5001-5035 dated 18.9.1980) substantiated by ground traverses. The air photo patterns are largely related to the gross changes in vegetation, soil type and local relief along with some features of rock and regolith outcrop. For example, the areas of red clay soils (Units $m\mathrm{D}_1$ and mD2) have a Eucalypt woodland (Salmon gum, York gum) association contrasting with extensive areas of yellow sand plain (Unit $f\mathrm{R}_2$) having a dense, commonly 2 to 3 m high shrubland (*Acacia resinomarginea*) association. These plant communities and others provide a useful surrogate relationship as a base for regolith mapping.

The landscape of Mt. Gibson district has been divided into three major regimes, namely residual, erosional and depositional — where the focus is on the degree of preservation or truncation of the lateritic residuum. These three primary groups of regolith-landform units have been further subdivided according to the provenance of the associated regolith. The regolith of one group is related to granitic rocks, that of the second group to the rocks of the greenstone belt, and a third has regolith of mixed origin. Several units were mapped within these groups, based on surface expression of regolith and topographic featues. Units are described in detail below (Section 4.3). The description includes the salient features of the regolith, landform, and vegetation.

4.1.1 RESIDUAL REGIMES

Residual regimes are characterized by a complete or near complete lateritic profile. Such areas occupy broadly-convex crests of low hills which are frequently partially flanked and peripherally truncated by low breakaways that are components of neighbouring erosional tracts. Four units were mapped within the residual regimes. They were subdivided according to the source of regolith ie mafic vs. felsic. The brown to red clay soils and a high proportion of ferruginous gravels on greenstone terrain contrast with the clayey sands of the soils of residual areas on weathered granites. Residual areas on mafic rocks are mantled by pisolitic-nodular duricrust and coarse lateritic nodules and pisoliths. Pockets of Fe-rich duricrusts may also occur. The soils are shallow gravelly acid earths comprising very friable brown fine sandy loam.

Residual areas on felsic rocks are characterized by gravelly sandy soils with nodular duricrust at a shallow depth. Lateritic lag comprising yellow-brown nodules is common on crests. This lag, however, does not occur on sandplains.

4.1.2 EROSIONAL REGIMES

In the erosional regimes there has been varying degrees of truncation of the weathering profile; often the lateritic residuum has been removed so that the mottled zone, saprolite, saprock, or fresh bedrock are either exposed, concealed beneath soils, or beneath locally-derived colluvium. These areas comprise hills, breakaways, pediments, and very gently-undulating tracts often comprising a complex of low broad rises and shallow broadly-concave drainage floors.

Mafic units in the erosional regimes are largely dominated by calcareous red earths on saprolite and there are scattered pockets of crumbly pedogenic calcrete. Felsic units are characterized by partially-indurated pallid and mottled zones. Pale grey-brown gritty sandy loam soils are common.

4.1.3 DEPOSITIONAL REGIMES

Depositional regimes comprise lower slopes and plains that occupy the extensive floors of the principal tributary valleys. These include colluvial and alluvial outwash plains and account for about 65% of the mapped area. Exploration drilling shows that both complete and truncated profiles are buried by valley fill.

Residual Regimes

Mafic terrain

- mR_3 Orange earths
- mR_2 Lateritic gravels (pisoliths, nodules)
- mR_1 Lateritic duricrust (pisolitic, nodular)

Felsic terrain

- fR_1 Yellow sands
- fR_2 Gravelly yellow sands

Erosional Regimes

Mafic terrain

- mE_1 Calcareous clays, carbonates, mafic saprolite
- mE_2 Mafic outcrops

Felsic terrain

- fE_1 Gritty soils on granitic saprolite
- fE_2 Granitic outcrops

Depositional Regimes

Mixed terrain

- miD_1 Clayey sand to sandy clay loam, very saline (lake sediments)
- miD_2 Clayey sand, gypsum dunes, saline (lake sediments)

Mafic terrain

- mD_2 Calcareous red earths
- mD_1 Acid red earths

Felsic terrain

- fD_1 Gritty acid to calcareous red earths

- S Mine pits
- Road A, B
- A, B See text

mi = mixed,
m = mafic,
f = felsic,
R = residual,
E = erosional,
D = depositional

N

1 km

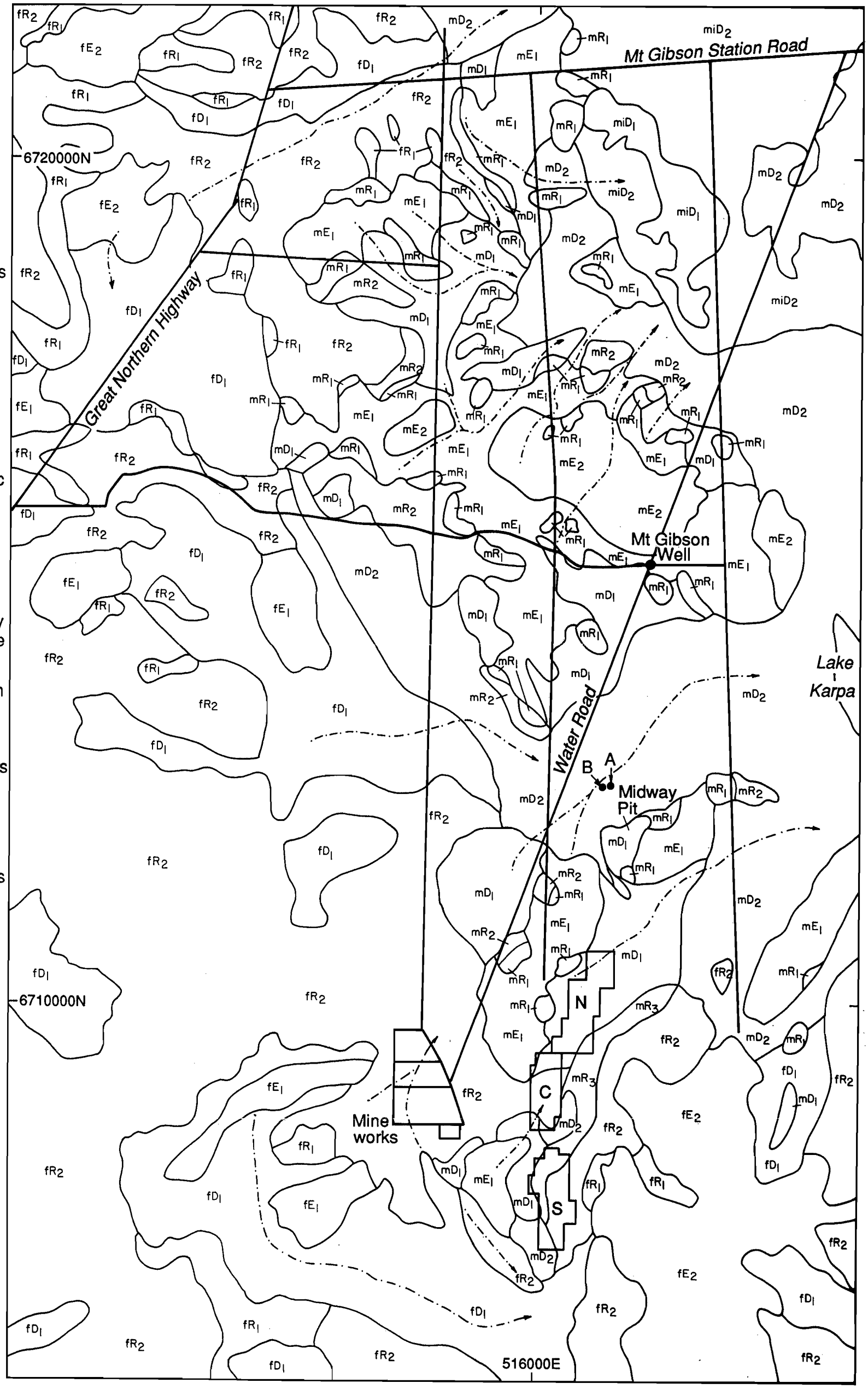

Fig. 4. Map showing the surface distribution of regolith-landform units for the Mt. Gibson district

Fine ferruginous granules form a sparse lag on depositional areas associated with mafic rocks. Acid to calcareous red earths have developed in colluvium, while extensive sheets of pisolitic-nodular duricrust form the principal substrate to soils. Hardpan, commonly developed in soils at a depth of 50 to 75 cm, continues for several metres within underlying lateritic residuum. Scattered pockets of calcrete can be present in the hardpan.

Depositional areas on felsic rocks are dominated by colluvium/alluvium (referred to as co-alluvium) largely from granitic rocks. There is an appreciable amount of quartz grit associated with the generally-clayey mass. Carbonates appear to be much less common than in the valleys associated with the mafic rocks.

4.2 The Regolith Stratigraphy

For successful application of geochemical exploration programmes in deeply-weathered terrain, it is important to have a more complete picture of the regolith, than presented above, including an understanding of the distribution of the regolith units and their stratigraphic relationships. In the Mt. Gibson district, exposures of the regolith stratigraphy have been provided by the open pit mining operations at S, C, N, and Midway North Pits. Opportunities to examine subsurface regolith relationships were also provided by the spoil from many exploration drill holes. In regional terms, the regolith stratigraphy of the Mt. Gibson district is complex because of the cyclic history of erosion and deposition and this has resulted in a diversity of regolith types being present in any particular area. The regolith stratigraphy and characteristics of regolith units for the Mt. Gibson district are given in Table 1.

4.2.1 REGOLITH STRATIGRAPHY — S, C, AND N PITS

The regolith stratigraphy of the S, C, and N Pits has already been described in detail in the report by Anand *et al.* (March 1989) and is briefly summarized below.

In the S, C, and N Pits, the regolith is related to residual, erosional, and depositional regimes. Units of friable red earths occupy a NS zone surrounded by extensive yellow sands. The continuity of the NS zone is broken by a narrow zone of yellow sand across the centre (Fig.4). The areas of red earths generally follow the broad crest of a sloping ridge immediately W of the mine site. Two types of red soils are associated with the greenstone sequence, namely, calcareous red earths associated with an occassional mafic outcrop and acid red earths overlying hardpanized colluvium. The distribution of these contrasting types of soil is related to the complex history of deep weathering as well as erosion and deposition. Calcareous red earths occur on broadly-concave erosional tracts set below areas of acid red earths separated by a change of slope. Here, on concave tracts, there are sporadic exposures of weathered mafic rocks and these areas are interpreted as being erosional tracts. The calcareous red earths show a close association with weathered or subcropping mafic rocks and appear to result from *in situ* weathering. By contrast, acid red earths associated with the long gentle slopes flanking these erosional tracts have formed in colluvium derived from the erosion of the weathered profiles in the upland erosional areas. The acid red earths are underlain by hardpanized gravelly colluvium which, in turn, overlies lateritic duricrust. The most common substrate to the calcareous red earths is non-calcareous dark, red-brown plastic clays which merge with mafic saprolite at a depth of 3 to 4 metres.

Figure 5 (from Anand *et al.*, March 1989) is an E-W cross section through the N1 pit at line 3800N (mine grid). The local upland area to the W is characterized by red earths overlying saprolite with sporadic subcrops of amphibolite. In the W part of this cross section, lateritic pisoliths, nodules, or lateritic duricrust have largely been removed by erosion. The local upland area is thus interpreted to be a partly-stripped laterite profile.

In the central part of Fig. 5, acid red earths are underlain by nodular sandy and gravelly colluvium in which hardpan has developed. The colluvium was derived by erosion of a laterite profile interpreted to have once covered the adjacent upland area. Wispy carbonate cementation along bedding and partings is common in the hardpan unit and, at the base of the hardpan, calcrete reaches 1 m in thickness. The hardpanized colluvium generally lies upon one or more of the lateritic units, namely loose lateritic pisoliths/nodules, nodular duricrust, or, in places, the

Table 1. Regolith stratigraphy and characteristics of regolith units, Mt. Gibson district

TYPE OF REGIME	RESIDUAL REGIMES					EROSIONAL REGIMES				DEPOSITIONAL REGIMES				
REGOLITH UNIT AT SURFACE	mR1	mR2	mR3	fR1	fR2	mE1	mE2	fE1	fE2	mD1	mD2	fD1	MiD1	MiD2
REGOLITH DERIVED FROM	GREENSTONE BELT			FELSIC ROCKS		GREENSTONE BELT		FELSIC ROCKS		GREENSTONE BELT		FELSIC ROCKS	MIXED	
LANDFORM	Broad crests	Upper to mid-gentle slopes	Lower slopes	Broad crests	Gentle slopes	Gently-undulating tracts	Low to medium hills	Minor breakaways, pediments	Low domes	Lower slopes	Floors of tributary valleys	Broad floors	Major drainage system	Dune
VEGETATION	Acacia	Acacia	Acacia	Casuarina	Acacia	Salmon gum	Eucalypts	Eucalypts	Eucalypts	Malle, Eucalypts	Eucalypts	Eucalypts	Saltbush	Saltbush
LAG	Lateritic nodules/ pisoliths	Lateritic nodules/ pisoliths	Lateritic nodules/ pisoliths	Lateritic nodules	-	Saprolite/ saprock	Fresh rock	Pallid zone	Granite	Fine ferruginous granules	-	-	-	-
SOILS	Gravelly acid red earths	Gravelly acid brown earths	Gravelly acid orange earths	Gravelly acid sand	Acid yellow-brown clayey sand	Calcareous red clays, Plastic acid red clays	Calcareous red clays , Plastic acid red clays	-	-	Acid red earths	Calcareous red earths	Acid to calcareous red earths	Red brown clayey sand	Brown clayey sand
COLLUVIUM	-	Minor	Minor	-	Minor	Minor	Minor	-	-	Red sandy clay with or without lateritic debris (2-10m)	-	-	-	-
CO-ALLUVIUM	-	-	-	-	-	-	-	-	-	-	Extensive White granitic clays, Red mafic clays, may be up to 25 m thick	Extensive, thickness unknown	Extensive co-alluvium	Extensive co-alluvium
CARBONATES/ CALCRETES	-	-	-	-	-	Pedogenic calcrete	Pedogenic calcrete	-	-	Nodular calcrete within hardpan unit	Soft carbonates at 50 to 80cm	Soft carbonates can be present	Soft carbonates rare	Soft carbonates rare
HARDPAN (developed in colluvium/alluvium)	-	Minor	-			-	-	-	-	Hardpan present at 0.5-10 m	May be present	-	May be present	-
LATERITIC RESIDUUM	Pisolitic duricrust, some Fe-rich duricrust	Pisolitic-nodular duricrust (weakly indurated) 1-4 m	Pisolitic/ nodular duricrust (weakly indurated) 1-3 m	Nodular duricrust 0.5-1.5 m		-	-	-	-	Pisolitic-nodular duricrust (weakly indurated) (1-4 m)	Can be buried up to 6 m thick	-	-	-
MOTTLED ZONE		Present 1-4 m		-	-	-	-	-		Present 2-5 m		?	?	?
SAPROLITE	Multicoloured clay-rich saprolite, variable thickness			Granitic white saprolite		Multicoloured clay-rich saprolite		Granitic white saprolite	-	Multicoloured clay-rich saprolite variable thickness		Granitic white saprolite	?	?
BEDROCK	Mafic to felsic volcanics and sediments, amphibolite			Granitic		Mafic to felsic volcanics, amphibolite, sediments		Granitic	Granitic	Fine-grained mafic volcanic and metasediments		Granitic	?	?

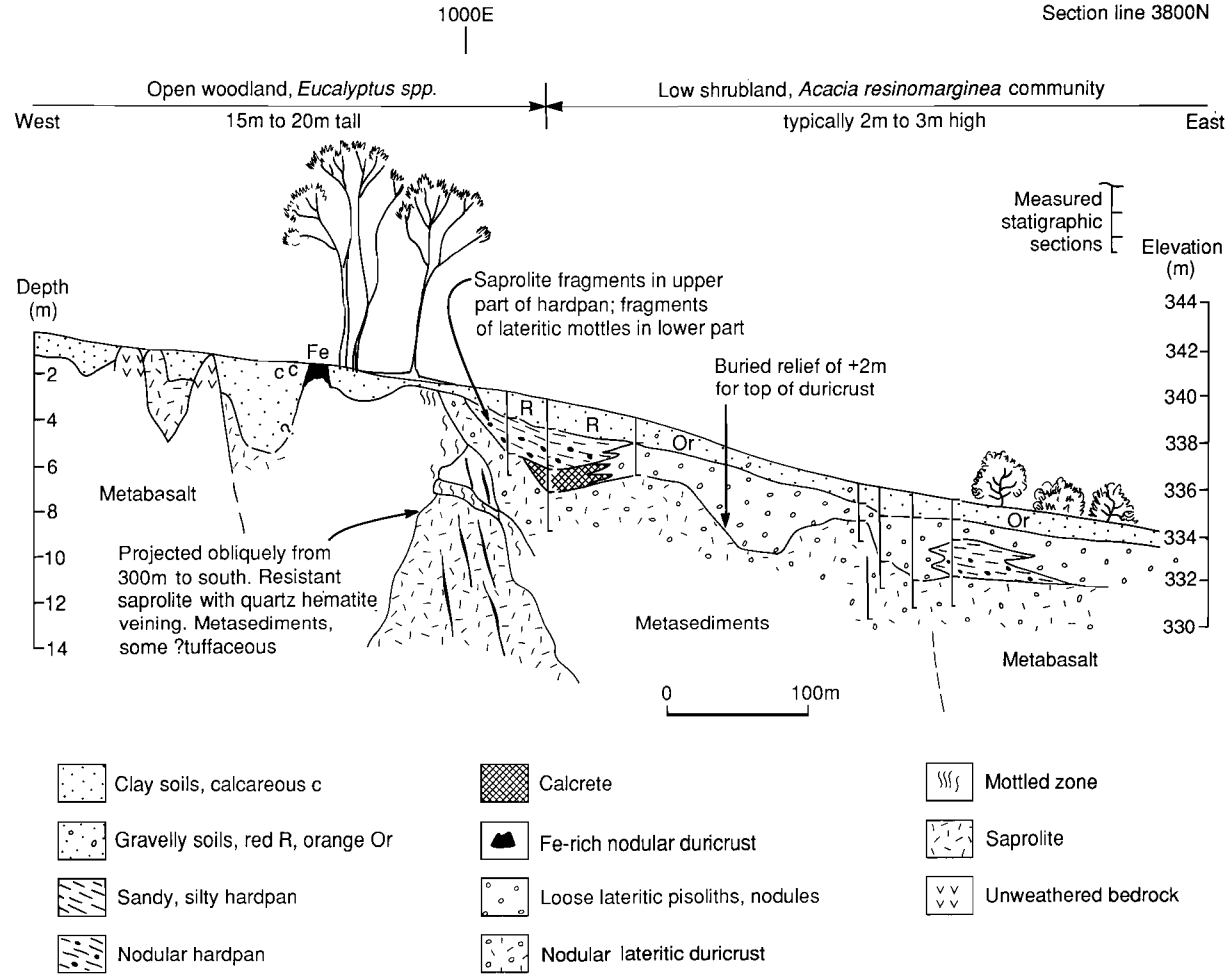

Fig. 5. Cross-section through the N1 pit (Line 3800N) showing upper regolith and vegetation relationships, from Anand *et al.* (March 1989).

mottled zone. The base of this hardpanized colluvium is thus interpreted as a local unconformity in the detailed regolith stratigraphy.

Red earths merge laterally, downslope, with orange sandy clay soils. Hardpan and carbonates were not seen as a substrate to the orange sandy clays. Rather the typical substrate is poorly-indurated, nodular, massive, or mottled duricrust which occurs at a depth of 1 to 1.5 m.

Extensive yellow clayey sands dominate the sand plain at Mt. Gibson and the surrounding region. These typically overlie coarse lateritic nodules which in turn may overlie nodular-pisolitic duricrust.

4.2.2 REGOLITH STRATIGRAPHY — MIDWAY NORTH PIT

In the Midway North Pit, the pattern of regolith relates closely to the erosional and depositional modification of a deeply-weathered mantle (Fig. 6A). Regolith of the depositional regime is exposed in the S and W walls of the pit (Figs 6B, 7A). The E wall provides an example of regolith of the erosional regime (Fig. 7B).

The depositional regimes at Midway are characterized by acid red earths (50-80 cm) overlying harpanized colluvium (Figs 6B, 7A). Hardpanized colluvium ranges in thickness from 2.5 to 10 m. A thick body (8-10 m) of hardpanized silty colluvium appears near the N end of the W wall and continues N of the pit. The hardpan unit lies upon pisolitic-nodular lateritic residuum which is present as an almost continuous horizon, varying from 2 to 4 m thick. In places, the introduction of silica-cement has modified the lateritic residuum resulting in a coarsely-laminated appearance. Lateritic residuum merges at depth with a mottled zone (2-4 m), thence to a clay-rich saprolite which in turn merges into fresh mafic bedrock. Calcareous clays are present in areas where erosion has removed the lateritic residuum and mottled zone such as in the E face of the pit. Here 2-4 m of calcareous clays overlie a plastic non-calcareous red clay (Fig. 7B). Large pockets of soft carbonates occur within the upper 3-4 m of the surface. However, zones of hard carbonate nodules may also be widely distributed in calcareous clays. Beneath the non-calcareous red clay is a saprolite, which itself merges at depth to saprock.

4.2.3 REGOLITH STRATIGRAPHY — ON THE VALLEY FLOORS

The regolith stratigraphy of the valley floors was provided by logging a series of exploration drill holes. Whilst gritty pallid clays occur extensively at the surface of the valley floors in granitic terrain, they also form an important substrate along some of the valleys that transverse the mafic terrain. Spoil from several exploration drill holes (e.g. at 6950N 1950E, 6950N 2000E, local mine grid) suggest two main sedimentary units (Fig. 4:A,B). The upper unit comprises about 6 m of brown calcerous clays, without appreciable quartz grit, but with ferruginous granules to about 5-mm diameter. The lower sedimentary unit of gritty pallid clays is about 8-10 m thick and is underlain by 3 to 6-m thick lateritic residuum containing clays with abundant pisoliths, a regolith type that is residual. The lateritic residuum merges at depth to a pale mafic saprolite. In other cases, lateritic residuum is absent and transported clays (felsic and mafic) up to 25 m thick directly overlie clays from mafic rocks.

4.3 Description of the Regolith-Landform Mapping Units

The regolith-landform mapping units shown in Fig. 4 are described below.

4.3.1 REGOLITH-LANDFORM UNITS ON MAFIC ROCKS

4.3.1.1 Residual Regimes

mR_1
This unit occupies broadly-convex crests of low hills which are, in part, flanked and peripherally-truncated by low breakaways that are components of neighbouring erosional tracts.

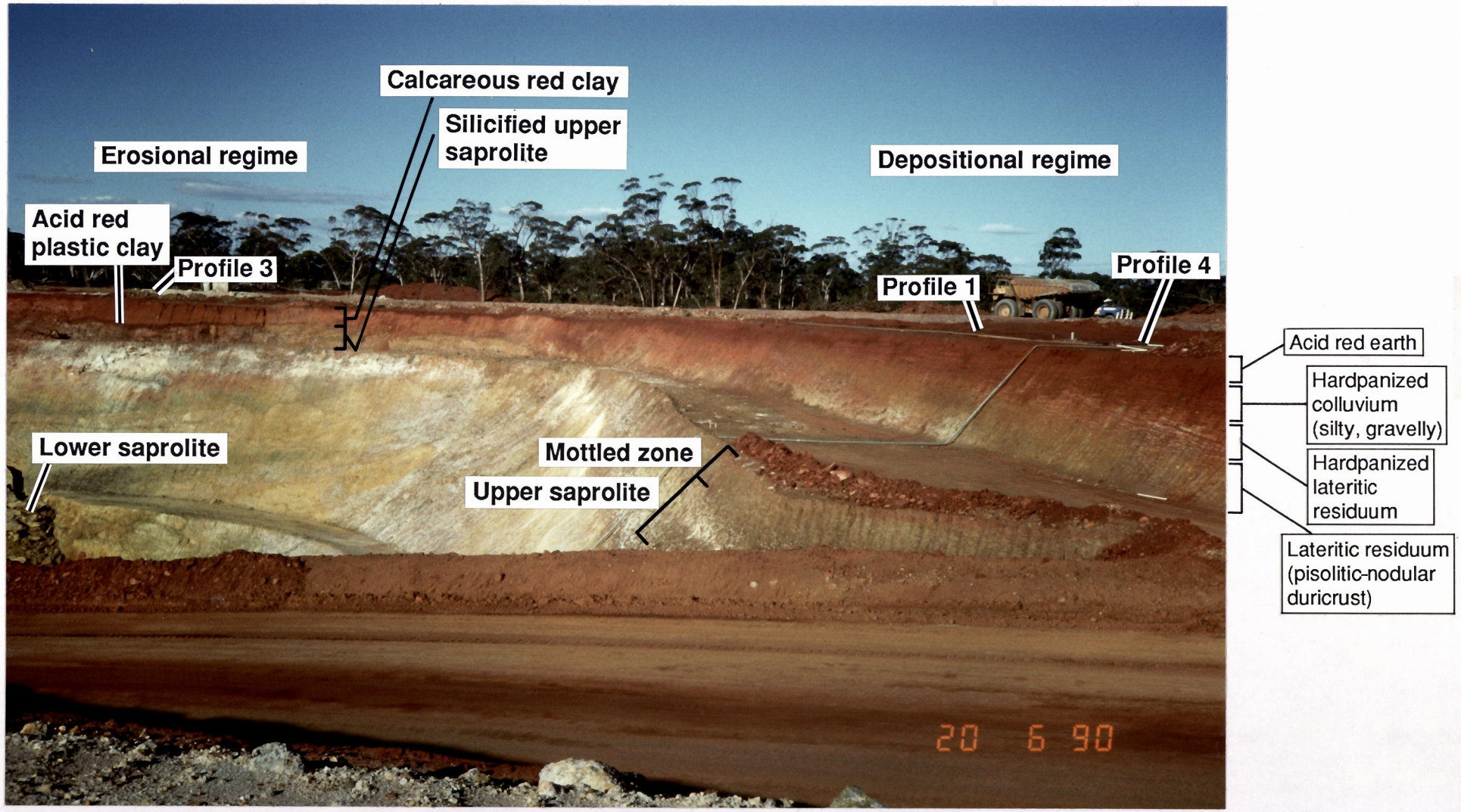

Fig.6A. Mine exposure of erosional and depositional regimes in Midway North Pit.

1 Acid red earth SU203

2 Hardpanized silty colluvium CV102HP

3 Lateritic residuum (pisolitic nodular duricrust) LT203

4 Mottled Zone MZ

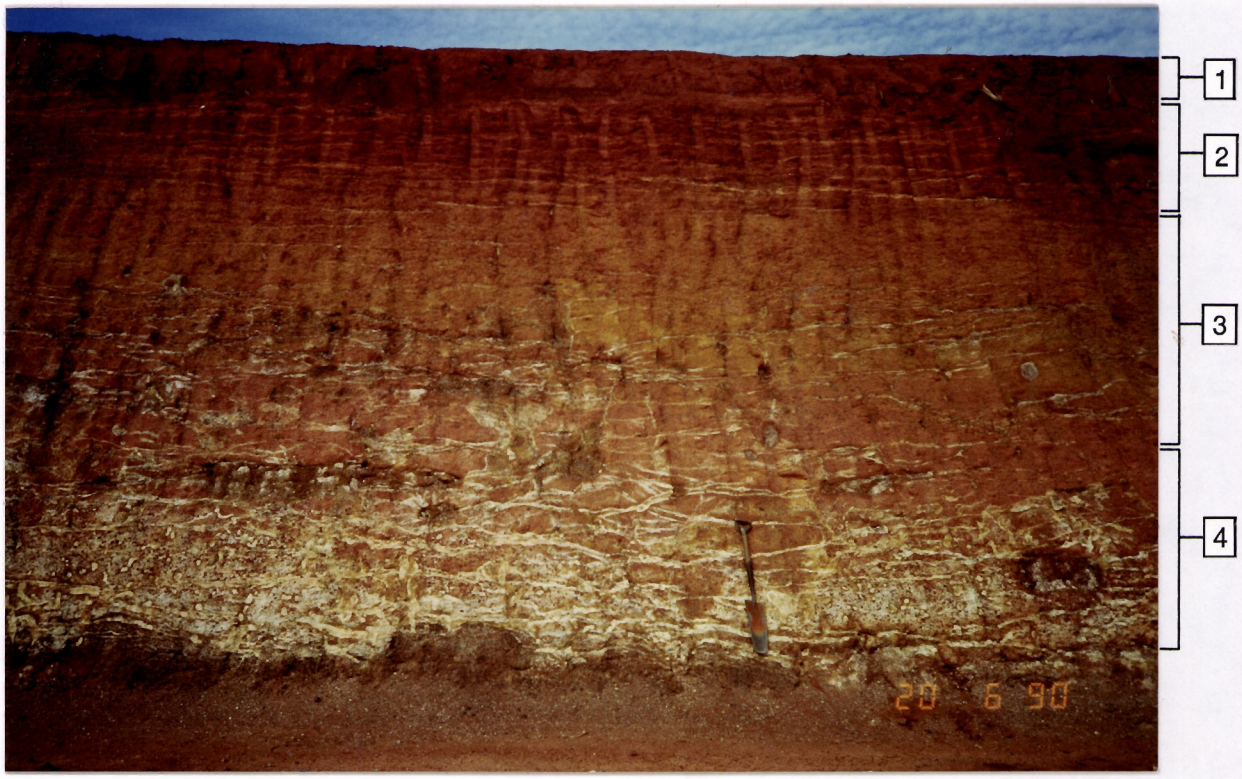

Fig.6B. Vertical profile showing regolith stratigraphy of depositional regime shown in A: hardpanized colluvium overlying lateritic residuum and mottled zone, location southern wall of Midway North Pit, profile No.1.

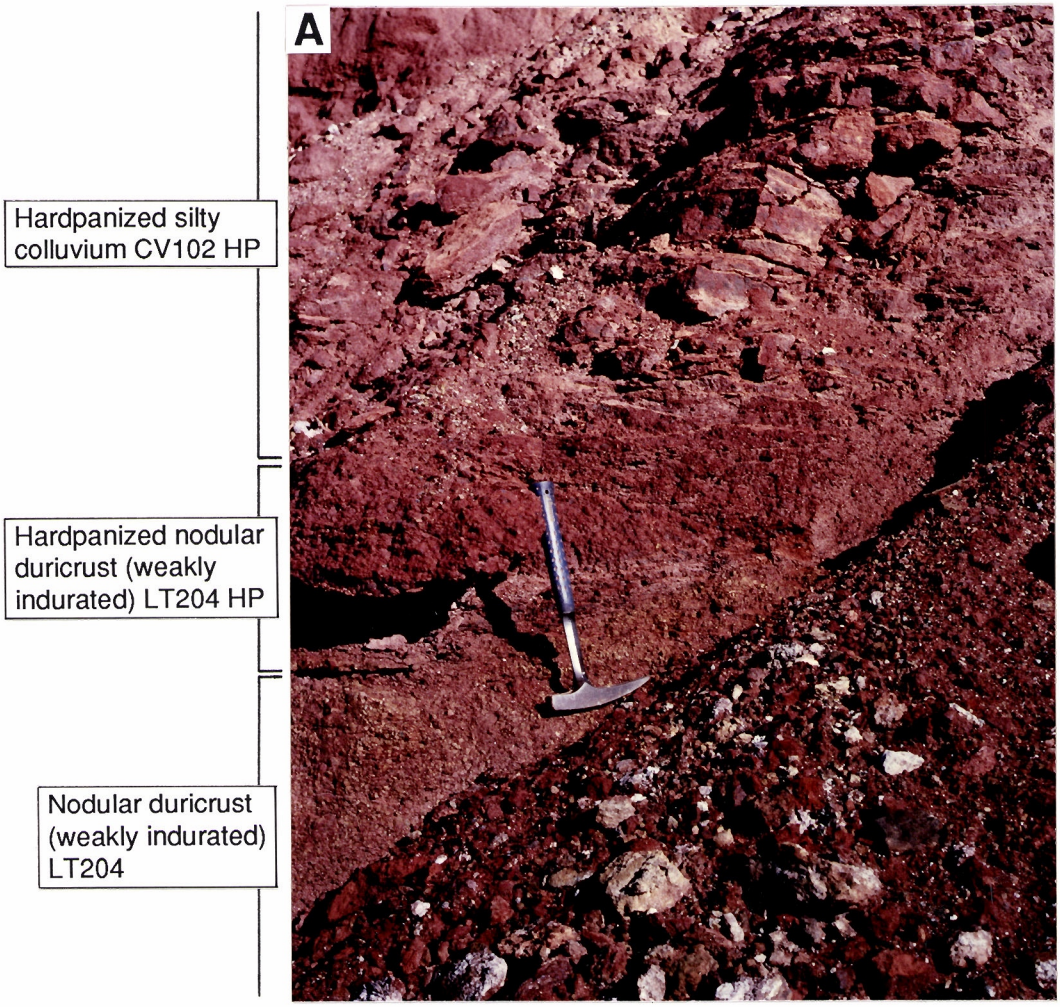

Fig.7A. Vertical profile showing regolith stratigraphy of depostional regime: hardpanized colluvium overlying residual nodular lateritic duricrust, Location western wall Midway North Pit, profile No.2.

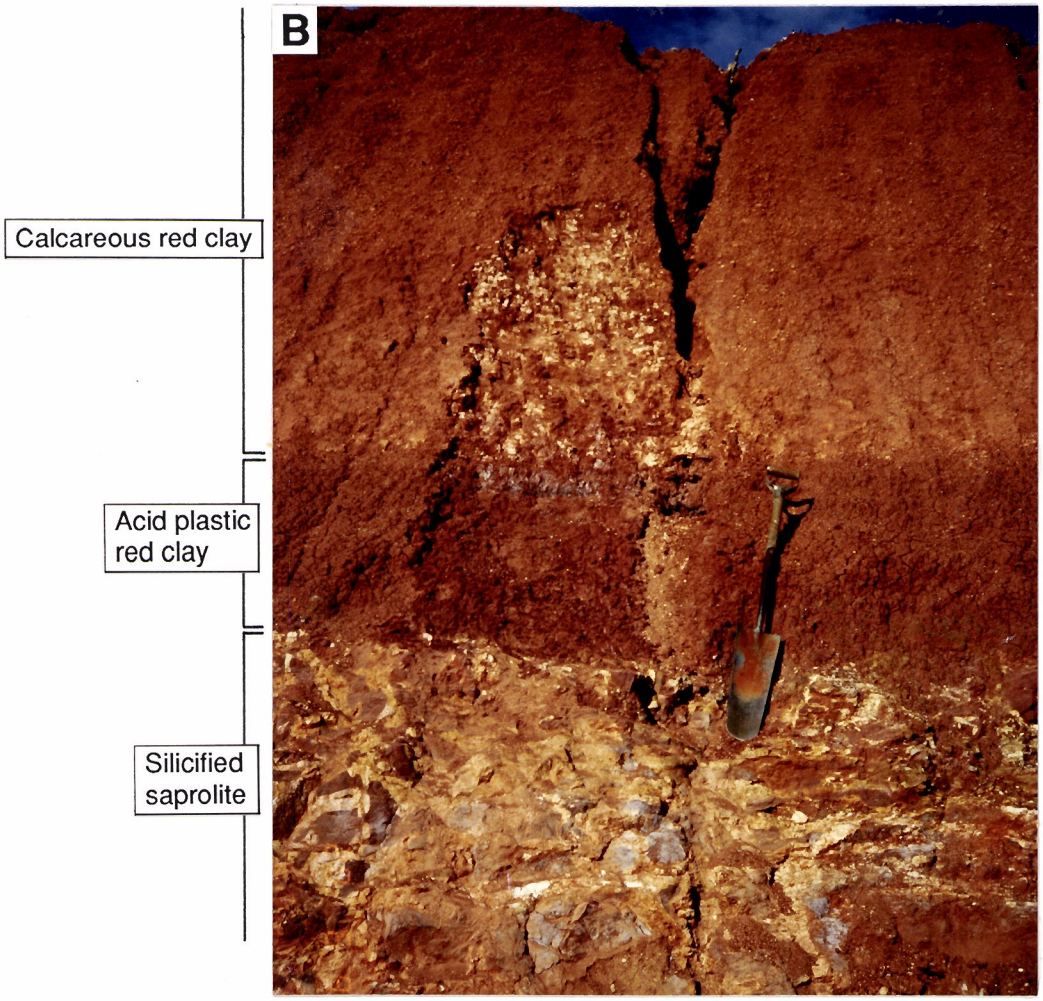

Fig.7B. Vertical profile showing regolith stratigraphy of erosional regime: calcareous clays overlying acid red plastic clays and silicified saprolite, Location eastern wall of Midway North Pit, profile No.3.

The upper regolith is dominated by a pisolitic lateritic residuum. Pockets of Fe-rich duricrust may also occur. Blocks and small slabs of these duricrusts outcrop while ferruginous saprolite is rare. Crumbly pedogenic calcrete is very rare and occurs as small pockets.

The lag is mostly of pisoliths and nodules, these are mainly derived from the breakdown of pisolitic duricrust and Fe-rich duricrust.

The soils are shallow gravelly acid earths comprising very friable brown fine sandy loams.

Dense thickets are common and usually comprise casuarina (*Allocasuarina campestris*), melaleuca (e.g. *Melaleuco cordata*), and *Hakea sp*. There can be scattered native pine (*Cellitris sp.*).

mR_2
This unit typically occurs on the upper to mid-gentle slopes down from mR_1, forming "backslopes" to breakways.

The dominant surface regolith type is a dense lag of lateritic pisoliths with some coarse lateritic gravels derived from Fe-rich duricrusts. Outcrops of pisolitic lateritic duricrust are very rare. The soils are gravelly acid earths comprising very friable red-brown to light brown fine sandy loams which are, in part, of colluvial origin.

Weakly-indurated pisolitic lateritic duricrust is an extensive substrate to these regolith types. Hardpan is commonly developed in this lateritic residuum.

Wattle (*Acacia sp.*) and cypress pine (*Callitris columellaris*) scrub communities are dominant and there are scattered eucalypts.

4.3.1.2 Erosional Regimes

mE_1
This unit is represented by very gently-undulating tracts often comprising a complex of low broad rises and broad shallow concave drainage floors. These tracts are frequently incised below the long smooths slopes of mR_2 and are separated from them by occasional low breakaways.

Saprock forms frequent outcrops or subcrops and there are scattered pockets of crumbly calcrete. Shallow red calcareous earths are the dominant soils.

Salmon gum (*E. salmonophloia*) woodlands are dominant communities, usually with a chenopod (salt bush, etc.) low understory.

mE_2
This unit comprises low to medium-sized hills. There are frequent exposures of fresh and weathered greenstone rocks as well as pockets of crumbly pedogenic calcrete. Shallow stony calcareous grey-brown to red earths are common.

Salmon gum (*E. salmonophloia*) woodland is the dominant vegetation community with a chenopod (salt bush, etc.) low understory.

4.3.1.3 Depositional Regimes

mD_1
This unit occurs on gently-graded lower slopes down from and continuous with the "backslopes" formed by mR_1 and mR_2.

The upper regolith type, a colluvium, comprises red-brown fine sandy clay loams with occasional fine (< 1 cm dia.) ferruginous gravels, which can be present as bands and lenses. Fine ferruginous gravels form a sparse lag. Acid red earths have developed in the colluvium, while extensive sheets of pisolitic lateritic residuum, often as a weakly-indurated duricrust, form the principal substrate to the soils. These sheets are from 1 to 4 m thick. Hardpan, developed in the soils at a depth of about 50 to 75 cm, continues for several metres within the underlying lateritic residuum. There can be scattered pockets of calcrete in the upper metre of the regolith.

Characteristic are tall shrubs and low closed woodland dominated by pine (*Callitris columellaris*) and wattle (*Acacia sp.*), but with a scatter of large ("bull") mallee ecualypts.

mD_2
This unit comprises plains that occupy the extensive floors of the principal tributary valleys. The present surface is without clearly defined streams or channels and appears to be the subject of sheet floods so that much of the upper regolith comprises co-alluvium. Exploration drill spoils suggest two main transported regolith types. The upper unit consists of brown calcareous clays, without appreciable quartz grit but with ferruginous granules to about 5 mm diameter. These clays are about 6 m thick. Underlying this unit is the second, consisting of pale grey gritty clays that have coarse yellow-brown mottles. This lower transported unit is about 8 to 10 m thick. It is underlain by grey and pale brown clays (without grits) containing pisoliths with yellow-brown cutans, a regolith type that has developed *in situ*. It merges at depth with pale saprolite. In other drill spoils, lateritic residuum is absent. Here transported granitic and mafic clays are up to 25 m thick overlying residual mafic saprolite.

Red earths with soft carbonate appearing at about 50 to 80 cm are the dominant soils of this unit. Ecualypt-native pine woodland with a dense wattle understory is extensive on this unit. The eucalypts are mainly large ("bull") mallee (*Eucalyptus loxophleba* and *E. salubris*), but there can be an occasional salmon gum (*E. salmonophloia*).

4.3.2 REGOLITH-LANDFORM UNITS ON FELSIC (GRANITOID) ROCKS

4.3.2.1 Residual Regimes

fR_1
This unit comprises broad crests, often as local divides or capping low breakaways, in weathered granitoid rocks. The lag is of coarse to fine yellow-brown to light brown lateritic nodules.

Gravelly sandy soils with pisolitic-nodular duricrust at a shallow depth are common. These soils are dominated by coarse lateritic nodules which are set in a sandy loam to clayey sand matrix. Lateritic duricrust commonly occurs within 40 cm of the surface and comprises mottled clay with frequent nodules. This lateritic residuum merges at depth with pallid saprolite derived from granitoid rocks.

Areas of this unit often support dense thickets dominated by casuarina (e.g. *Allocasuarina campestris*).

fR_2
This unit shows long gentle slopes down from fR_1 merging with broadly-concave gently-sloping floors.

This unit has extensive deep clayey sand colluvium with no gravelly lag. The soils are acid yellow-brown to brownish yellow clayey sand merging at depth to coarse sandy clay loams with an acid pH. Nodular duricrust forms the principal substrate to these soils.

The vegetation ranges from wattles and gravillia (*G. excelsior*) scrub to low meleleuca heath, some whipstick mallee is present.

4.3.2.2 Erosional regimes

fE_1
These tracts are a complex of minor breakaways and local pediments.

The low breakaways in weathered granite commonly comprise a partially-indurated pallid zone and an associated overlying mottled zone. Pediments below these are mantled by pale grey-brown gritty sandy loam over pallid brownish grey kaolinitic clay at a depth of from 30 to 50 cm.

Tall shrub communities are common in this unit with some patches of heath of mallee. Casuarina (*Allocasuarina campestris*) and York Gum (*E. loxophleba*) can be present as low trees.

fE_2
This unit is dominated by outcrops of granite as low domes and tors. These are associated with local wash slopes. Minor slopes from local granite outcrops are mantled by gritty coarse sands, light brown to light grey-brown in colour.

4.3.2.3 Depositional Regimes

fD_1
This unit consists of broad floors and very gentle lower slopes of tributary valleys. There are no clearly defined fluvial channels and the upper regolith is dominated by co-alluvium largely from granitic rocks. There is an appreciable amount of grit associated with the generally-clayey mass. Pedogenic carbonate appears to be much less common than in the broad valleys associated with the greenstone sequence.

The soils are red earths which have a light reddish brown sandy clay loam at the surface; this merges at depth to a sandy brownish red light clay by 30 cm. The soil has an alkaline pH at depths greater than 50 cm and some soft carbonate can appear at depths of 50 to 100 cm. As is the case in the valley floor of the greenstone terrain, it is expected that granitic saprolite forms the main substrate to the upper transported regolith types. The upper regolith types are derived from a granitic saprolite source area.

The vegetation is dominated by tall closed woodlands of native pine, "bull" mallee and York gum (*E. loxophleba*); some salmon gum (*E. salmonophloia*) can be present.

4.3.3 REGOLITH-LANDFORM UNITS — MIXED ORIGIN

4.3.3.1 Depositional Regimes

miD_1
This unit consists of valley plains adjacent to and, in part, occupied by the major drainage systems. The regolith has an uncertain origin. Information is only available for the upper metre. This is dominated by red-brown clay sand to sandy clay loam soils with rare carbonate, hardpan is sometimes present at about 75 cm depth.

The vegetation is predominantly salt bush communities with some areas of open low woodland of native pine, wattle, and tea tree (*Melaleuca lanceolata*)

miD_2
This unit represents the immediate surround of the salt lakes. Low gypsum dunes can flank the lakes. The intervening areas have brown clayey sand soils which sometimes contains soft carbonate.

The vegetation is dominated by shrub communities of salt bush (*Atriplex sp.*) with tea tree (*Melaleuca thymoides*) thickets. Samphire is extensive near the margins of the lake floors.

4.4 Synthesis of Regolith Development

A schematic cross section showing regolith-landform relationships for the Mt. Gibson district is shown in Fig. 8. Facies relationships for the formation of lateritic residuum and the relationships between mapped regolith units are shown in Fig. 9. These figures are based upon the regolith-landform assessment throughout the Mt. Gibson district coupled with the detailed study at S, C, N, and Midway North Pits.

The generalized regolith-landform model summarizing the regolith stratigraphy for three dominant regimes derived from the Mt. Gibson study is shown in Fig. 10.

Lateritic horizons, hardpanized colluvium (hardpan), calcrete, and soils are conspicuous components of both the landscape and the regolith stratigraphic column in the Mt. Gibson district. The landforms and regolith of the complex lateritic sandplain of the Perenjori/Ninghan region, typified by the Mt. Gibson district, can be related to a complex physiographic history, including deep weathering and processes of erosion and deposition. Stripping of the weathered profiles to varying degrees is an important process, giving several different apparent land surfaces related to what may have been a single older weathering profile. Stripping is clearly expressed on low ridges and hills. In contrast, the deeply-weathered materials in footslopes are little affected by erosion. Materials from erosional areas have been moved from crests into upper and midslope areas with the consequent burial of the residual laterite profile. In the process, local erosional/depositional couples have resulted in colluvial/alluvial sequences, some of which show an inversion of the sequence of the former weathering profile, now dismantled (Anand *et al.*, March 1989).

Depositional processes have had a role in the modification of the ancient surface and the emplacement of an array of regolith types. Gritty clays occupy the broad tributary velleys in the granite terrain. There are sporadic occurrences of carbonates in these soils which, in general, could have been derived from weathering of the occasional dolerite dyke that intrudes these granites. It is also possible that the carbonates in granitic terrain are aeolian in origin. While surface expression of these more gritty clays is in general limited to granitic terrain, it forms a substrate along some of the valleys that traverse the mafic terrain where the upper regolith member comprises red clays with little apparent quartz grit but appreciable carbonate. It seems that the processes of landform and regolith development are multiphase. An earlier phase showed more effective transport of gritty clays from the extensive granitic terrain to the W and SW. These were deposited on a deeply-weathered land surface, subsequently, it was buried by calcareous clay from erosional tracts in the greenstone terrain. Presumably, sedimentary processes, such as sheet flodding, ceased to be as regionally effective, so that calcareous clays from adjacent greenstone exposures then contributed much more sediment than did the granites to the west. These resulted in extensive superposition of calcareous clays on the gritty clays.

Both the hardpan and calcrete are clearly much younger than the weathered surface and developed in detritus resulting from the erosional modification of the old surface. The influx of silica and carbonates is a relatively recent addition to the landscape and were not involved in the creation of the original deep weathering profiles in which they are now found. The origin of carbonates is discussed in detail in Section 6.3. Hardpanization processes have affected both transported and residual regolith units. There is a strong development of hardpan on lower slopes compared to valley floors. The acid, intensively-weathered settings on crests and lower slopes are very different from the alkaline conditions of the main tributary valley floor and could well have provided more favourable conditions for the development of hardpan.

The lateritic duricrust formed during the Tertiary period has been partly replaced/displaced by silica or carbonates, with the beginnings of a replacive silcrete or calcrete.

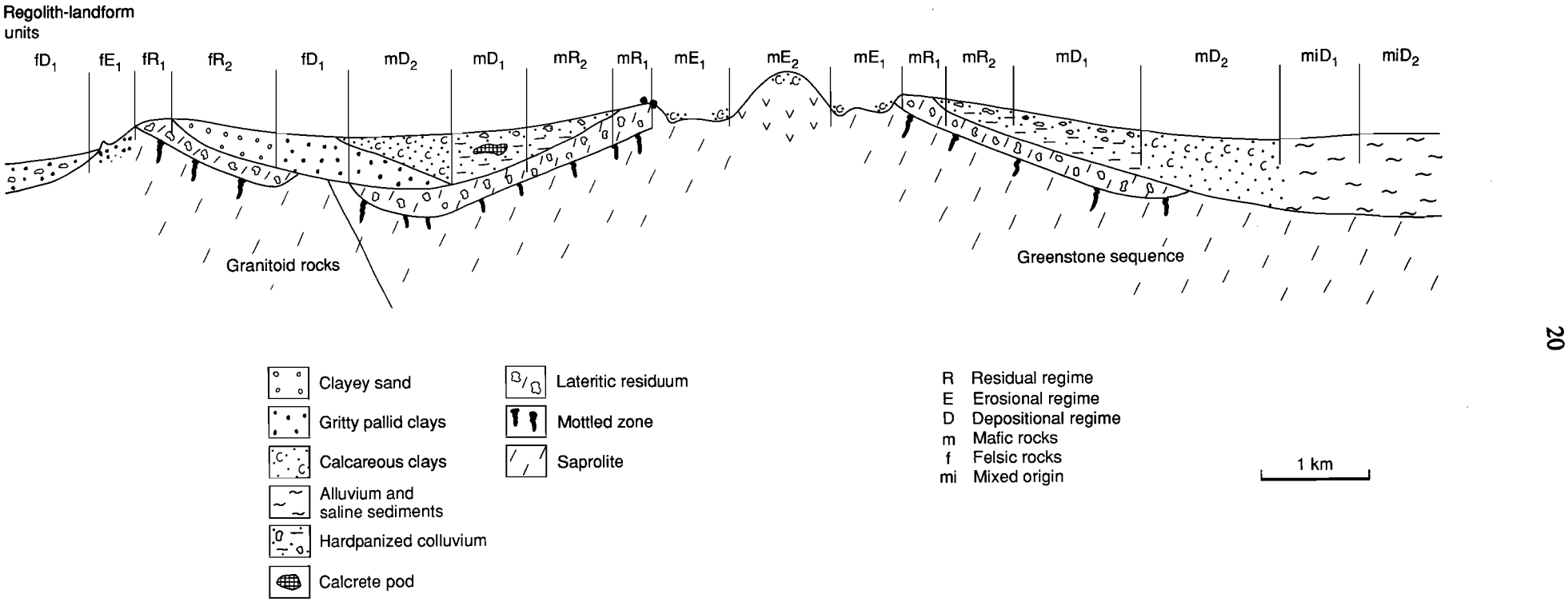

Fig. 8. Schematic cross section for the Mt. Gibson district showing regolith stratigraphy and landforms.

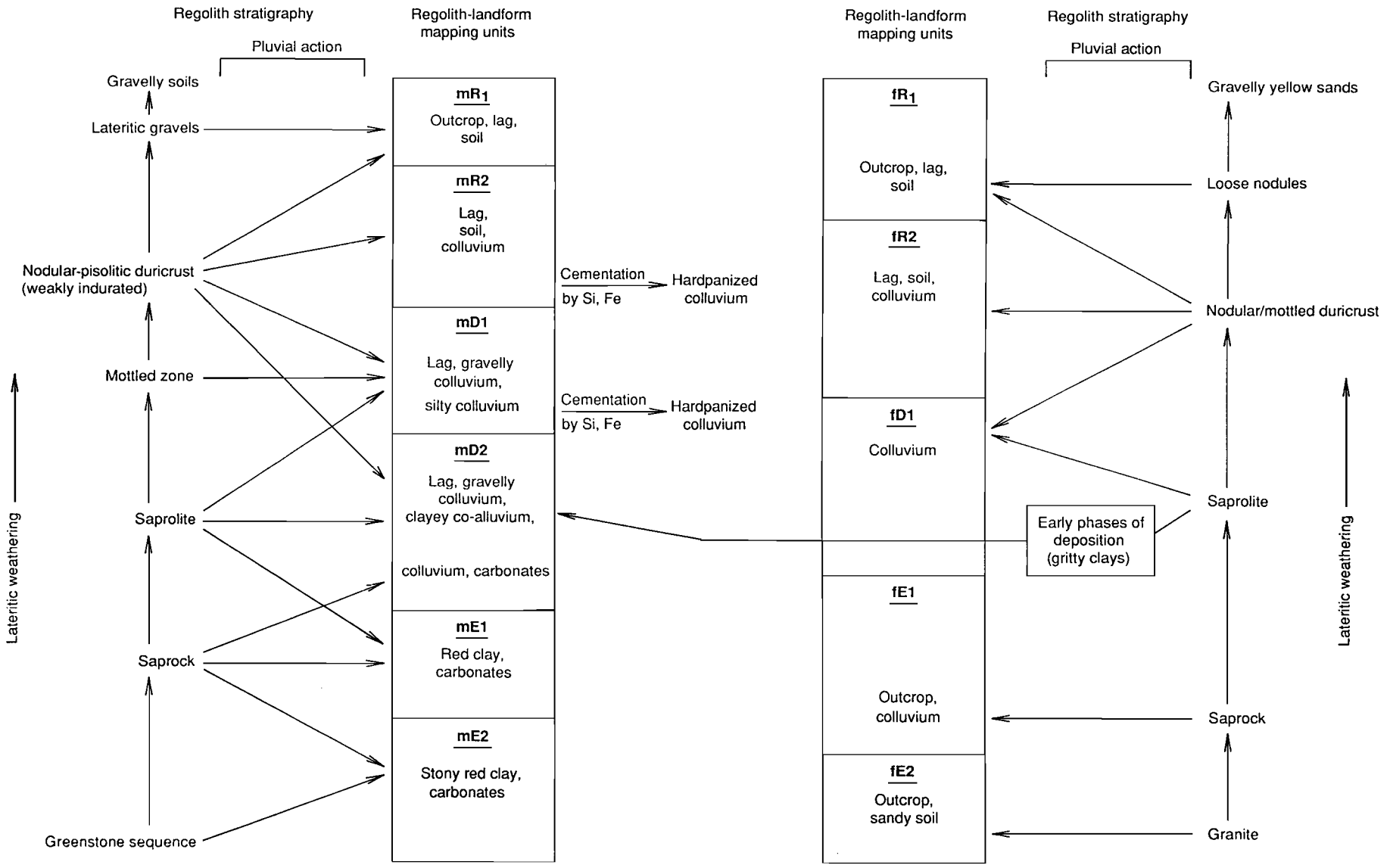

Fig. 9. Schematic facies relationships for the formation of lateritic residuum and relative contribution of deep weathering profiles to upper regolith units.

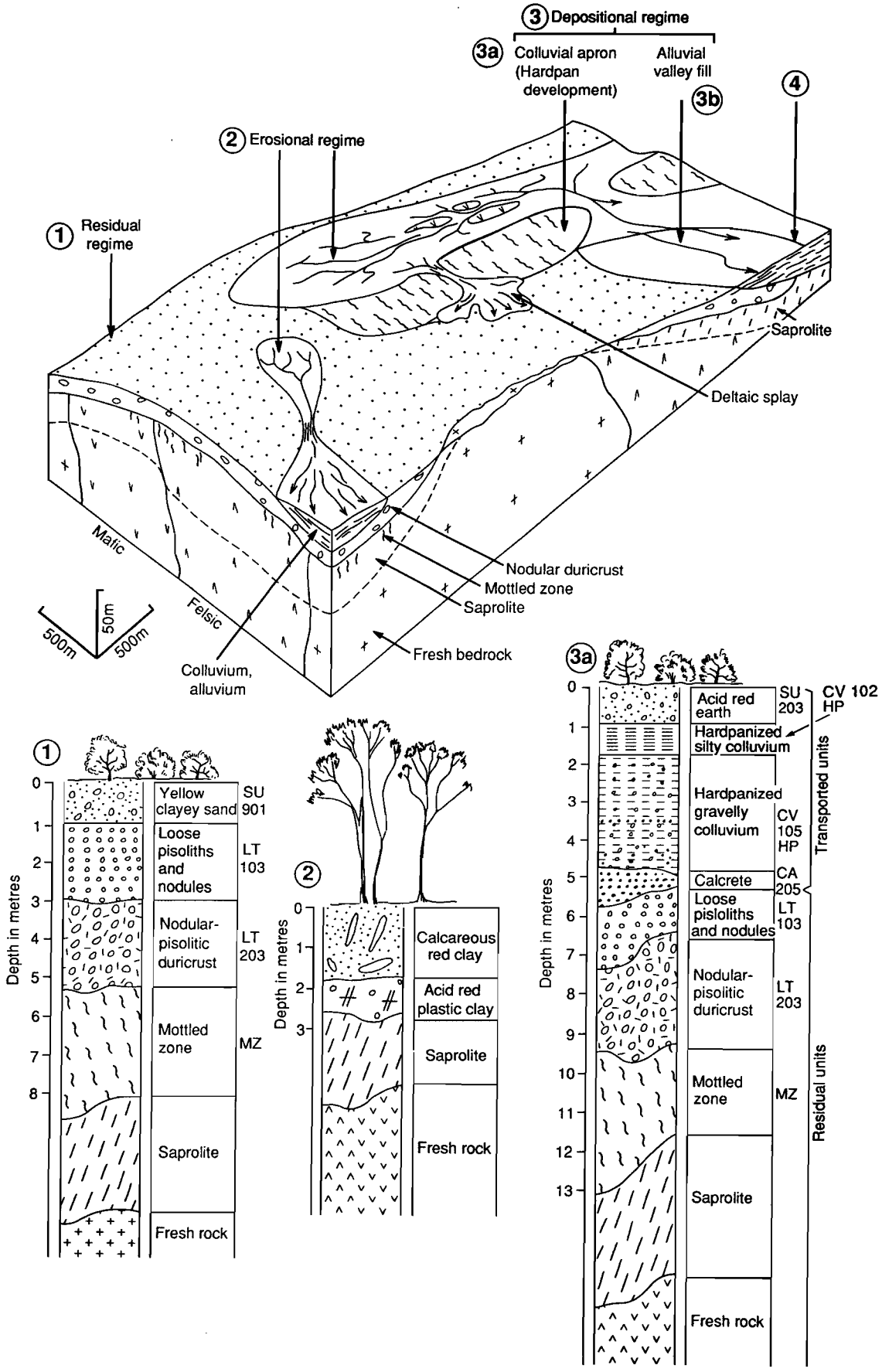

Fig 10. Generalized regolith-landform facies model based upon the Mt. Gibson district.

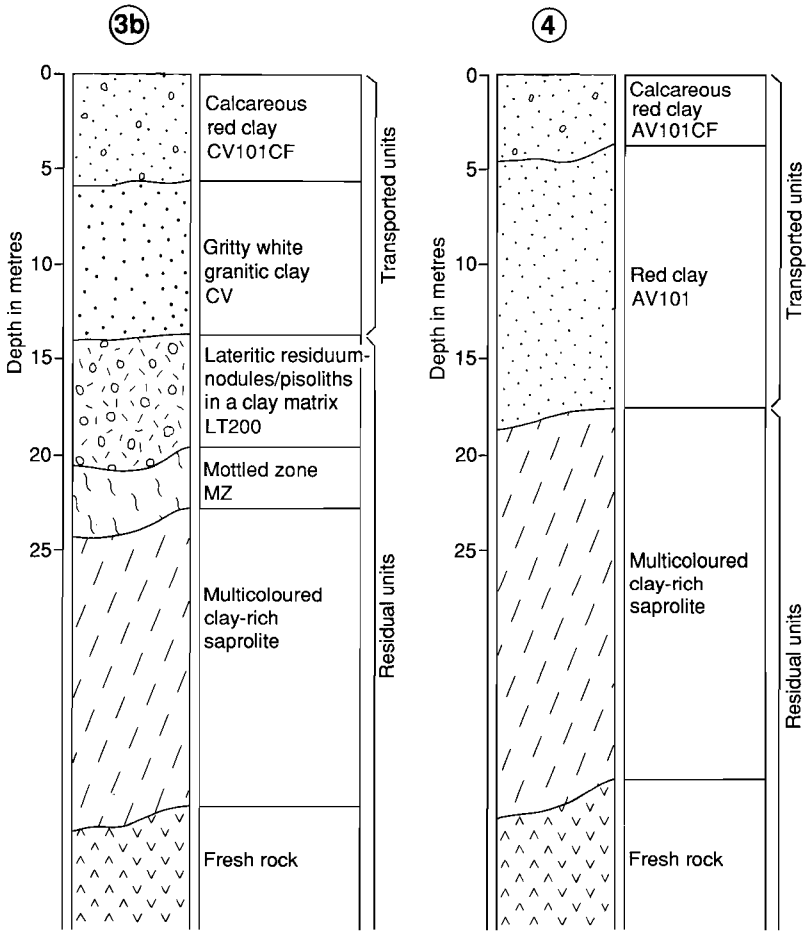

Fig. 10 Contd. Generalized regolith-landform facies model based upon the Mt. Gibson district.

5.0 STRATIGRAPHY, MINERALOGY, AND GEOCHEMISTRY OF REGOLITH UNITS AT MIDWAY NORTH

5.1 Regolith

The regolith at the Midway North Pit relates closely to the erosional and depositional modification of a deeply-weathered mantle (see Fig. 6). The regolith of the depositional regime is exposed in the S and W walls of the pit. The E wall provides an example of regolith of an erosional regime.

The depositional regimes at Midway are characterized by acid red earths (50-80 cm) overlying hardpanized colluvium (Figs. 11, 12). The hardpanized colluvium ranges in thickness from 2.5 to 10 m. A thick body (8-10 m) of hardpanized silty colluvium appears near the N end of W wall and continues N of the pit. The hardpanized colluvium overlies pisolitic-nodular lateritic residuum which is present as an almost continuous horizon, varying from 2 to 4 m thick. In places introduction of silica cement has modified the lateritic residuum resulting in a coarsely-laminated appearance. Lateritic residuum merges at depth to a mottled zone (2-4 m thick), thence to a clay-rich saprolite which in turn merges into a fresh mafic bedrock. Areas of calcareous clays occur where erosion has removed the lateritic residuum and mottled zone. In these areas (eastern face of the pit), calcareous clays merges at a depth of 3-4 m to plastic, non-calcareous red clay (Fig. 13). Large pockets of soft carbonates occur within the upper 3-4 m of the surface. However, zones of hard carbonate nodules may also be widely distributed in calcareous clays. Beneath the non-calcareous red clay is a saprolite, which itself merges at depth to a bedrock.

Soils

The *acid red earths* overlying hardpanized colluvium are friable sandy clay loam containing abundant fine quartz and small amounts of black ferruginous gravels. The red earths are formed from colluvium and show very little or no development of A and B horizons. *Calcareous clays* are friable, pinkish, with soft powdery carbonates dispersed throughout the whole soil matrix. *Acid plastic clays* which form the substrate to calcareous clays are red, clayey and contain moderate amounts of black 2 to 4-mm ferruginous granules. The clay substrate is very plastic and has a neutral or mildly acid pH. Plastic red clays are residual soils and are the result of weathering of the underlying leached saprolite.

Hardpanized Silty and Gravelly Colluvium

Hardpanized colluvium is commonly present beneath the red friable earths at depths of 50 to 100 cm and is brittle, dull, earthy, porous, silicified, red to dark red or red-brown in colour (2.5 YR 4/6-4/8). The hardpans are coarsely laminated on a scale of 1 to 5 cm thick. Some of the horizontal and vertical partings can be coated with very fine silica. Accumulations of black Mn oxides are characteristic and can occur on subhorizontal partings and on vertical hardpan fracture surfaces. The hardpan is developed within layers of silty or gravelly colluvium which reaches 10 m in thickness. The gravelly colluvium contains abundant fine quartz and black lateritic nodules, clay pisoliths, and few lithorelics. Silty units occur throughout the hardpan unit and dominate the top 1-4 m of the hardpan where nodular lenses are rare. The nodular gravel occurs as lensoid beds which typically reach 5 to 15 cm in thickness.

Lateritic Residuum

Lateritic residuum is pisolitic, nodular, or, more rarely, fragmentary, it is either weakly-indurated or more strongly-cemented as duricrusts. The pisolitic-nodular duricrust comprises abundant black to reddish brown hematite-rich nodules and pisoliths set in a pale to reddish brown matrix (Fig. 14A). Pale coloured patches also suggest local mobilization of Fe from those areas. Nodules are generally subrounded to irregular with a diameter from 3-10 mm. Angular and platy shapes of nodules are also common in some samples. These nodules/pisoliths are well defined against a very porous kaolinite-rich matrix by their yellowish brown cutans which are up to 0.5 mm thick. The porous matrix also contains abundant clay balls which are either Si-rich or Si-Al-rich.

In the southern wall of the pit pisolitic-nodular duricrust laterally merges with fragmentary duricrust. It consists of large (20-30 mm) angular, brown, hematite-rich fragments of ferruginous saprolite in which relict fabric, such as foliation remains set in a yellow to reddish brown, kaolinite/Si-rich sandy matrix. The large fragments may have a reticulate mottling and have thin (0.5 mm) yellowish cutans. Smaller fragments, in the 5 to 10-mm range, are somewhat rounded, and consist of yellowish to reddish brown hematite/goethite-rich materials.

Mottled Zone
This zone is transitional between the saprolite and the lateritic residuum. It comprises red, 5 to 10-mm mottles in a pale grey kaolinite-rich matrix (Fig. 14B). Mottling is due to discrete, local accumulations of hematite cementing the clayey matrix. In some samples a few incipient pisoliths were also developed within the mottling. The upper part of this zone lacks bedrock primary structures, but relict primary structures are recognizable at lower levels.

Saprolite
The saprolite forms a broad zone 30-40 m thick. The transition from unweathered to weathered rock occurs at the base of the pit at about 40 m depth. The saprolite becomes softer and increasingly clay-rich towards the surface. The saprolite is commonly friable and retains primary fabric of the parent rock. The clays are normally grey to green in colour. Pockets of reddish-brown ferruginous saprolite occur within the saprolite at a depth of about 30-35m. In this study, saprolite is designated to all that weathered material beneath the mottled zone to saprock.

5.2 Mineralogy and Geochemistry of Regolith Units

At Midway, four vertical profiles typical of the depositional and erosional regimes were sampled to assess the variations in mineralogical and geochemical response according to the regolith units sampled. A total of 25 samples representing various regolith units has been analysed for 30 elements. Data on individual samples are shown in Appendices I and II. Mineralogical and geochemical compositions for three of the profiles correlated with detailed logging are shown in Figs. 11, 12, and 13. Methods of analysis are given in Table 2.

(Profiles 1, 2 and 4 from the depositional regime - see Figs. 6A,B and 7A)
Acid red earth in colluvium
Acid red earths largely consists of quartz and kaolinite with small amounts of hematite, goethite, and feldspars. The presence of feldspars suggests a saprolitic origin, and the feldspars may have been mechanically introduced by colluvial transport.

Silica in the form of quartz is a major constituent and decreases down the profile. Aluminium oxide and Fe_2O_3 occur in small amounts and generally increase with depth. Minor amounts of K_2O (0.38-0.61%) occur as muscovite and feldspars. The levels of Cu, Pb, As, Ag, Sb, and Bi are depleted in red earths relative to the underlying regolith units. Gold values are anomalous (to 74 ppb) but low and are believed to have been mechanically introduced by colluvial transport.

Hardpanized Colluvium
Hardpanized colluvium is dominated by quartz and kaolinite with small amounts of hematite, goethite, feldspars, and mica. In gravelly colluvium, hematite becomes the dominant mineral reflecting the presence of hematite-rich lateritic nodules.

Silica contents of hardpanized colluvium are lower than in the red earths; Al_2O_3 and Fe_2O_3 contents are relatively higher than in the red earths reflecting the presence of kaolinite and hematite/goethite-rich lateritic nodules/pisoliths. Hardpanized colluvium shows significantly higher values of Cu, Pb, Zn, As, and Ag than the red earths. Manganese values peak in this unit reaching values of up to 700 ppm, a function of pedogenic processes. This enrichment is often visible in exposed field profiles, manifested in coatings of black Mn oxide on ped surfaces. Gold values are significantly high (100-230 ppb).

Lateritic Residuum
Iron oxides (hematite, goethite, maghemite) and kaolinite constitute the two mineral phases, both can represent about 60-80% of total. Among the Fe oxides, hematite is the dominant mineral.

Table 2. Analytical methods and lower limits of detection

Element	Reported as	Method	Detection Limit
SiO_2	wt%	ICP	0.2
Al_2O_3	wt%	ICP	0.04
Fe_2O_3	wt%	ICP	0.03
MgO	wt%	ICP	0.004
CaO	wt%	ICP	0.007
Na_2O	wt%	ICP	0.007
K_2O	wt%	ICP	0.06
TiO_2	wt%	ICP	0.003
Mn	ppm	ICP	15
Cr	ppm	ICP	20
V	ppm	ICP	5
Cu	ppm	AAS	2
Pb	ppm	XRF	2
Zn	ppm	AAS	2
Ni	ppm	AAS	4
Co	ppm	AAS	4
As	ppm	XRF	2
Sb	ppm	XRF	2
Bi	ppm	XRF	2
Mo	ppm	XRF	1
Ag	ppm	AAS	0.1
Sn	ppm	XRF	2
Ga	ppm	XRF	4
W	ppm	XRF	4
Ba	ppm	ICP	5
Zr	ppm	ICP	5
Nb	ppm	XRF	2
Se	ppm	XRF	2
Be	ppm	ICP	1
Au	ppm	Graphite furnace AAS Aq req.	0.001

ICP = inductively coupled plasma optical spectroscopy, Si, Al, Fe, Ti, Cr, V after an alkali fusion, others after $HCl/HClO_4/HF$ digestion.

XRF = X-ray fluorescence

AAS = Atomic absorption spectrophotometry, after $HCl/HClO_4/HF$ digestion

Profile 1

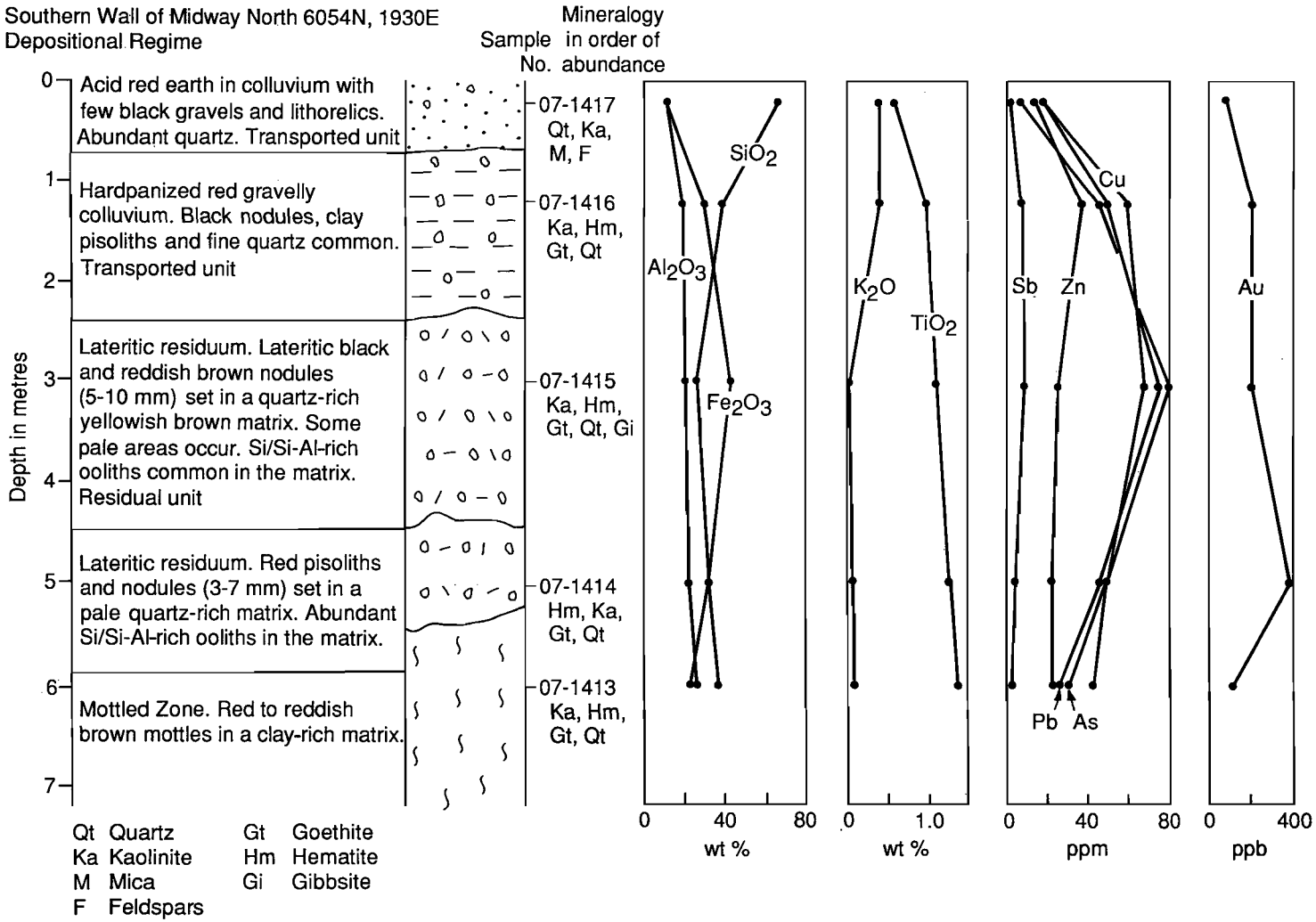

Fig. 11. Vertical profile showing the stratigraphy, mineralogy, and geochemistry of regolith units for the depositional regime.

Profile 2

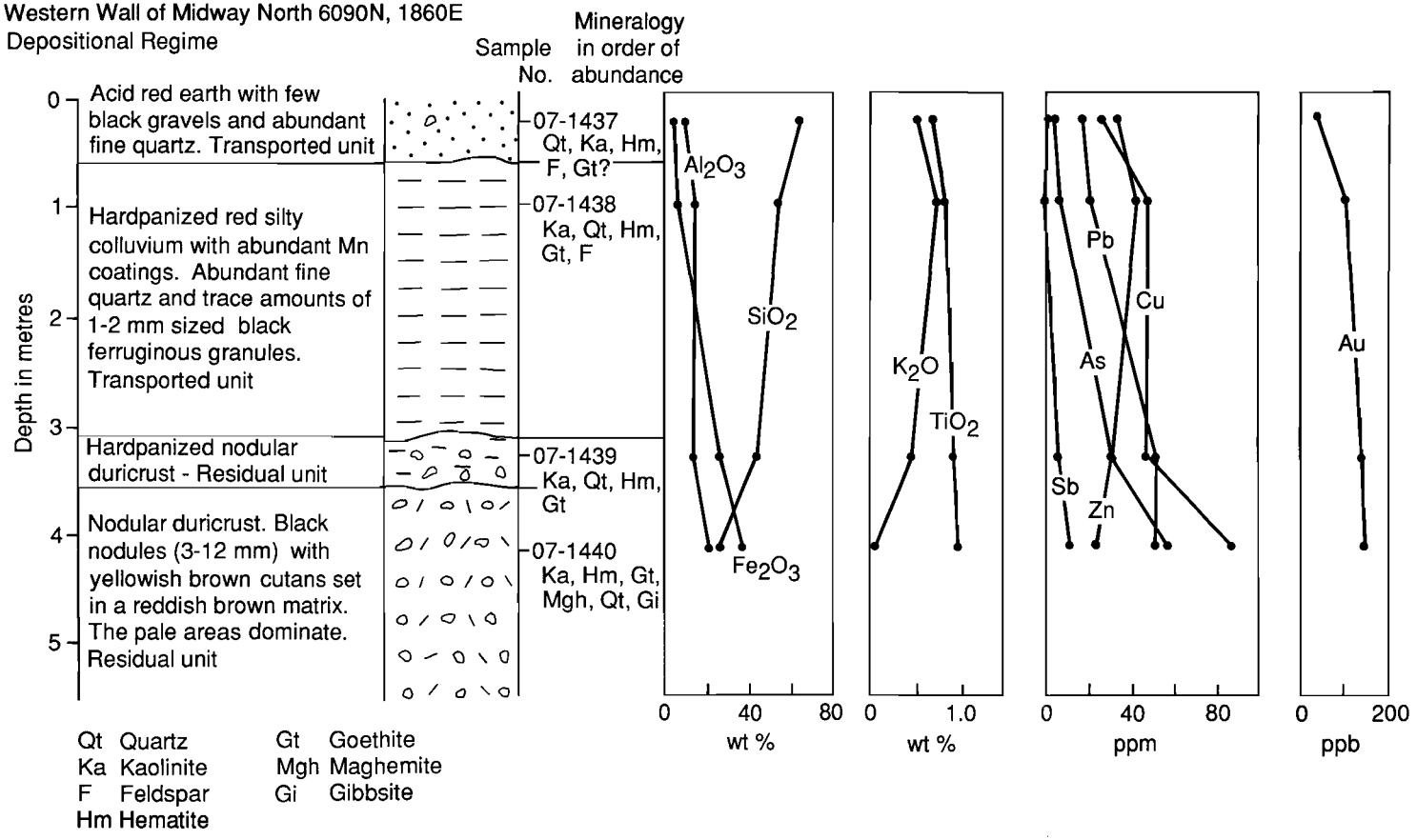

Fig. 12. Vertical profile showing the stratigraphy, mineralogy, and geochemistry of regolith units for the depositional regime.

Profile 3

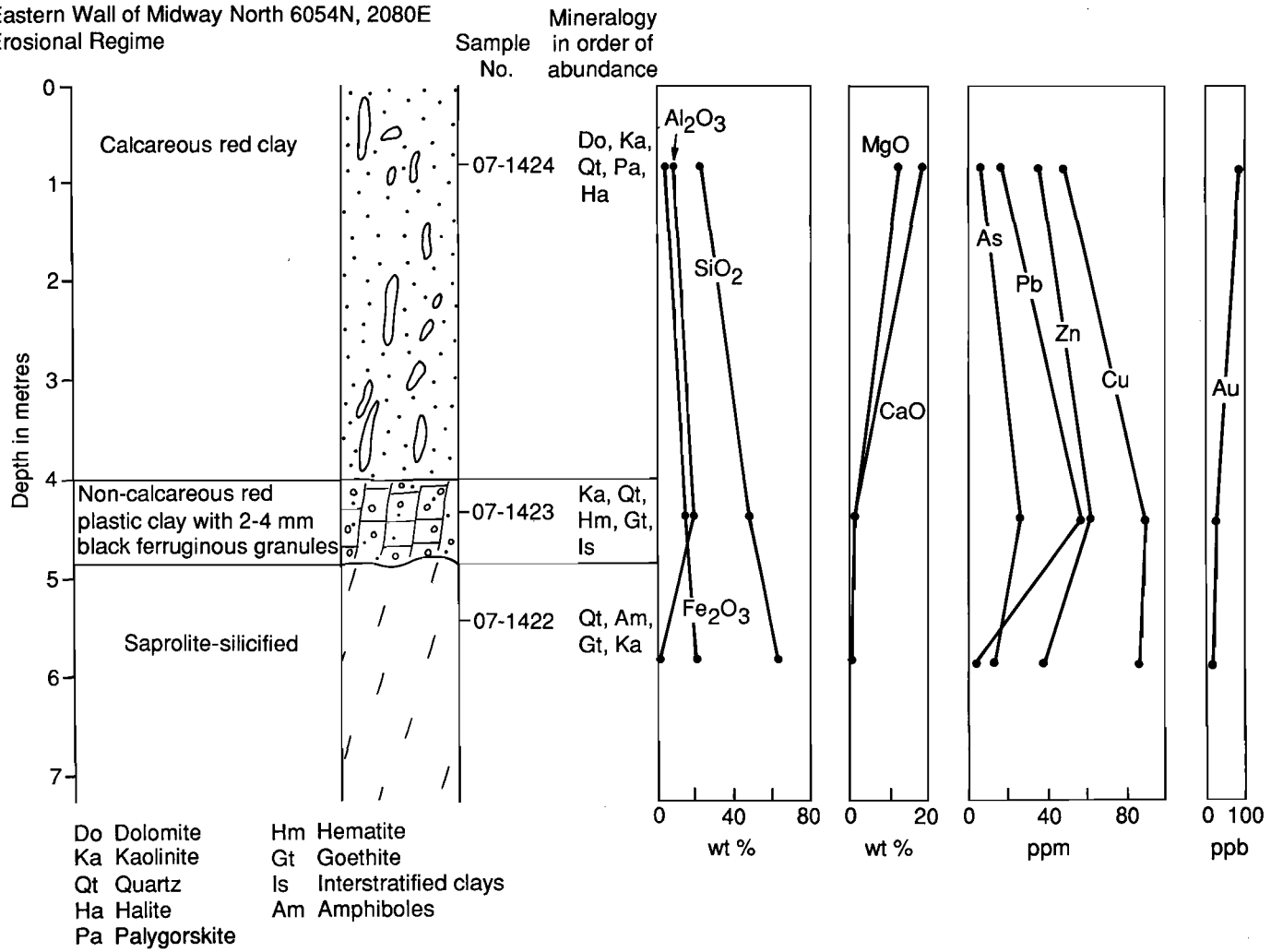

Fig. 13. Vertical profile showing the stratigraphy, mineralogy, and geochemistry of regolith units for the erosional regime.

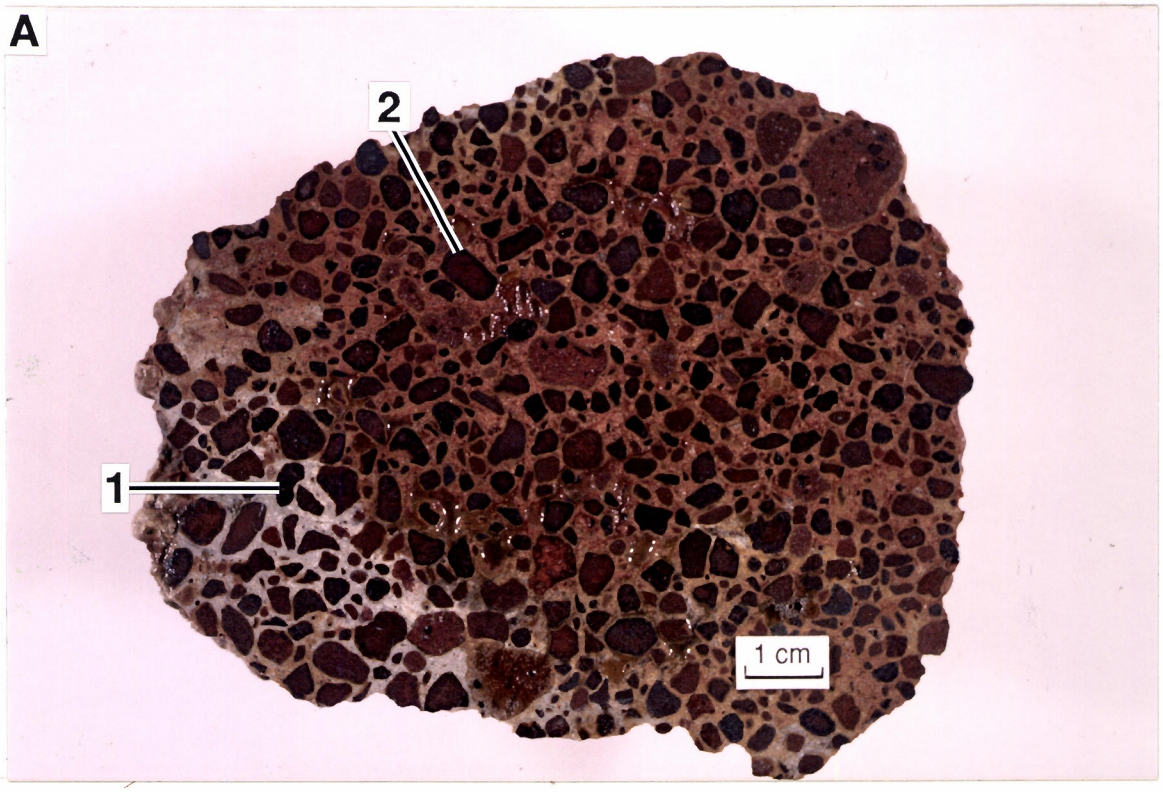

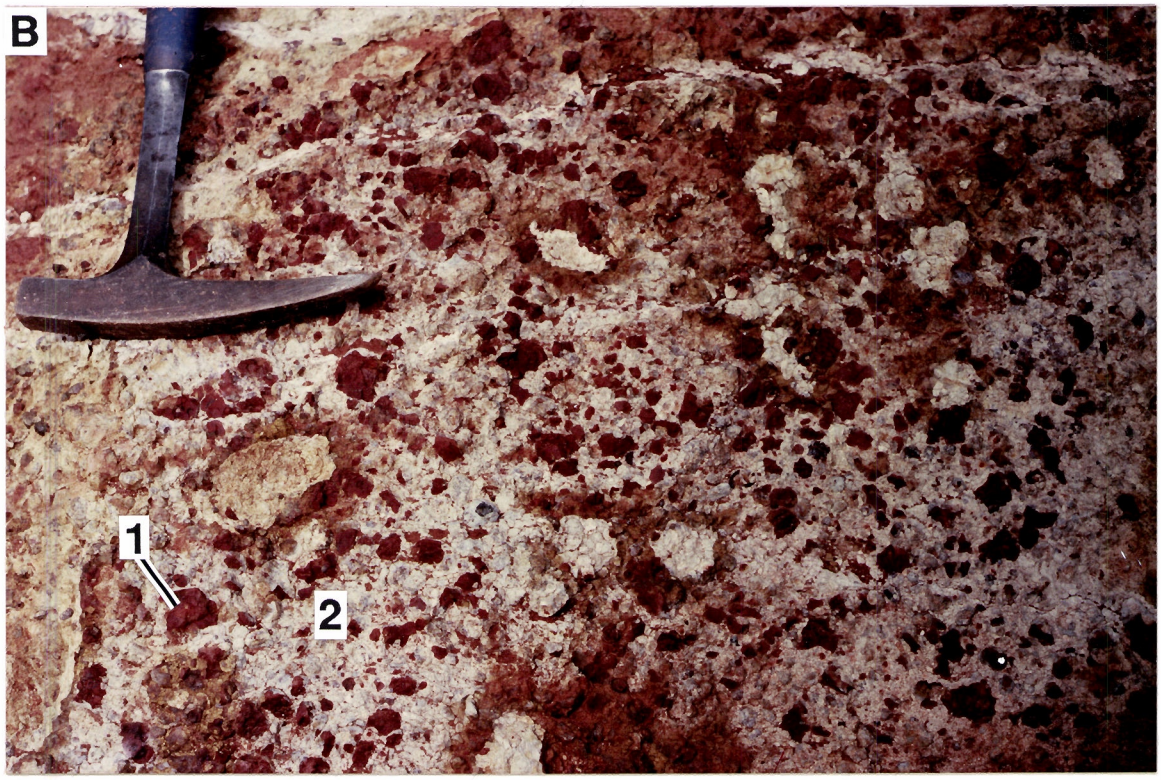

Fig.14A. Slice through a nodular duricrust showing irregularly-shaped reddish brown hematite-rich nodules (1), platy shaped nodules (2) set in a kaolinite-rich matrix, Location southern wall of Midway North Pit, Profile No.1, Sample No.07-1414.

Fig.14B. Field photograph of mottled zone showing dark reddish brown mottles (1) set in a white kaolinitic matrix (2), Location southern wall of Midway North Pit, Profile No.1.

Quartz is also present in significant amounts. Gibbsite occurs in small amounts in residual laterite. The restricted amounts of gibbsite in the material probably reflecting the semi-arid environment where the leaching conditions are not optimum for desilification.

Aluminium substitution in goethites ranges between 15-18 mole %. The kaolinite present in nodules and pisoliths is generally poorly crystalline.

This regolith unit differs from the overlying transported sedimentary unit in having a lower SiO_2 content but higher Fe_2O_3 and Al_2O_3 contents. Higher Fe_2O_3 and Al_2O_3 concentrations are associated with the occurrence of hematite and kaolinite. It is interesting to note that hardpanized lateritic residuum contains higher concentrations of SiO_2 than the lateritic residuum reflecting the presence of amorphous Si. Magnesium, Ca, Na and K are strongly leached. Titanium is concentrated in lateritic residuum (to 1.29% TiO_2) and is present as secondary anatase and primary rutile. Lateritic residuum has higher values of Cr and V than the overlying transported regolith units. Chromium can substitute for Fe^{3+} in goethite because of a similar ionic radius and therefore can concentrate in Fe-oxide-rich materials. The values of chalcophile elements excluding Zn are much higher in lateritic residuum than in the overlying transported regolith. The trace elements (Cu, Pb, As) and Au appear to follow the Fe_2O_3 curve (See Fig. 11 and 12) suggesting these elements may be associated with secondary Fe-oxides. The concentrations of Mo, Sn, Ge, Se, and Be are very low. The occurrence of high metal values in the pisoliths/nodules of lateritic residuum render them amenable to the multi-element exploration approach (Smith, 1987).

Mottled Zone
The mottled zone largely consists of kaolinite, hematite, quartz, and goethite. The grey matrix consists of kaolinite and quartz while the red mottles contain hematite and goethite. Gibbsite was not detected in the mottled zone. Goethite contains about 13 mole % Al.

Iron is less abundant in the mottled zone than in the lateritic residuum. The trace elements including Cu, Pb, Zn, and As, are depleted relative to the values of these elements in lateritic residuum. Gold levels are relatively low (120 ppb).

Lower Saprolite
In these profiles, upper saprolite is an equivalent to mottled zone, and therefore samples of upper saprolite were not collected.

Kaolinite, quartz, goethite, and hematite are present in saprolite. Kaolinite is the most abundant of these four minerals. Smectite is also present, but in small proportions only. Significant amounts of unweathered feldspars and ferromagnesian minerals can also be present. Aluminium substitution in goethite ranges between 3-8 mole %. Kaolinite is generally well crystalline.

Major element chemistry of saprolite can be expected to vary according to parent rock type and the intensity of weathering. The saprolite has large contents of SiO_2 and lower contents of Al_2O_3 and Fe_2O_3 (Appendix II). Magnesium (to 4.31% MgO) and sodium (to 2.67% Na_2O) can be present in appreciable amounts. Pockets of ferruginous saprolite occur within the saprolite at a depth of about 30-35 m; these are characterized by higher concentrations of Fe_2O_3 (to 26.5%) relative to the adjoining white clay-rich saprolite (to 9.40%). Iron in ferruginous saprolite occurs as hematite and goethite. The saprolite shows significantly-higher values of Cu (to 400 ppm), Pb (to 480 ppm), Zn (to 630 ppm), As (to 300 ppm), and Bi (to 125 ppm). In general, high values of these elements occur in ferruginous saprolite. High values of Au (to 1180 ppb) are associated with higher values of Pb, Zn, As, and Bi; however, the range of Au levels in saprolite is large (2 to 1900 ppb).

(Profile 3 from the erosional regime - See Figs. 6A and 7B)
Calcareous Clays
The principal minerals in the calcareous clays are dolomite, quartz, kaolinite, and palygorskite. Small amounts of calcite and halite are present.

Calcium oxide, MgO, and SiO_2 are the major components of calcareous clays. Calcium and Mg occur in the form of dolomite. Most chalcophile elements Cu, Pb, Zn, and As are relatively low in abundance compared with the underlying acid red plastic clays, but Au is significantly higher (88 ppb). The lowest Au concentration occurs at the base of the profile sampled, at a depth of 5 m.

Acid Red Plastic Clays
Red clays underlying calcareous clays are dominated by kaolinite and quartz with small amounts of hematite, goethite, smectite, and mixed layer minerals. In contrast, black ferruginous granules separated from these clays largely consist of hematite and goethite, with small amounts of maghemite, kaolinite, and quartz.

Silica, Al_2O_3, and Fe_2O_3 are the major components of red clays. These elements are much higher in acid red clays than in calcareous clays. High levels of these elements are reflected in the presence of significant amounts of kaolinite, quartz, and hematite. Chalcophile elements are relatively more abundant in acid red plastic clays than in calcareous red clays suggesting an association of these elements with Fe-oxides. Copper and Zn are even more abundant in acid red clays than in lateritic residuum. The gold level however is low (28 ppb).

Upper Saprolite
The upper saprolite largely consists of quartz, amorphous silica, and goethite.

This saprolite is extensively silicified. Aluminium is present in very small amounts. Iron occurs as goethite. Goethite contains about 9 mole % Al. All the trace elements analysed including Cu, Pb, Zn, As, and W are low in abundance. Gold levels are very low (16 ppb).

5.3 Conclusions on the Midway North Area

- The regolith relationships for the Midway North area relate closely to the erosional and depositional modification of the deeply-weathered mantle. Lateritic residuum 1-3 m thick-forms a continuous blanket beneath the transported hardpanized colluvium.

- Systematic mineralogical and geochemical differences occur between transported and residual regolith units. The colluvial units contain higher amounts of kaolinite and quartz relative to the underlying lateritic residuum. The colluvial units also contain minor feldspar.

- Hematite (with maghemite) increases upwards in the weathering profile. Goethite rather than hemaite is the more common Fe-oxide in saprolite. The Al content in goethite also tends to increase towards the top of the residual profile.

- The kaolinites present in the lateritic residuum are generally more poorly-ordered than the kaolinites forming in the deeper layers where the structure of the parent rock is preserved.

- The lateritic residuum at Midway, in comparison with the upper saprolite and mottled zone, is enriched in Au, Cu, Pb, Zn, As, W, and Ag which are associated with secondary Fe-oxides. These elements are less abundant in the red earths and calcareous clays.

- The upper saprolite is depleted compared with the lower saprolite in Au and chalcophile elements.

- Gold levels in the red earths (41-88 ppb) and calcareous clays (88 ppb) are low but are anomalous.

6.0 CALCAREOUS CLAYS AND CALCRETES

6.1 Introduction

One of the characteristics of the widespread, thick red clay regolith units in areas with arid or semi-arid climate in the Yilgarn Block is the development of carbonates within soil profiles. Some workers (e.g. Lintern, 1989) have shown that the Au in these red clays is intimately associated with the carbonates. They believe that the association between Au and pedogenic carbonates is of more recent origin, related to weathering under recently-imposed semi-arid climates. Furthermore, Au accumulation in carbonates is probably related to cycling of Au and Ca by vegetation. Certain authors have pointed out that the development of such carbonates affects the contents and locations of those metallic elements including Au that either formed a pre-existing geochemical anomaly and could be detected before the formation of such calcretes (Briot, 1978; Guedria, 1981) or that are forming an anomaly through a calcrete crust (Garnett *et al.*, 1982). Such a phenomenon could have a major impact on geochemical soil exploration, as it introduces modifications that threaten to compromise the interpretation of geochemical surveys. The mode of the formation of carbonates, however, is not well understood and the mode of formation may be important in explaining the nature and origin of certain geochemical anomalies. Carbonates originate from several sources or combination of sources, either directly in the form of carbonates, or by a solution precipitation mechanism. Several mechanisms, including dissolution of Ca-bearing minerals, mineralization of plant materials, transport by wind, rain and ground water have been put forward by many workers. To investigate which of these mechanisms applied at the Mt. Gibson mine, a scanning electron microscopic study of calcareous clays and nodular calcrete was carried out. This report presents the preliminary work on the origin of carbonates.

The morphology of the calcrete varies significantly according to the position of the weathering profile in the landscape. The major facies of carbonates are illustrated in Fig. 15. In the depositional regimes, carbonates are present in a number of forms including powdery carbonates, nodular/platy calcrete, calcrete pods, and calcrete sheets. Powdery carbonates and nodular calcrete occur beneath the acid/calcareous red earths and may contain transported lateritic pisoliths and nodules which are calcified (Fig. 15A). Powdery carbonate is loose, finely-divided carbonate and lacks any nodular development. Nodular calcrete is typically composed of coarsely platy/irregular, white to pinkish nodules, varying from 1 to 5 cm in diameter, set in a loose calcareous soil matrix. The calcrete horizon can be up to 1.5 m thick and is commonly underlain by lateritic residuum at the S, C, and N Pits. Calcrete pods and calcrete sheets occur beneath or within hardpanized colluvium as indurated horizons which show evidence of having partially- to completely-replaced regolith materials (Fig. 15B).p

Calcareous clays up to 2 m thick occupy the erosional regimes dominated by mafic lithologies (Fig. 15C). These soils are underlain by acid red plastic clay which in turn overlies saprolite. Such is the case at Midway North and the western ends of S, C, and N Pits. Carbonates in calcareous clays occur as coatings or stringers on soil matrix.

6.2 Morphology

The morphology of carbonates is variable. On the basis of observations of samples collected from several profiles, it appears that the *needle-fibre calcite* occurs frequently in nodular calcrete from the depositional regime (Fig. 16). This morphology was not observed in the calcareous clays overlying plastic red clays from the erosional regime. Here euhedral *rhombohedral crystals of dolomite* and *calcite* occur (Fig. 17).

The morphology of needle-fibre calcite is related to calcified remains of fungi, algae, root hairs and bacteria (Phillips *et al.*, 1987; Klappa, 1979). The calcified filaments are concentrated in dense mats or mycelia which are conspicuous with a hand lens or binocular microscope on nodular calcrete. The samples of needle-fibre calcite from the Mt. Gibson area may be divided into two distinct morphological groups, similar to those described by Phillips *et al.* (1987). The first morphological group of needle-fibre calcite consists of small single rods (Fig. 18A, B) or

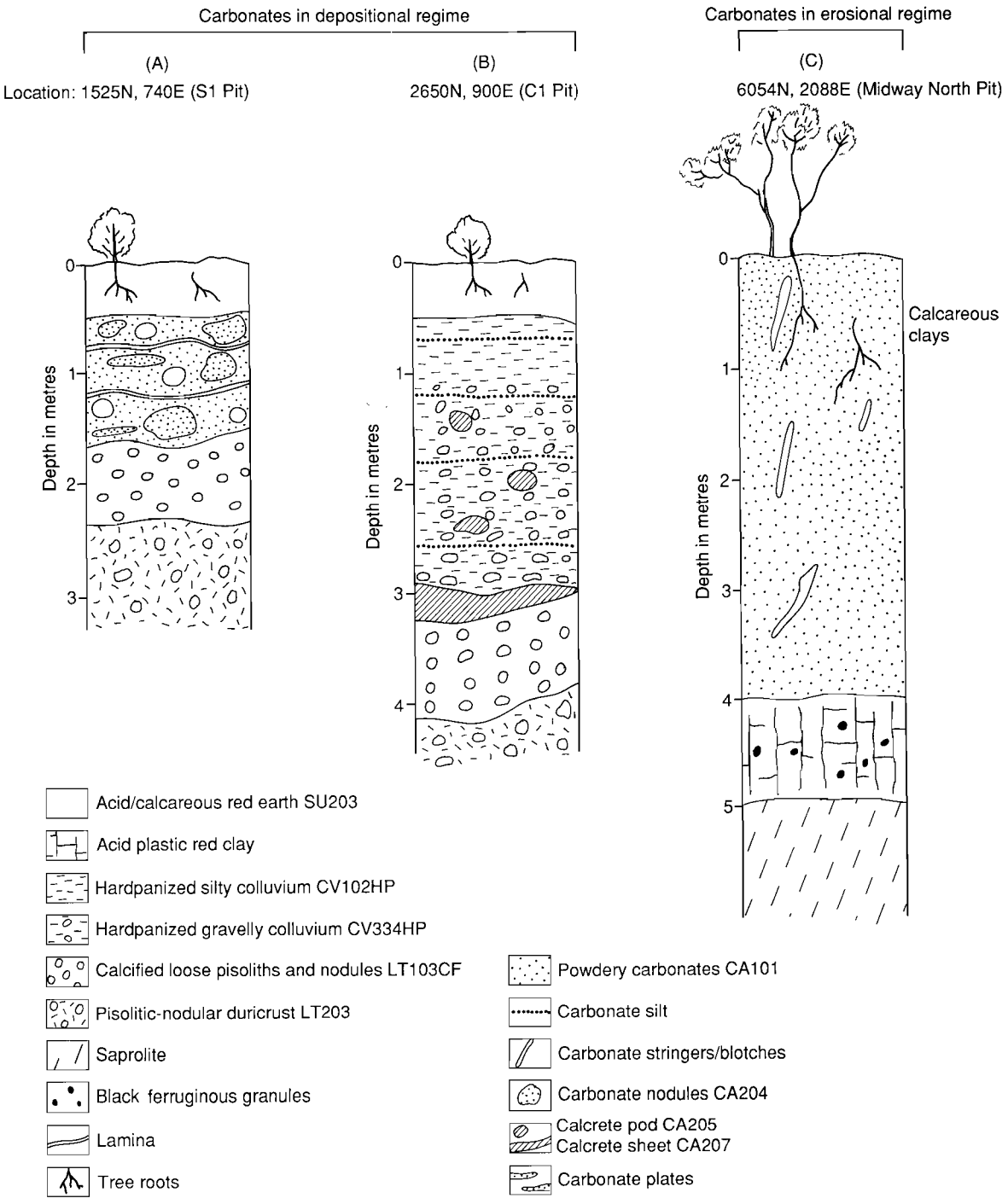

Fig. 15. Diagrams of calcrete profiles showing variation in morphology and facies.

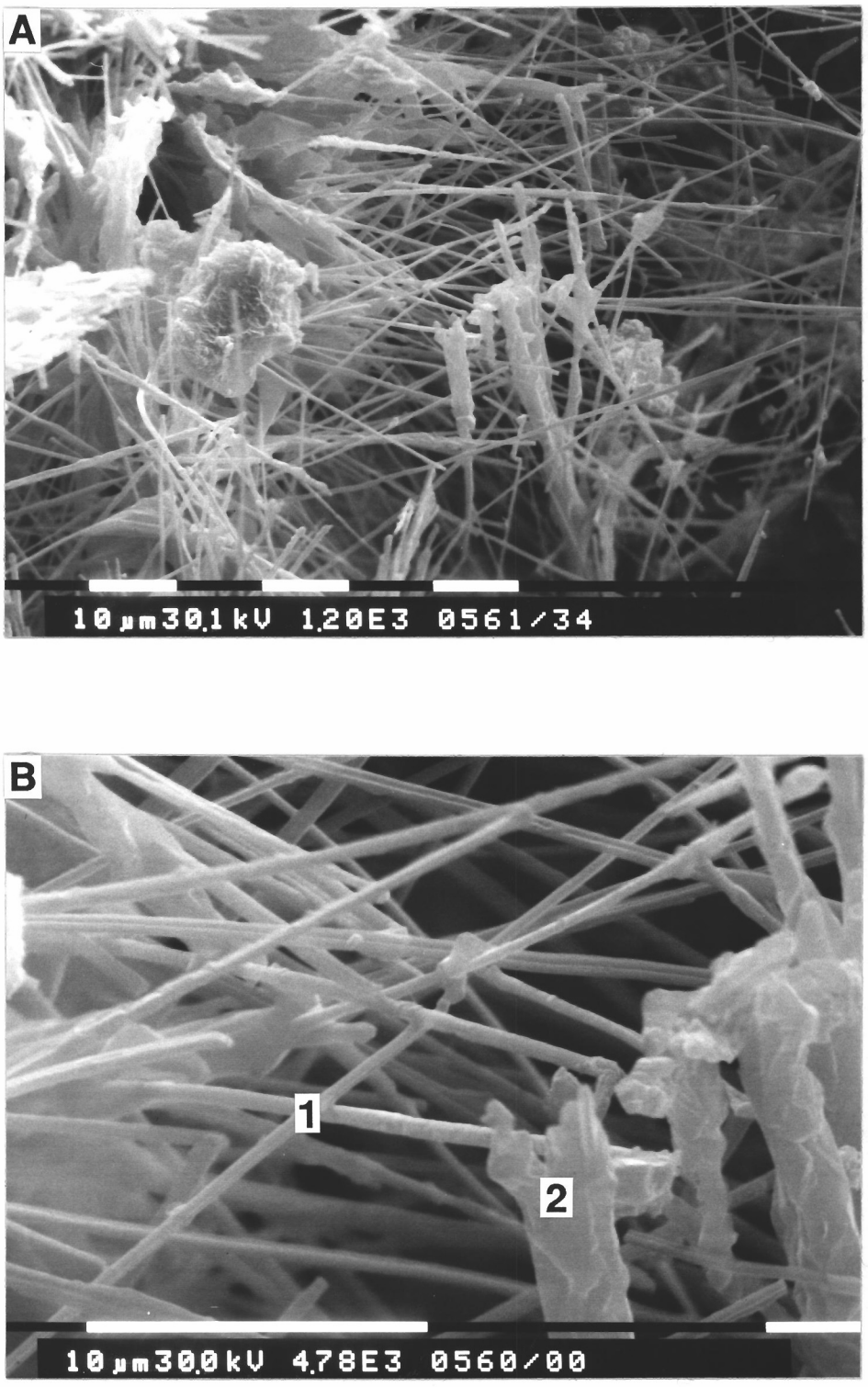

Fig.16. Low (A) and high (B) magnification scanning electron micrographs of carbonates from nodular calcrete (CA204) showing needle-like fibre crystals of calcite (1) and lath-shaped calcite crystals with saw-tooth edges (2), Location 1525N, 740E, Sample No.07-0504, S1 Pit.

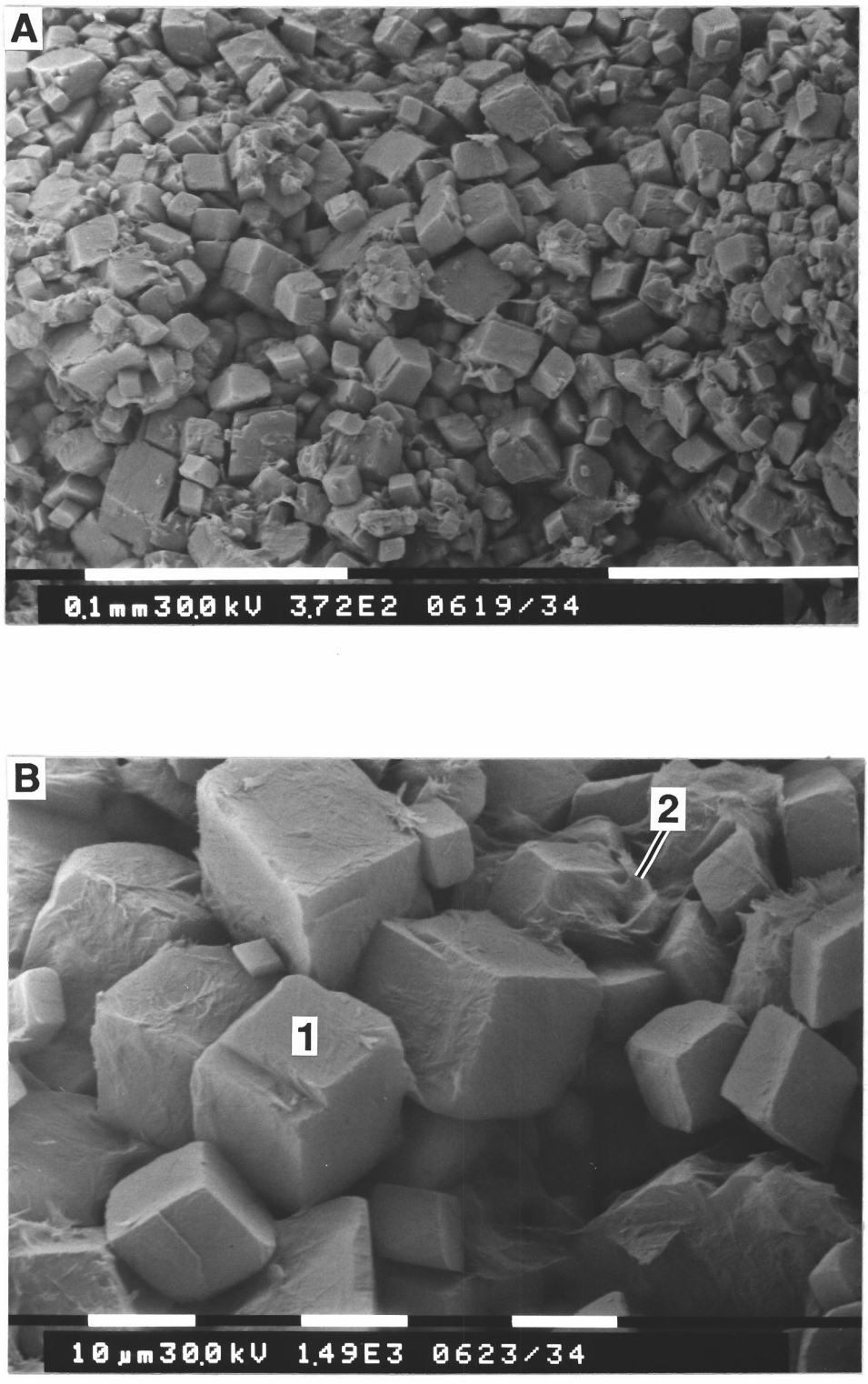

Fig.17. Low (A) and high (B) scanning electron micrographs of powdery carbonates from calcareous clays showing euhedral rhombohedral dolomite (1) and fibrous crystals of palygorskite (2) attached to the surface of dolomite, Location 6054N, 2088E, Sample No.07-1424, Midway North Pit.

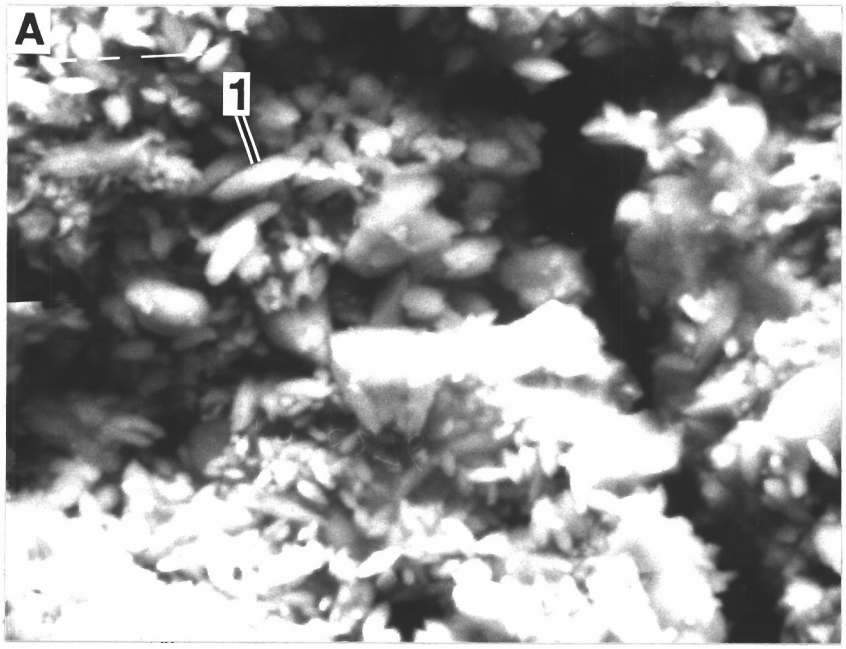

Fig.18A. Scanning electron micrograph of carbonates from nodular calcrete (CA204) showing rods of calcite (1), Location 1900N, 1100E, Sample No.07-0276, S2 Pit.

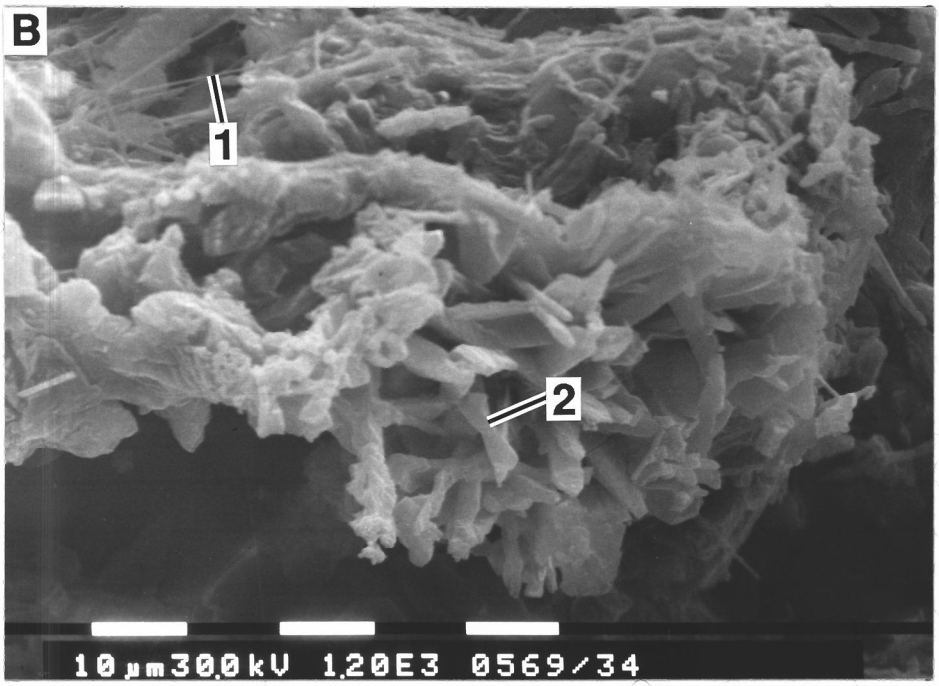

Fig.18B. Scanning electron micrograph of carbonates from nodular calcrete (CA204) showing needle like fibre crystal (1) and rods/platy crystals (2) of calcite, Location 1525N, 740E, Sample No.07-0503, S1 Pit.

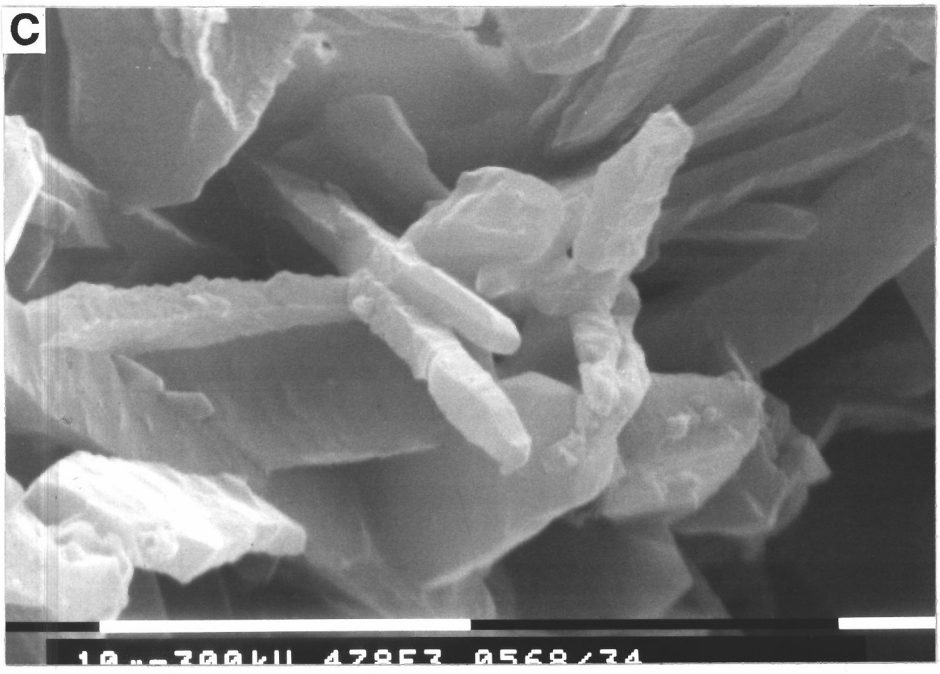

Fig.18C. Scanning electron micrograph of carbonates from nodular calcrete showing laths of calcite with saw tooth edge, Location 1525N, 740E, Sample No.07-0503, S1 Pit.

microrods. The micro rods are up to 20 μm in length. They have rounded terminations and may be straight or curved along their length.

Needle-fibre calcite in the second morphological group has a much larger size than the micro-rods of the first group (Fig. 16). Needles have lengths from 20 μm to 160 μm and vary in width from 0.5 to 2 μm depending upon the rods that make up the fibre. These needle-fibres may be straight or curved. Branching is common, with short subsidiary filaments or extensive ramifying networks. In the needle-fibre group, elongated laths with serrated edges are also common. Relatively flat serrated laths are 5 to 25 μm long, 2 to 5 μm wide and are straight along their length with saw-tooth edges (Fig. 18C). The frequency of serration varies along the length of the lath.

The most common spatial arrangement of the second morphological group of needle-fibre calcite is a self-supporting random open mesh, infilling the centres of voids and root channels in weak to moderately-indurated nodular calcrete. Fibres composed of curved and straight rods up to 160 μm long are most frequent in the random open mesh.

In the calcareous soils, euhedral rhombohedral crystals of dolomite and calcite occur. These crystals range in diameter from 5 to 40 μm. Needle-fibre calcite crystals occur rarely in calcareous soils.

The dolomite and calcite crystals are sometimes coated with fibrous crystals of palygorskite $(OH_2)_4(OH)_2Mg_5SiO_8O_{20}4H_2O$ (Fig. 17B-2). Presence of palygorskite was confirmed by energy dispersive analysis of X-rays. Palygorskite occurs as dense mats which are up to 1 μm wide and 8 μm long. Palygorskite has been reported to be a common component of arid and semi-arid soils of Australia (Stace *et al.*, 1968). Its formation is favoured by high pH and high Mg^{2+} and $Si(OH)_4$ concentrations. Its origin and significance are discussed below.

6.3 Origin of the carbonates

The morphology of the carbonates provides the main clue for the mechanism of their formation, the two distinct morphologies suggest two modes of formation. Euhedral rhombohedral crystals of dolomite and calcite in calcareous clays suggest their inorganic precipitation from solution. In contrast needle-fibre crystals in nodular calcrete suggest the role of biological agencies in the carbonate accumulation process.

Carbonates in the erosional regimes

As discussed above, several mechanisms for the formation of pedogenic calcrete have been proposed. The *in situ* model of forming carbonates from the weathering of underlying mafic lithologies is inappropriate for the Mt. Gibson area, as there are no weatherable Ca and Mg minerals present in an already highly-weathered regolith. Furthermore, this is supported by the formation of acid red plastic clays which are strongly leached as indicated by the low base status and large amounts of kaolinite. This suggests that these carbonates are not formed from the weathering of underlying lithologies. However, scattered pockets of fresh mafic rocks occur in the erosional areas which may on weathering provide Ca and Mg-rich solutions that could infuse the upper parts of the regolith. Several workers (e.g. Stace *et al.*, 1968) also believe that the carbonates in calcareous red clays are aeolian in origin. The occurrence of alkali and alkaline earth elements as aerosols with rainfall has been well established (Hingston and Gailitis, 1976). It is possible that the materials containing alkali and alkaline elements are transported some distance, perhaps from Lake Karpa, by wind, and are deposited on the surface as dust or in rain. Subsequent relocation within the soil by solution and reprecipitation is possible.

Palygorskite is known to occur in close associations with carbonates in lacustrine environments of semi-arid to arid regions of Australia. It seems that pedogenic conditions leading to carbonate formation are also favourable for palygorskite formation. These occurrences are associated with aquatic conditions characterised by alkaline solutions with high activities of Si and Mg. Such environments may be created by various combinations of factors. The most common environmental setting for lacustrine palygorskite authigenesis is playa deposits (Lake

Karpa). The high Mg and Si activities in this closed catchment are attributed to the concentration of ground water solutions by evaporation close to the surface, or to cyclic inundations and subsequent concentration of solutions by evaporation. The palygorskite formed in calcareous clays may have been derived from Lake Karpa. It has been shown to be transported long distances in the form of aerosolic dust and thus could have been introduced into calcareous clays from Lake Karpa.

Carbonates in the depositional regimes

The origin of carbonates in the depositional areas may have involved lateral transportation and redeposition of weathered fragments of calcrete derived from the erosional areas which are then dissolved and precipitated at the top of profile. The most commen form of calcrete is authigenic calcite precipitated from laterally moving groundwater. The introduced carbonates probably develop initially as a void filling and act as a chemical diluent. An initial period of diffuse accumulation is followed by the development of carbonate cutans, soft nodules, veins, etc. It is concluded that fluctuating high solubilities of carbonate minerals in the groundwaters have resulted in segregation and the development of secondary structures, the growth of which may displace existing material. An abundance of growth of authigenic carbonate results in disruptions, brecciation, and displacement of existing material.

Calcified filaments in the form of needle-fibre calcite suggest the part played by organisms in the deposition of calcite and the creation of nodular calcretes. The calcite forming the filaments has a variety of crystal habits; the nature of microcrystals is specific to each filament, but varies significantly between adjacent filaments. Phillips *et al.* (1987) demonstrated that calcretes from South Australia reveal a fossilized community of soil micro-organisms dominated by filamentous structures preserved in fine detail by calcite. There are various stages between the primary filaments and the calcite encrusted structures characteristics of calcretes, suggesting that *in vivo* biochemical processes dominate the mechanism of calcification. They further suggested that the organisms deposit calcite microcrystals within the mucilaginous sheath or in the cell wall (or both) as a detoxification mechanism in response to their highly calcareous environment.

7.0 SITING AND BONDING OF ELEMENTS AND DISPERSION PROCESSES

7.1 Introduction

The objectives of this research are to establish (a) the morphology of Au; (b) the siting and bonding of Au and the ore-associated elements within selected samples from various upper regolith units including laterite, hardpan, and carbonate units in order to establish any relationships of these elements to iron oxides, clay minerals, or carbonates; and (c) to complement petrographic studies on the types of nodules in lateritic environments. This research should lead to an improvement of geochemical exploration sampling methods, a better understanding of the mobility and behaviour of Au and chalcophile elements in weathering profiles, provide information on whether anomalies may exist from which Au is leached, but chalcophile elements remain, and aid the understanding of the genesis of nodules and the accompanying dispersion processes.

7.2 Laboratory Procedures

7.2.1 SAMPLING PARAMETERS

A total of 53 samples of various regolith units including soils, lateritic residuum, hardpanized colluvium (red-brown hardpan), and calcrete were collected from the S, C, and N Pits (Fig. 19). An example of a typical weathering profile is shown in Fig. 20. Samples of units within vertical profiles generally consisted of a 2.0-kg grab sample. Appendix III gives the locations (as AMG co-ordinates) for all the samples investigated, together with the analytical data. Field sheets record the regolith stratigraphy of the particular vertical profile and the depth at which samples were taken.

Clasts is used as a general term for an individual constituent or fragment produced by mechanical weathering of a rock mass or hardened regolith material, particularly in the granule, pebble or cobble size range. As used here, the term clast includes fragments of ferruginous saprolite, hardened mottles, as well as lateritic pisoliths and nodules. Other terms used in this report are taken from the *Terminology, Classifications and Atlas* of Anand *et al.*, (August, 1989).

7.2.2 SAMPLE SEPARATION

Bulk samples were split into three parts. One part was retained for reference, one was milled in an agate mill and submitted for analysis as a whole. The remaining third part was separated into morphological groups which were analysed separately. The separation procedure for each morphological group is shown in the flow chart (Fig. 21).

Magnetic and Non-Magnetic Gravel Fractions of Soils
Magnetic and non-magnetic gravel fractions were separated from soils. The substrate to the soils is hardpanized colluvium and/or lateritic residuum. Soils are red (2.5YR 4/8 to 4/6 moist) to orange (5YR 6/8 to 4/6 moist) and contain significant amounts of gravels. Soil samples were passed through a 2 mm sieve to separate the gravel (>2 mm) fraction. Vegetable matter and large stones were rejected. The plus 2-mm fraction was ultrasonically treated in water to remove the soil and fine organic debris attached to the surface of the gravels and dried at 50°C. The gravel fraction, which makes up between 17 and 76% of the soil and ranges in size from 2 to 15 mm (Table 3), was separated into magnetic and non-magnetic gravels using a hand magnet. Care was taken to discard the clay fragments, calcrete, and quartz fragments from the non-magnetic fraction. These fractions were weighed for some samples. The measurements showed that the non-magnetic fraction generally makes up about 50-70% of the gravel fraction.

The <2-mm fraction of the total was separated into sand (0.02 to 2 mm), silt (2-20 μm) and, clay (<2 μm) sized-fractions (Table 3). The sand-sized fraction, 51-70 wt%, largely consists of quartz and ferruginous granules. The clay fraction (22-44 wt%) is dominated by kaolinite, hematite, goethite, and quartz.

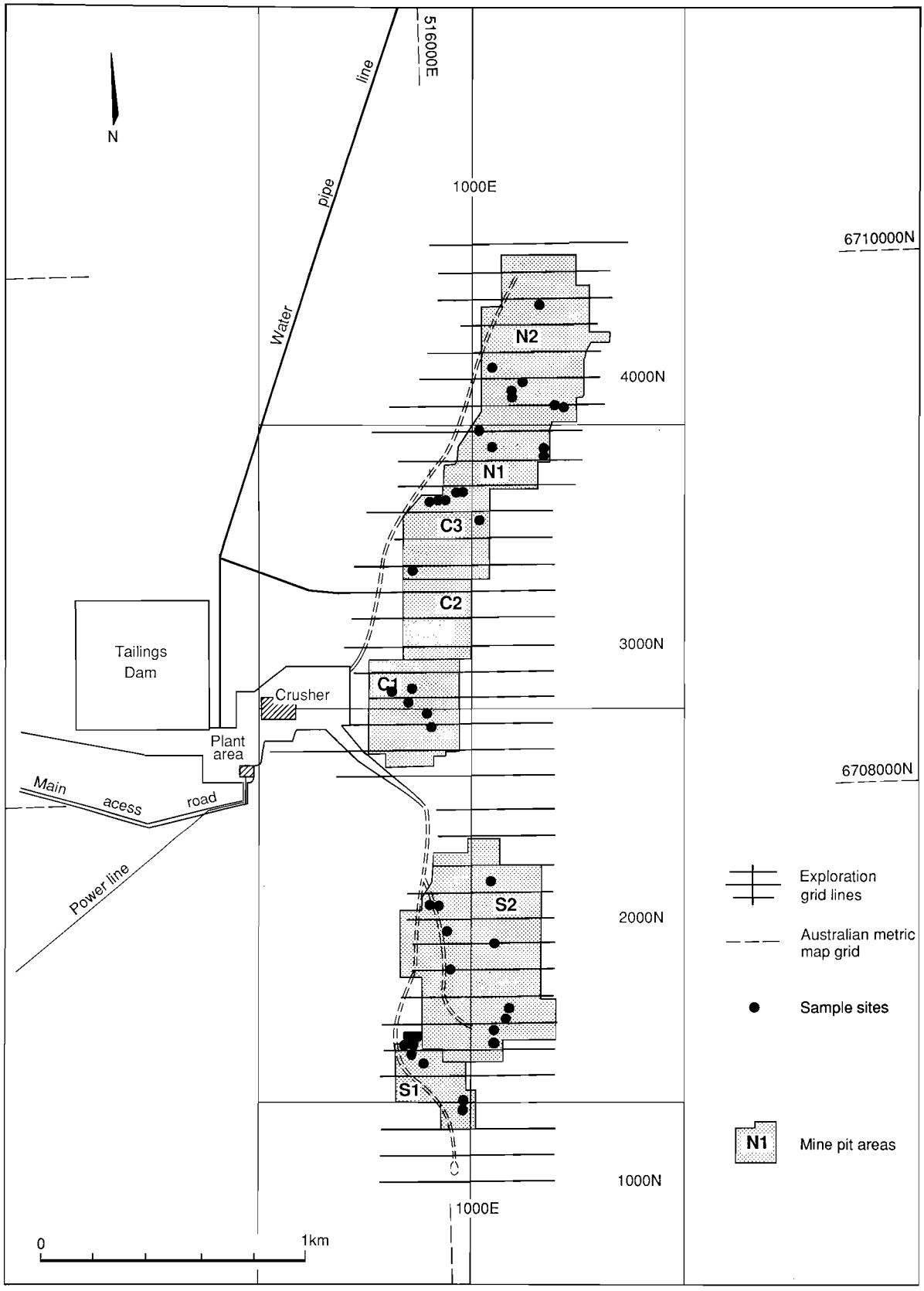

Fig. 19. Map of the Mt. Gibson orientation area showing the positions of the mine grid, open cut mining area, sample sites, and other features.

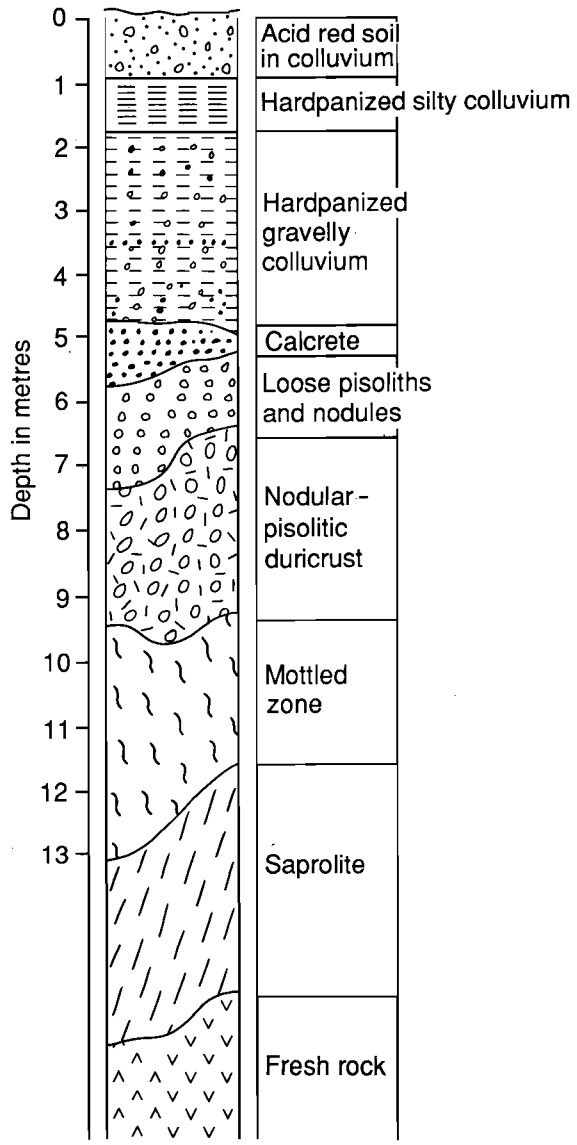

Fig. 20. Example of a typical weathering profile in the depositional regime.

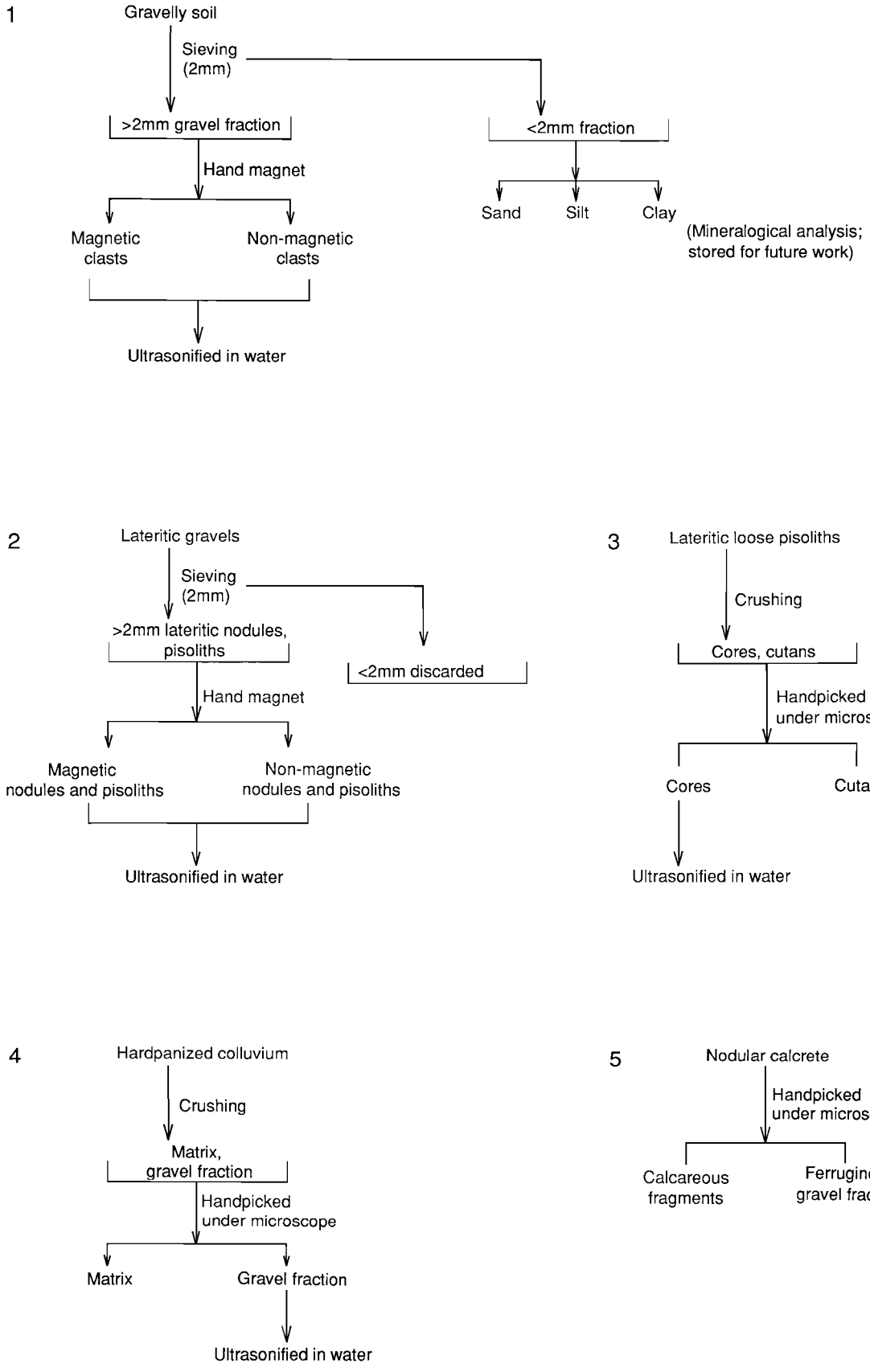

Fig. 21. Sample preparation flow chart.

Table 3. Particle Size Analysis of Soils

Sample No.	Texture	Gravel % >2 mm	< 2 mm		
			Sand % 50-2000μm	Silt % 2-50μm	Clay % <2μm
07-0253	Sandy clay	26	51	5	42
07-0261	Sandy clay loam	64	69	5	24
07-0265	Sandy clay loam	49	70	5	25
07-0296	Sandy clay loam	29	68	7	25
07-0301	Sandy clay	18	54	5	41
07-0337	Sandy clay	17	55	4	42
07-0502	Sandy clay	27	51	6	42
07-0511	Sandy clay	29	52	4	44
07-0516	Sand loam	64	77	5	18
07-0528	Sandy clay	35	54	6	39
07-0533	Sandy clay	69	56	6	38
07-0536	Clay	57	45	7	46
07-0541	Sandy clay loam	33	56	5	36
07-0550	Sandy clay loam	68	62	7	29
07-0555	Sandy clay	27	52	6	42
07-0557	Sandy clay loam	76	68	7	22
07-0579	Sandy clay	48	55	5	39
07-0595	Sandy clay	64	55	4	43
07-0614	Sandy clay loam	71	71	7	21
07-0795	Sandy clay loam	53	69	7	24
07-0797	Sandy clay loam	55	68	7	23

Magnetic and Non-Magnetic Nodules/Pisoliths from Lateritic Residuum
Magnetic and non-magnetic nodules/pisoliths were separated from the loose gravelly unit of lateritic residuum. The lateritic gravelly unit largely consists of lateritic nodules/pisoliths and is generally overlain by soils and/or red-brown hardpanized colluvium. The separation procedure is essentially the same as that described for the separation of magnetic and non-magnetic gravel-fractions of soils.

Cores and Cutans of Loose Pisoliths
The separation of cores and cutans from lateritic pisoliths was only practical for large pisoliths which have thick (5-10 mm) cutans. Whole pisoliths were gently crushed between zirconia plates. Cores and cutans so freed were then handpicked under the binocular microscope. Cores were ultrasonified in water to remove the fine clay particles attached to the surface of cores.

Silicified Matrix and Gravel Fraction from Hardpanized Colluvium (Red-brown Hardpan)
The hardpanized colluvium has developed within gravelly colluvium which largely consists of matrix and lateritic pisoliths and nodules. The matrix constitutes about 60-70% of the specimens. Two main components, namely matrix and lateritic nodules were separated from hardpanized colluvium. In order to separate the matrix from hardpanized colluvium, the samples were first crushed to detach the matrix from the nodules. The fragments of matrix and nodules were then handpicked under a binocular microscope. Care was taken to exclude matrix fragments which had inclusions of small ferruginous granules. Nodules were ultrasonically treated in water to remove the soil attached to the surface of nodules.

Calcareous Fragments and Gravel Fraction from Calcrete
Calcareous fragments and gravels were handpicked under the microscope. Gravels were washed to remove the carbonates attached to the surface of clasts.

7.2.3 SAMPLE PREPARATION

Samples were crushed and ground using non-metallic methods described by Smith (1987). Large fragments, particularly the coarse gravel fraction were reduced to minus 8 mm by crushing between zirconia plates in an automated hydraulic press with the undersize then being processed through an epoxy resin lined disc grinder with alumina plates and reduced to minus 1 mm. Final milling was done in a motorized agate mill.

7.2.4 ANALYTICAL METHODS

Chemical methods
A combination of chemical analytical methods including inductively coupled plasma spectroscopy (ICP), X-ray fluorescence (XRF), and atomic absorption spectrophotometry (AAS) were used to determine a total of 30 elements.

Petrography
Samples were prepared for petrographic study under a binocular microscope. Polished and thin sections of selected samples were prepared and examined using a reflected and transmitted light petrographic microscope in order to provide information on mineralogy and internal fabrics.

X-ray Diffraction
XRD patterns of pulverized representative samples of various morphological groups were obtained using Cu Kα radiation with a Philips vertical diffractometer and graphite diffracted beam monochromator. The diffraction peaks were recorded over the 2θ range of 3-65° and data collected at 0.02° 2θ intervals. The semi-quantitative abundance of minerals in each sample was estimated using a combination of XRD and chemical analyses of bulk samples. The relative proportions of constituent minerals were estimated from peak intensities of selected characteristic lines on the XRD traces. This approach provides a reconnaissance assessment of relative mineral abundances. The following diffraction lines were used — 111 and 110 lines of goethite, 012 and

202 lines of hematite, 313 and 220 lines of maghemite, 001 of kaolinite, 101 of anatase, 110 of rutile and 101 of quartz.

Aluminium substitution in Fe-oxides
The type, crystallinity, and Al substituion of Fe-oxides are influenced by pedogenic environments (Fitzpatrick and Schwertmann, 1982). Because of its identical valency and its similar size (ionic radius 0.51 Å for Al^{3+} and 0.64 Å for Fe^{3+}), the Al^{3+} ion can replace Fe^{3+} in its octahedral position in Fe (III) oxides. An important characteristic of Al-substituted Fe (III) oxides is their smaller unit cell size (shift in XRD peaks) caused by the slightly smaller size of Al^{3+}. In all samples, the concentrations of goethite and hematite were high enough to be easily detected by XRD without any pre-treatment. For Al-substitution measurements, a NaCl or quartz internal standard was added. Measurement errors in the position of peaks were estimated and the positions of diffraction lines corrected. Aluminium substitution in goethite was determined from the 111 reflection using the relationship of mole % Al = 2086-850.7 d (111) as established by Schulze (1984).

Scanning electron microscopy
The micromorphology and qualitative energy dispersive analysis of materials in polished sections and hand picked gravels were carried out using a JEOL Geo SEM 2.

Microprobe analysis
Geochemical analysis of each bulk sample provided the average chemical composition of that sample type. The chemical composition of individual grains, however, was determined by microprobe analysis which also provided information on the association of elements within particular mineral species. Selected mineral grains in polished sections were thus analysed using a Cameca SX-50 microprobe (specimen current 100 nA beam, accelerating voltage 25 kV). A suite of major and minor elements including Si, Al, Fe, Ti, Mg, Ca, Na, K, As, Cr, Cu, Mn, Ni, Sn, V, and Zn were determined.

7.3 Morphological, Mineralogical, and Geochemical Characteristics of the Separated Fractions

The main characteristics of the various fractions separated from soils, hardpanized colluvium, calcrete, and lateritic residuum are summarized in Table 4. Semi-quantitative mineral abundances are shown in Figs 22 and 23.

Tables 5A, 5B, 6A, 6B, 7A, 7B, 8A, 8B, 9A, and 9B present the mean, standard deviation, median, minimum, and maximum values of major minerals and chemical composition for separated fractions. The chemical abundances of selected elements for separated fractions is also shown in Figs 24, 25, 26, 27, and 28. Geochemical and mineralogical data on individual samples are given in Appendix III.

7.3.1 MAGNETIC AND NON-MAGNETIC GRAVEL FRACTIONS OF SOILS

The magnetic and non-magnetic gravel fractions of soils consist of ferruginous granules and lateritic pisoliths/nodules (Fig. 29A) all of which are referred to as clasts. However, ferruginous granules dominate the gravel fraction. The magnetic clasts are rounded, dark reddish brown to black, non-porous and are commonly 2-6 mm in size. They have only a very thin cutan or no cutan at all and generally have a smooth shiny surface. Non-magnetic clasts are also reddish brown to black but have a dull to shiny porous surface. The clasts of the soils exhibit morphological features that are indicative of an inherited, transported origin. These features include roundness, loss of cutans, and different particle size-distribution of sand and silt grains contained within adjacent nodules from the same sample. The field observations support the micromorphological interpretation that the clasts in the soils are re-worked and are derived from the erosion of lateritic residuum in upland areas.

The magnetic fraction consisted mostly of hematite and maghemite with small amounts of goethite and kaolinite (Fig. 22). Goethite was absent from some samples. The non-magnetic

Table 4. Main characteristics of the morphological groups separated from soils, hardpanized colluvium, calcrete unit, and lateritic residuum.

Property	Magnetic Gravel Fraction		Non-magnetic Gravel Fraction		Matrix from Hardpanized Colluvium	Calcareous Fragments
	Soils	Lateritic Residuum	Soils	Lateritic Residuum		
Colour	Reddish-brown to black	Yellowish brown to red	Reddish brown to black	Yellowish brown to red	Red to reddish brown	Cream to pinkish
Hardness	Hard to very hard	Hard to very hard	Hard to very hard	Hard to very hard	Brittle	Moderately firm
Shape	Rounded to irregular, some elongated	Rounded to subrounded	Rounded to irregular, some elongated	Rounded to irregular	-	Platy
Surface Texture	Smooth, shiny, non-porous	Dull, rough porous	Dull to shiny, porous surface with fine to very fine quartz grains	Dull, porous, fractured surface may be infused with silica	Porous, partly silicified, Mn staining	Rough, porous
Internal Fabric	Massive, black, no cutans visible with hand lens	Massive, black with cutans, kaolinite, goethite-pseudomorphs after muscovite common	Porous, reddish brown to black, no cutans, some contain abundant quartz	Porous, reddish brown with cutans, kaolinite, goethite-pseudomorphs after muscovite common, abundant round clay balls	Oriented bands of clay, goethite and amorphous silica	Carbonate replaced fabric

fraction consisted mostly of hematite, kaolinite, goethite with small amounts of quartz (Fig 22). Maghemite was not detected in the non-magnetic fraction of the gravel. It is interesting to note that the concentrations of maghemite are much higher (to 40%) in these magnetic samples compared to those of the Darling Ranges where the levels are commonly between 10-20%. Thus, apart from the differences in Fe oxide mineralogy between magnetic and non-magnetic clasts, the association with other minerals was also different. The non-magnetic clasts contained greater amounts of the non-Fe-oxide (e.g. kaolinite, quartz) minerals. This is consistent with the findings of Taylor and Schwertmann (1974) who observed in an examination of magnetic and non-magnetic concretions from a variety of Australian soils, that the magnetic samples had much less layer lattice silicate in their matrix than did the morphologically similar non-magnetic concretions with which they were associated. The origin of maghemite is discussed below.

Anatase and ilmenite were detected in some samples, but there was no pattern to their occurrence.

Aluminium substitution in goethite ranged between 11 and 21 mole % over all the samples (Table 10). The degree of Al substitution in goethite in non-magnetic (mean - 16 mole%) and magnetic (mean - 15 mole %) clasts is similar.

By far the most abundant chemical constituent is Fe_2O_3 with mean values greater than 55 wt% in both the magnetic and non-magnetic gravel fractions. The magnetic gravel fraction has a high mean Fe_2O_3 content (77.8%) and low SiO_2 (7.5%) and Al_2O_3 (8.8%) contents relative to the non-magnetic gravel fraction (Tables 5A, 5B). Iron occurs as hematite, maghemite, and goethite, Al_2O_3 as kaolinite, and SiO_2 as kaolinite and quartz. There is a large range of values for Fe_2O_3 (39.6 - 70.5%) in the non-magnetic gravel fraction reflecting the presence of clay-rich to Fe-oxide-rich clasts. The minor oxides CaO, MgO, Na_2O, and K_2O are strongly depleted relative to Fe, Al, and Si. The non-magnetic gravel fraction contains slightly less TiO_2 (1.6%) relative to the magnetic fraction (2%).

The magnetic fraction is richer in Mn, Cr, V, Pb, Zn, As, W, and Ga than the corresponding non-magnetic fraction. In contrast Ag, Au, Cu, and Ni are enriched in the non-magnetic fraction relative to the magnetic fraction. The levels of Co, Sb, Bi, Mo, Sn, and Se are not significantly different between magnetic and non-magnetic fractions.

Bulk soils are included for comparison. As expected, the soils are high in SiO_2, Al_2O_3 and low in Fe_2O_3 compared with the gravel fractions separated from these soils. The levels of Cu are much higher in soils than in the magnetic gravel fraction. Although mean Au concentrations are low in soils relative to the magnetic and non-magnetic fraction, levels are significant and anomalous.

7.3.2 MAGNETIC AND NON-MAGNETIC NODULES AND PISOLITHS FROM LATERITIC RESIDUUM

Nodules and pisoliths in lateritic residuum may be present in roughly equal amounts; however, nodules are generally dominant (Fig. 29B). Magnetic nodules are rounded to subrounded in shape with a size range of 2-10 mm and they consist of 1-3 mm thick yellowish brown to red cutans around black cores (Fig. 30A). The cores of non-magnetic nodules are reddish brown to red and contain abundant kaolinite and/or siliceous balls (Fig. 30B). The kaolinite-rich balls (0.2-0.5 mm) are less common in the cores of magnetic nodules. Non-magnetic nodules are slightly larger (5-15 mm) than magnetic nodules and may also contain quartz grains in the nucleus. Large nodules are observed enclosing smaller ones both in magnetic and non-magnetic nodules. In lateritic residuum, the nodules/pisoliths display none of the features described for clasts from soils or evidence for transportation and appear to have formed *in situ*.

In polished thin sections, the central parts of both magnetic and non-magnetic nodules show the preservation of pseudomorphs of goethite, hematite, and kaolinite after muscovite typical of *in situ* weathering as described by several authors (e.g. Bisdom *et al.*, 1982; Muller and

Bocquier, 1986). This may suggest that these nodules and pisoliths are formed from the weathering of underlying muscovite-quartz schist. The presence of pseudomorphs after muscovite was confirmed by the electron microprobe analysis. Typical distributions of Si, Al, K, Fe in a pisolith containing muscovite pseudomorph are shown in Fig. 31. Most of the muscovite has weathered, leaving some fresh muscovite fragments separated by an Fe-oxide and clay-rich matrix. The distribution of K shows the residual unweathered muscovite. Aluminium and Si are present as kaolinite and Fe as goethite.

The mineralogical compositions of the magnetic and non-magnetic nodules/pisoliths are similar to those described for magnetic and non-magnetic gravel fractions of soils (Fig. 22). However, gibbsite occurred both in magnetic and non-magnetic nodules of lateritic residuum, but was not detected in the gravel fractions of soils. Goethite and kaolinite occurred in larger amounts in magnetic nodules of lateritic residuum compared to those of magnetic clasts from soils. These differences in mineralogy may be, in part, explained by the absence of cutans in clasts from soils; cutans are generally rich in goethite and kaolinite.

Scanning electron microscopic and electron microprobe analysis of areas within cores of nodules show compositions ranging from Al-Si-rich (kaolinite) through Al-Si-Fe-rich (Kaolinite and Fe-oxides) to Fe-rich (Fe-oxides). This may suggest the various stages of replacement of kaolinite by Fe-oxides to form the Fe-oxides rich nodules. Hematite is the dominant Fe-oxide mineral.

Aluminium substitution in goethite ranged from 13 to 23 mole % over all the samples (Table 10). The degree of Al substitution in goethite in non-magnetic (mean - 17 mole %) and magnetic (mean - 19 mole %) is similar. These values of Al substitution are not significantly different from those of magnetic and non-magnetic clasts in the soils suggesting similar pedogenic environment of their formation.

The distributions of major and minor elements, including Au, in magnetic and non-magnetic nodules are similar to those for the magnetic and non-magnetic gravel fractions of soils (Tables 6A, 6B). The levels of abundances of major and minor elements, however, are different. For example, the mean values of Fe_2O_3, Mn, Pb, Zn, As, and Ba are relatively low in magnetic nodules of lateritic residuum compared with the corresponding magnetic gravel fraction of soils. In contrast, magnetic nodules of lateritic residuum show higher mean concentration of Au and Ag than the magnetic gravel fraction of soils. Similar relationships apply to non-magnetic nodules.

7.3.3 CORES AND CUTANS OF LOOSE PISOLITHS

Cores and cutans could only be separated from large pisoliths which have thick cutans. The individual pisoliths which were studied are round, 20-50 mm in diameter and contain black to red cores. The cutans around cores are generally 2-15 mm in thickness, consisting of light and dark red banded zones. Light zones are kaolinite and/or goethite-rich, whereas dark zones are hematite-rich. Lenses of quartz grains may occur in cutans. Pisoliths can also be partly replaced or surrounded by authigenic calcium carbonate and silica. Such pisoliths are relatively weak and their cutans can be readily removed by hand. These pisoliths are comparable with classical types described in the literature, but are atypical for the Mt. Gibson area. The cores are dominated by hematite and maghemite with lesser amounts of goethite, kaolinite, quartz, and gibbsite. Primary rutile up to 4% was also present. The cutans largely consist of kaolinite, hematite, and gibbsite with small amounts of goethite and quartz. Maghemite is typically absent in cutans.

The cores contain higher mean concentrations of Fe_2O_3 (64.7%) and lower concentrations of SiO_2 (12.5%) and Al_2O_3 (12.5%). In contrast, cutans contain almost equal mean concentrations of Fe_2O_3, Al_2O_3, and SiO_2 (Tables 7A, 7B). The Fe in the cutans occurs as hematite and goethite and Al_2O_3 as gibbsite and kaolinite, and SiO_2 as kaolinite and quartz. Both cores and cutans show relatively large concentrations of TiO_2 (up to 4.6%) which are significantly higher than values for the nodules of lateritic residuum. The cores and cutans of loose pisoliths contain more TiO_2 (averaging 3.24-4%) compared with 1.7-2.2% for the nodules of lateritic residuum.

This may suggest that the large pisoliths with thick cutans have developed from the weathering of Ti-rich basic rocks.

The levels of Cr, V, Pb, Zn, As, and Ga are enriched in cores relative to cutans. The cores show very high concentrations of Au averaging about 11 ppm compared with 2.7 ppm for the cutans. The mean Au values for these large pisoliths are five times higher than those for the commonly occurring nodules of lateritic residuum. In contrast, Ag levels are significantly higher in the cutans relative to the cores. The cutans are probably formed by concentric concentrations of Al and Fe-rich solutions around black nuclei and therefore may not have any genetic link with the formation of cores. This suggests the Au enrichment in the cores and cutans did not occur at the same time and indicates that Au has been mobile.

7.3.4 SILICIFIED MATRIX AND GRAVEL FRACTION OF HARDPANIZED COLLUVIUM (RED-BROWN HARDPAN)

Hardpanized colluvium consists of varying amounts of ferruginous silty clay/sandy matrix and gravels. The matrix fragments separated from hardpanized colluvium are brittle, dull, earthy red to dark red, or red-brown (2.5YR 4/6 - 4/8 or 5/6 - 5/8, moist) silicified masses of kaolinitic clays with some fine quartz invaded by Fe-oxides and Si. Accumulations of Mn oxides characteristically occur on the hardpan surface. The matrix shows zones of strongly-oriented kaolinite around quartz grains with isotropic material containing amorphous silica and zones of carbonates filling fissures. Microscopic evidence indicates a complex development of cementation resulting in hardpan development. This appears to be related to alternating authigenic deposition of silica, hematite/goethite, kaolinite, and carbonate phases.

The gravel fraction separated from hardpanized colluvium largely consists of various amounts of lateritic nodules, pisoliths, and hardened mottles which are most abundant in the lower and middle parts of the hardpan unit. The nodules and pisoliths are black to red, black ones generally being magnetic, and vary in diameter from 2 to 20 mm. Most pisoliths and nodules have thin cutans of goethite and kaolinite. Amorphous silica and carbonates may coat the ferruginous gravels.

The matrix largely consists of kaolinite, quartz, and amorphous silica with lesser quantities of goethite, hematite, calcite, and dolomite (Fig. 23). Samples are richer in calcite than dolomite. Smectite and illite were also present in some samples. Gibbsite was found to occur in one sample. Hematite is responsible for the red colour of the hardpan matrix.

The mineralogy of the gravel fraction largely consists of hematite and kaolinite with varying amounts of goethite, quartz, gibbsite, and calcite (Fig.23). Maghemite was present in moderate amounts in magnetic clasts. The mineralogy of the gravel fraction separated from hardpanized colluvium is similar to that described for nodules and pisoliths from the lateritic residuum suggesting a similar origin. Calcite occurred as coatings on gravels and is present in cracks.

Silica and Al_2O_3 are present in higher concentrations in the silicified matrix, whereas Fe_2O_3 dominates the gravel fraction of hardpanized colluvium (Tables 8A, 8B). With the increase in Fe_2O_3, there is therefore a concomitant decrease in SiO_2 and Al_2O_3. The Fe_2O_3 in the silicified matrix is present as hematite and goethite. The gravel fraction has higher mean values of TiO_2 than does the matrix. The matrix has higher concentrations of CaO and MgO in the form of calcite and dolomite. Silica and Al_2O_3 occur in kaolinite and SiO_2 occurs as amorphous silica.

The mean values of Mn, Cr, V, Pb, As, Sb, Bi, Ag, W, and Au are much higher in the gravel fraction than in the matrix. The levels of Zn and Cu are not significantly different between the two fractions. Nickel, Co, and Ba are enriched in the matrix relative to the gravel component. Care is needed in the interpretation of Ba values up to about 250 ppm because Ba is an unwanted impurity in the alumina disk grinding plates. However, the matrix shows significantly higher values of Ba (to 900 ppm). Furthermore, scanning electron microscopy shows that Ba occurs as barite in such samples.

Table 5A **Range of values for magnetic gravel fraction of soils (N=21)**

	Means	Medians	Std. Devs	Minima	Maxima
wt %					
SiO2	7.53	6.86	2.27	4.02	12.50
Al2O3	8.86	8.59	1.44	6.84	12.00
Fe2O3	77.87	78.30	3.41	71.21	82.80
MgO	0.066	0.060	0.024	0.041	0.132
CaO	0.092	0.067	0.052	0.046	0.222
Na2O	0.044	0.040	0.021	0.024	0.116
K2O	0.029	0.020	0.024	0.020	0.107
TiO2	2.072	2.035	0.582	1.070	3.170
ppm					
Mn	261	243	65	139	427
Cr	960	961	244	576	1690
V	1901	1880	319	1380	2640
Cu	27.0	26.0	7.9	17.0	46.0
Pb	120.4	115.0	35.9	66.0	200.0
Zn	26.8	24.0	8.5	16.0	56.0
Ni	15.9	14.0	5.2	10.0	28.0
Co	2.5	1.3	2.5	1.3	10.0
As	58.8	49.0	31.8	18.0	126.0
Sb	7.7	6.0	3.7	2.0	14.0
Bi	10.2	9.0	9.1	1.7	40.0
Mo	8.0	9.0	4.1	0.3	16.0
Ag	0.20	0.10	0.24	0.03	1.00
Sn	5.1	6.0	2.8	0.7	10.0
Ga	86.6	85.0	19.3	54.0	120.0
W	15.7	12.0	10.0	4.0	34.0
Ba	25	17	22	6	93
Zr	190	185	44	135	292
Nb	15.1	15.0	4.2	9.0	25.0
Se	5.1	5.0	3.1	0.7	11.0
Be	0.7	1.0	0.4	0.3	2.0
Au (ppb)	949	616	1152	104	4647
wt %					
Hematite	45	45	6	30	56
Goethite	4	0	6	0	18
Maghemite	31	30	11	0	40
Kaolinite	9	8	6	0	25
Gibbsite	0	0	1	0	5
Quartz	5	5	3	0	10

Table 5B **Range of values for non magnetic gravel fraction of soils (N=21)**

	Means	Medians	Std. Devs	Minima	Maxima
wt %					
SiO2	17.07	15.30	4.59	9.61	25.20
Al2O3	16.16	15.30	3.03	11.50	22.20
Fe2O3	57.85	59.30	9.09	39.60	70.50
MgO	0.078	0.072	0.033	0.047	0.193
CaO	0.097	0.067	0.087	0.035	0.438
Na2O	0.043	0.037	0.020	0.012	0.104
K2O	0.027	0.020	0.018	0.020	0.086
TiO2	1.644	1.700	0.377	0.842	2.268
ppm					
Mn	180	179	77	54	376
Cr	796	776	203	461	1320
V	1680	1680	290	972	2150
Cu	43.0	42.0	15.8	23.0	94.0
Pb	92.5	89.0	29.6	50.0	170.0
Zn	17.3	16.0	5.5	8.0	26.0
Ni	24.6	24.0	6.0	14.0	34.0
Co	2.9	1.3	2.2	1.3	6.0
As	55.1	44.0	31.6	28.0	154.0
Sb	6.0	6.0	2.2	3.0	12.0
Bi	8.2	7.0	4.8	1.7	20.0
Mo	6.7	7.0	3.0	0.3	12.0
Ag	0.68	0.70	0.47	0.03	1.60
Sn	4.7	5.0	2.4	0.7	9.0
Ga	73.8	72.0	16.8	50.0	120.0
W	10.9	9.0	5.9	2.0	19.0
Ba	44	19	49	9	184
Zr	167	169	27	127	252
Nb	13.3	13.0	4.3	4.0	24.0
Se	4.7	5.0	2.3	0.7	10.0
Be	0.8	1.0	0.5	0.3	2.0
Au (ppb)	1546	1178	1564	30	6128
wt %					
Hematite	46	50	13	20	65
Goethite	15	14	5	5	30
Maghemite	0	0	0	0	0
Kaolinite	26	25	10	5	45
Gibbsite	0	0	0	0	2
Quartz	7	5	3	3	12

Table 6A **Range of values for magnetic nodules/pisoliths from lateritic residuum (N=13)**

	Means	Medians	Std. Devs	Minima	Maxima
wt %					
SiO2	10.30	8.98	5.11	6.11	25.90
Al2O3	12.80	10.69	4.28	7.69	20.97
Fe2O3	68.01	70.78	8.07	53.48	79.22
MgO	0.102	0.079	0.084	0.041	0.348
CaO	0.248	0.066	0.584	0.020	2.170
Na2O	0.059	0.032	0.049	0.009	0.177
K2O	0.024	0.020	0.016	0.020	0.076
TiO2	2.271	2.002	0.927	1.380	4.587
ppm					
Mn	162	138	102	63	475
Cr	1008	1050	310	431	1570
V	1756	1790	307	1280	2180
Cu	26.8	24.0	11.7	16.0	58.0
Pb	100.8	94.0	29.6	54.0	165.0
Zn	17.7	16.0	6.4	11.0	34.0
Ni	17.3	18.0	5.5	10.0	26.0
Co	3.2	1.3	2.6	1.3	8.0
As	45.4	45.0	21.1	13.0	86.0
Sb	5.8	5.0	2.7	3.0	12.0
Bi	8.0	9.0	5.2	0.7	16.0
Mo	7.4	7.0	2.8	0.3	11.0
Ag	0.45	0.40	0.52	0.03	2.00
Sn	5.4	5.0	3.6	0.7	15.0
Ga	90.4	88.0	27.1	60.0	150.0
W	13.1	14.0	7.3	2.0	25.0
Ba	44	20	64	2	232
Zr	185	186	37	128	249
Nb	15.4	16.0	6.0	7.0	26.0
Se	8.5	8.0	4.2	3.0	19.0
Be	0.6	0.3	0.4	0.3	1.0
Au (ppb)	1603	845	1490	180	3954
wt %					
Hematite	38	40	7	30	50
Goethite	9	10	4	0	15
Maghemite	25	25	5	15	35
Kaolinite	13	15	6	0	20
Gibbsite	4	0	7	0	20
Quartz	5	5	5	0	20

Table 6B **Range of values for non magnetic nodules/pisoliths from lateritic residuum (N=13)**

	Means	Medians	Std. Devs	Minima	Maxima
wt %					
SiO2	19.89	21.30	7.17	6.40	31.40
Al2O3	19.60	20.40	2.61	14.72	23.23
Fe2O3	45.92	49.05	12.89	13.30	62.63
MgO	0.137	0.079	0.136	0.058	0.533
CaO	0.392	0.054	0.977	0.019	3.510
Na2O	0.067	0.031	0.062	0.011	0.213
K2O	0.028	0.020	0.019	0.020	0.076
TiO2	1.692	1.380	0.634	1.120	3.019
ppm					
Mn	131	106	113	19	474
Cr	784	729	287	396	1460
V	1381	1400	254	978	1780
Cu	35.8	36.0	8.3	24.0	58.0
Pb	74.8	60.0	29.9	38.0	140.0
Zn	14.5	14.0	2.9	11.0	19.0
Ni	26.3	26.0	5.6	18.0	36.0
Co	5.5	6.0	3.4	1.3	12.0
As	34.3	30.0	14.1	12.0	59.0
Sb	4.3	4.0	2.2	2.0	10.0
Bi	7.4	8.0	4.7	0.7	17.0
Mo	5.8	5.0	2.2	4.0	12.0
Ag	0.62	0.50	0.45	0.03	1.60
Sn	5.1	5.0	3.7	0.7	15.0
Ga	77.8	65.0	32.8	52.0	150.0
W	14.2	10.0	15.8	4.0	63.0
Ba	64	25	71	2	233
Zr	145	145	26	99	194
Nb	13.9	12.0	5.7	7.0	24.0
Se	7.5	6.0	3.5	3.0	14.0
Be	0.8	1.0	0.3	0.3	1.0
Au (ppb)	2657	2035	1960	140	5975
wt %					
Hematite	37	40	9	22	55
Goethite	16	15	4	10	23
Maghemite	0	0	0	0	0
Kaolinite	30	30	8	15	40
Gibbsite	3	0	5	0	15
Quartz	8	8	4	2	15

Table 7A **Range of values of cores of lateritic pisoliths (N=8)**

	Means	Medians	Std. Devs	Minima	Maxima
wt %					
SiO2	12.50	12.61	4.84	7.69	17.10
Al2O3	12.50	12.48	4.11	7.88	17.17
Fe2O3	64.74	65.35	4.92	58.34	69.93
MgO	0.121	0.145	0.054	0.040	0.154
CaO	0.086	0.101	0.038	0.029	0.112
Na2O	0.143	0.152	0.047	0.078	0.189
K2O	0.020	0.020	0.000	0.020	0.020
TiO2	3.244	3.178	0.595	2.619	4.003
ppm					
Mn	103	100	44	60	152
Cr	977	968	173	801	1170
V	1995	1970	142	1850	2190
Cu	23.3	22.0	4.7	19.0	30.0
Pb	95.3	77.0	46.0	64.0	163.0
Zn	12.3	12.0	2.9	9.0	16.0
Ni	11.8	11.5	3.9	8.0	16.0
Co	1.3	0.7	1.9	1.3	4.0
As	18.5	18.0	4.2	14.0	24.0
Sb	5.0	3.5	4.1	2.0	11.0
Bi	3.6	1.9	3.6	1.7	9.0
Mo	4.7	3.7	5.3	0.3	11.0
Ag	0.53	0.50	0.33	0.20	0.90
Sn	6.8	6.0	6.2	0.7	15.0
Ga	117.5	120.0	99.5	1.3	230.0
W	13.8	14.0	3.8	9.0	18.0
Ba	63.8	23.0	88.3	13.0	196.0
Zr	208.8	193.0	62.1	154.0	295.0
Nb	13.5	13.5	11.1	0.7	27.0
Se	5.3	5.5	5.5	0.7	10.0
Be	0.3	0.3	0.0	0.3	0.3
Au (ppb)	11145	13042	5365	3333	15163
wt %					
Hematite	34	34	4	30	40
Goethite	9	8	5	5	15
Maghemite	25	25	6	20	30
Kaolinite	9	9	9	0	20
Gibbsite	4	3	6	0	12
Quartz	10	9	4	5	15

Table 7B **Range of values of cutans of lateritic pisoliths (N=8)**

	Means	Medians	Std. Devs	Minima	Maxima
wt %					
SiO2	29.08	28.65	9.03	18.80	40.20
Al2O3	24.55	24.09	8.29	14.89	35.14
Fe2O3	30.25	29.25	4.24	26.31	36.18
MgO	0.263	0.266	0.033	0.221	0.300
CaO	0.091	0.105	0.034	0.040	0.113
Na2O	0.230	0.265	0.081	0.110	0.280
K2O	0.034	0.020	0.027	0.020	0.074
TiO2	4.003	3.887	0.482	3.553	4.687
ppm					
Mn	35	33	15	19	55
Cr	571	531	192	409	813
V	1270	1295	126	1110	1380
Cu	35.8	35.5	3.3	32.0	40.0
Pb	73.8	63.5	31.5	49.0	119.0
Zn	7.0	7.0	1.2	6.0	8.0
Ni	30.0	28.0	5.7	26.0	38.0
Co	3.5	3.0	4.1	1.3	8.0
As	13.8	14.0	4.4	9.0	18.0
Sb	3.5	2.5	2.4	2.0	7.0
Bi	4.9	5.0	2.6	1.7	8.0
Mo	2.7	2.2	2.8	0.3	6.0
Ag	1.23	1.00	1.20	0.03	2.90
Sn	16.3	15.0	6.3	10.0	25.0
Ga	68.8	72.5	21.7	40.0	90.0
W	12.3	12.5	3.2	9.0	15.0
Ba	32.8	29.5	17.4	17.0	55.0
Zr	239.8	247.0	98.1	120.0	345.0
Nb	32.0	30.5	10.2	22.0	45.0
Se	5.0	6.0	2.7	1.0	7.0
Be	0.7	0.7	0.4	0.3	1.0
Au (ppb)	2717	2264	2723	257	6084
wt %					
Hematite	24	24	4	20	28
Goethite	11	11	1	10	12
Maghemite	0	0	0	0	0
Kaolinite	30	28	11	20	45
Gibbsite	19	23	13	0	30
Quartz	16	14	7	10	25

Table 8A **Range of values of matrix of hardpanized colluvium (N=10)**

	Means	Medians	Std. Devs	Minima	Maxima
wt %					
SiO2	43.30	47.05	8.22	25.00	50.10
Al2O3	20.78	20.70	3.30	17.00	26.50
Fe2O3	13.51	13.15	4.34	7.89	21.40
MgO	0.840	0.751	0.595	0.000	1.860
CaO	3.796	1.512	4.424	0.401	12.400
Na2O	0.298	0.264	0.122	0.155	0.498
K2O	0.353	0.337	0.156	0.152	0.709
TiO2	0.896	0.943	0.223	0.469	1.153
ppm					
Mn	168	150	47	126	250
Cr	221	207	86	103	352
V	356	339	106	220	546
Cu	53.4	49.0	18.6	28.0	86.0
Pb	29.3	26.0	11.7	17.0	44.0
Zn	17.3	18.0	4.4	8.0	22.0
Ni	34.8	37.0	8.9	16.0	46.0
Co	8.2	8.0	3.2	4.0	16.0
As	11.3	11.0	6.1	4.0	22.0
Sb	1.5	1.0	1.2	0.3	4.0
Bi	1.3	0.7	1.1	0.7	4.0
Mo	1.3	0.3	1.6	0.3	4.0
Ag	0.48	0.50	0.32	0.03	0.90
Sn	3.7	3.5	1.4	1.0	6.0
Ga	38.1	36.0	6.0	30.0	50.0
W	3.8	3.5	1.6	2.0	7.0
Ba	339	202	306	54	931
Zr	92	96	18	65	117
Nb	10.5	11.0	2.0	7.0	13.0
Se	1.3	0.9	0.7	0.7	2.0
Be	1.2	1.0	0.4	1.0	2.0
Au (ppb)	1572	1559	693	673	2866
wt %					
Hematite	5	4	5	0	14
Goethite	12	10	4	8	20
Maghemite	0	0	0	0	0
Kaolinite	41	43	6	30	50
Gibbsite	2	0	5	0	15
Quartz	19	20	6	10	25

Table 8B **Range of values of gravels of hardpanized colluvium (N=10)**

	Means	Medians	Std. Devs	Minima	Maxima
wt %					
SiO2	18.68	17.15	7.34	10.40	28.80
Al2O3	17.74	18.40	3.30	11.70	21.40
Fe2O3	49.90	52.05	11.42	35.30	66.80
MgO	0.281	0.278	0.101	0.171	0.521
CaO	0.901	0.417	0.945	0.136	2.590
Na2O	0.164	0.153	0.071	0.082	0.277
K2O	0.110	0.096	0.037	0.071	0.174
TiO2	1.933	1.875	0.693	1.170	3.286
ppm					
Mn	203	172	139	66	545
Cr	711	690	244	347	1290
V	1343	1305	407	697	1900
Cu	59.2	61.0	13.8	36.0	80.0
Pb	85.5	81.0	36.1	32.0	140.0
Zn	15.5	16.5	3.0	10.0	19.0
Ni	25.6	28.0	6.4	14.0	32.0
Co	4.3	4.0	1.4	1.3	6.0
As	28.8	31.0	12.9	7.0	49.0
Sb	4.3	4.0	1.3	2.0	6.0
Bi	6.1	6.5	2.9	0.7	10.0
Mo	6.3	6.0	1.7	4.0	10.0
Ag	0.95	1.00	0.49	0.10	1.50
Sn	5.3	5.0	3.1	0.7	10.0
Ga	81.3	75.0	26.9	44.0	125.0
W	10.0	9.5	6.7	3.0	24.0
Ba	241	204	165	61	484
Zr	153	152	26	116	188
Nb	15.3	14.0	4.7	11.0	26.0
Se	3.9	4.0	2.9	0.7	9.0
Be	1.2	1.0	0.6	0.3	2.0
Au (ppb)	3966	3204	3071	629	9941
wt %					
Hematite	29	30	5	20	35
Goethite	13	10	5	5	20
Maghemite	13	20	11	0	25
Kaolinite	27	28	8	15	40
Gibbsite	4	0	6	0	15
Quartz	7	6	5	0	15

Table 9A **Range of values of calcareous fragments from calcretes (N=5)**

	Means	Medians	Std. Devs	Minima	Maxima
wt %					
SiO2	19.68	23.30	6.76	8.51	25.10
Al2O3	8.70	9.77	3.09	3.93	12.11
Fe2O3	4.28	4.73	2.58	1.30	8.05
MgO	2.595	2.100	1.206	1.691	4.659
CaO	35.312	34.000	12.118	19.166	47.986
Na2O	0.235	0.204	0.094	0.123	0.357
K2O	0.282	0.259	0.134	0.112	0.480
TiO2	0.422	0.340	0.307	0.132	0.941
ppm					
Mn	145	108	101	41	305
Cr	105	110	31	55	140
V	116	108	66	35	216
Cu	30.4	30.0	9.5	16.0	40.0
Pb	14.4	14.0	3.8	9.0	18.0
Zn	16.2	13.0	8.3	11.0	31.0
Ni	13.9	16.0	7.9	1.3	22.0
Co	2.9	1.3	3.2	1.3	8.0
As	5.2	4.0	2.7	2.0	8.0
Sb	0.3	0.3	0.0	0.3	0.3
Bi	2.6	0.7	3.6	0.7	9.0
Mo	0.4	0.3	0.3	0.3	1.0
Ag	0.04	0.03	0.03	0.03	0.10
Sn	2.8	2.0	2.5	1.0	7.0
Ga	13.3	15.0	7.7	1.7	20.0
W	1.4	1.0	0.5	1.0	2.0
Ba	110	88	52	54	171
Zr	52	60	19	21	67
Nb	6.0	5.0	4.2	1.0	12.0
Se	1.6	1.0	0.9	1.0	3.0
Be	0.3	0.3	0.0	0.3	0.3
Au (ppb)	931	763	578	322	1803
wt %					
Hematite	0	0	0	0	0
Goethite	6	4	5	0	12
Maghemite	0	0	0	0	0
Kaolinite	14	15	7	5	25
Gibbsite	1	0	2	0	5
Quartz	11	10	7	3	20

Table 9B **Range of values of gravels from calcretes (N=5)**

	Means	Medians	Std. Devs	Minima	Maxima
wt %					
SiO2	22.28	18.50	10.96	11.30	38.30
Al2O3	22.97	25.50	9.78	6.23	31.55
Fe2O3	37.33	37.18	19.00	15.30	66.80
MgO	0.394	0.403	0.116	0.252	0.560
CaO	2.346	1.441	2.036	0.360	4.750
Na2O	0.205	0.146	0.145	0.067	0.441
K2O	0.049	0.067	0.026	0.020	0.069
TiO2	1.668	1.239	0.971	0.862	3.253
ppm					
Mn	171	137	96	79	308
Cr	742	805	148	486	842
V	1034	736	554	645	1970
Cu	79.6	53.0	40.2	50.0	135.0
Pb	45.4	40.0	15.3	35.0	72.0
Zn	18.4	12.0	10.6	10.0	30.0
Ni	26.4	25.0	12.1	14.0	45.0
Co	2.8	4.0	2.7	1.3	6.0
As	37.6	27.0	15.5	25.0	56.0
Sb	4.0	5.0	1.9	2.0	6.0
Bi	8.7	8.0	5.4	1.7	15.0
Mo	4.7	7.0	3.3	0.3	7.0
Ag	3.07	2.00	3.12	0.03	7.50
Sn	9.4	6.0	8.8	4.0	25.0
Ga	58.8	55.0	22.5	35.0	84.0
W	6.4	5.0	4.0	3.0	12.0
Ba	249	134	331	23	834
Zr	146	140	36	103	203
Nb	13.6	8.0	11.6	4.0	32.0
Se	6.4	7.0	2.2	3.0	9.0
Be	0.6	0.3	0.4	0.3	1.0
Au (ppb)	6822	3891	5519	1920	15145
wt %					
Hematite	20	17	10	8	35
Goethite	18	18	6	9	24
Maghemite	3	0	8	0	17
Kaolinite	28	20	23	3	58
Gibbsite	12	14	11	0	25
Quartz	10	10	6	3	18

Table 10 - Range of values of Al substitution in goethite for magnetic and non-magnetic lateritic nodules/clasts.

	Lateritic nodules and pisoliths from lateritic residuum				Clasts from Soils			
	Non-Magnetic N = 10		Magnetic N = 10		Non-Magnetic N = 14		Magnetic N = 14	
	Range	Mean	Range	Mean	Range	Mean	Range	Mean
Al in goethite (mole %)	14-21	17	13-23	19	11-20	15	12-21	16

It is interesting that the mean values of Au and Ag in the matrix of harpanized colluvium are higher than, or very similar, to those for nodules of lateritic residuum and the gravel fractions of soils. The Au enrichment in the hardpan matrix may reflect the original levels of Au in the materials derived from the erosion of the upper part of the weathering profile in upland source areas. Introduction of Au into the hardpan matrix at a much later stage is also a possibility.

7.3.5 CALCAREOUS FRAGMENTS AND GRAVELS FROM CALCRETE

Calcareous fragments are platy, cream to pinkish in colour and vary in diameter from 1 to 5 cm. Clasts consisting of lateritic nodules and pisoliths separated from calcrete are reddish brown to black and are infused with carbonates. The distribution of Ca and Mg in the nodules shows that calcite and dolomite have formed coatings around nuclei and have also infiltrated the Fe-oxide matrix. Petrological evidence suggests that this process, taken to completion, would eventually result in replacement of the pre-existing lateritic nodules and pisoliths.

The calcareous fragments show higher mean concentrations of CaO (35.3%) and MgO (2.6%) and lower concentrations of Fe_2O_3 (4.2%) and Al_2O_3 (8.7%) relative to the gravel fraction (Tables 9A, 9B). The clasts have higher concentrations of Fe_2O_3 (37.3%), SiO_2 (22.2%), and Al_2O_3 (22.9%). Calcium is present as calcite and dolomite; Mg as dolomite; SiO_2 as kaolinite and quartz, and Al_2O_3 as kaolinite and gibbsite, and Fe_2O_3 as goethite and hematite.

The gravel fraction is enriched in all the trace elements analysed including Au relative to calcareous fragments. Although the mean value of Au (931 ppb) is low in the the calcareous fragments, it is highly significant. The low levels of Fe_2O_3 (4.2%) in calcareous fragments may suggest that most of the Au is associated with carbonates in the regolith. However, more work is needed to confirm this.

At the Mt. Gibson Au mine, carbonates have replaced or displaced pre-existing regolith fabrics (soils, lateritic duricrust) so that the Au which now occurs in carbonates may represent Au that was originally in soils. It is also possible that Au-enrichment in calcrete has taken place during the formation of carbonates.

7.4 Location and Distribution of Ore-associated Elements and Dispersion Processes

7.4.1 GENERAL

During weathering, the elements comprising the original mineral deposits are generally dispersed to a greater or lesser degree. These ore-associated elements including As, Cu, Zn, Ni, Co, Sb, and Bi can then be incorporated with or absorbed onto Fe-oxides and other secondary minerals during laterite formation. Thus dispersion increases the size of a geochemical anomaly, but reduces the chemical magnitude of an anomaly. Dispersion is basically of two types — hydromorphic and mechanical — although both types are frequently combined and are associated with residual accumulation. Hydromorphic or chemical dispersion is a function of the mobility, i.e. solubility of an element. The solubility of an element can vary widely, depending upon the chemical environment and in particular pH, Eh, associated dissolved ions and the matrix. Some mechanical disperson takes place during residual accumulation. The most extensive mechanical dispersion, however, results from physical erosion processess that carry the fragments of gossans or mineral grains from the source of the occurrence. Gossan fragments can be incorporated into pisoliths and nodules during lateritic weathering.

A study of polished sections of lateritic nodules and pisoliths for anomalous samples from Mt. Gibson suggested that, besides residual accumulation, both hydromorphic and mechanical processes have commonly operated. These are now discussed.

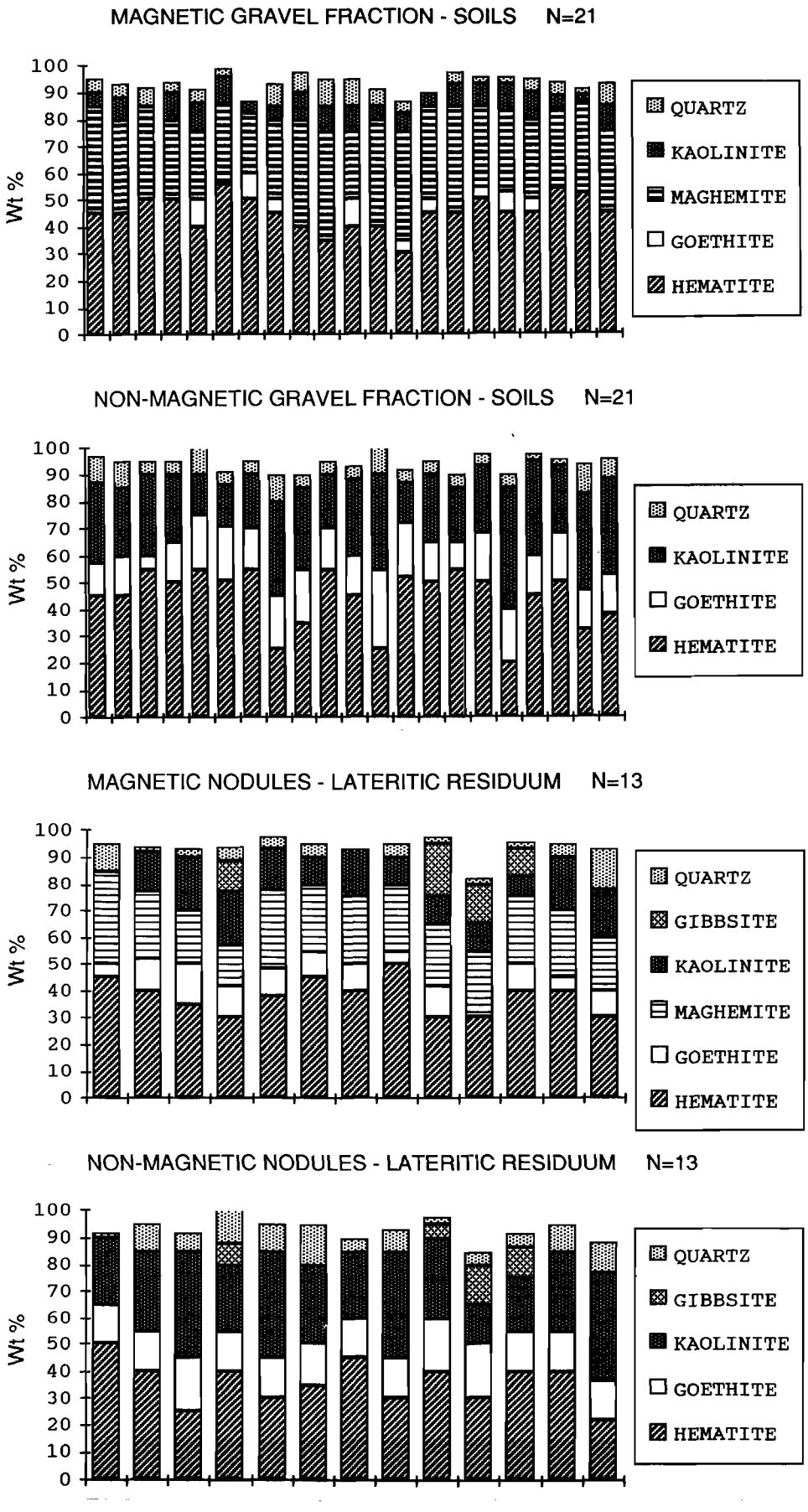

Fig. 22. Bar chart showing mineral abundances of an individual sample in four categories of samples.

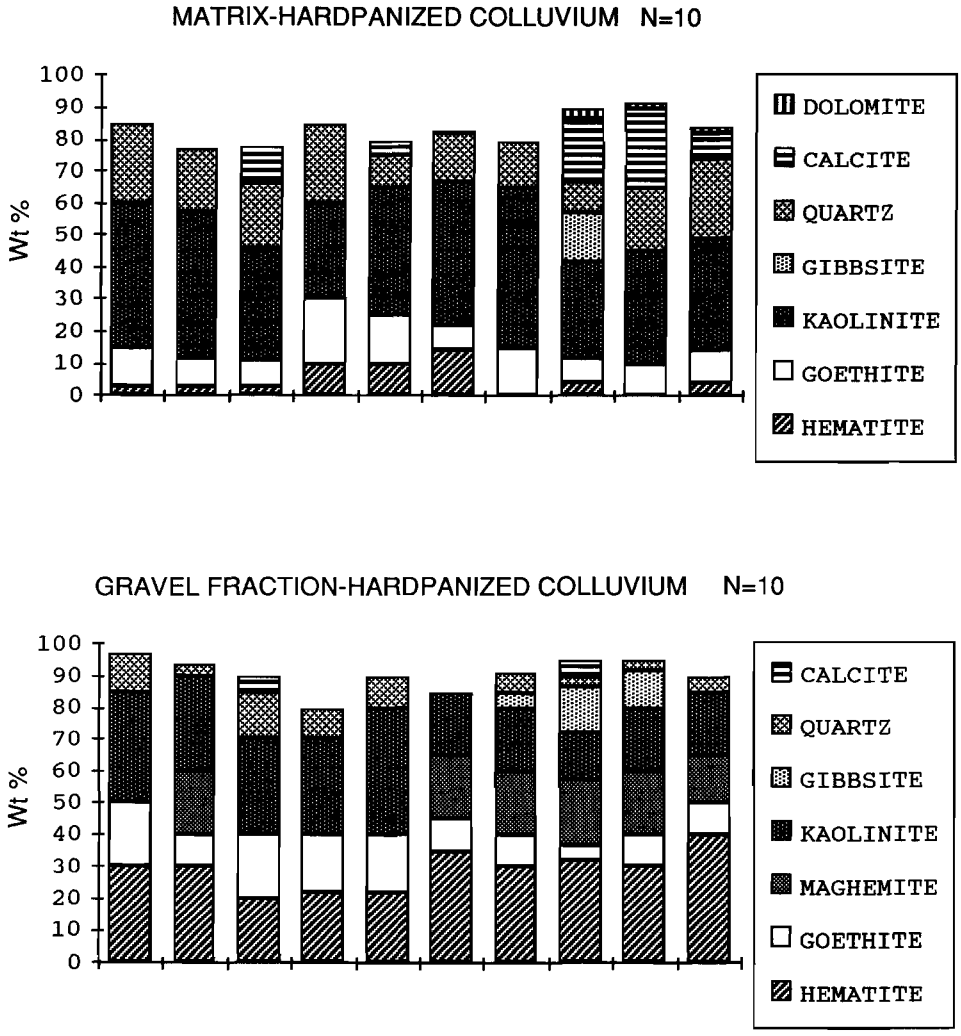

Fig. 23. Bar chart showing mineral abundances of an individual sample in four categories of samples.

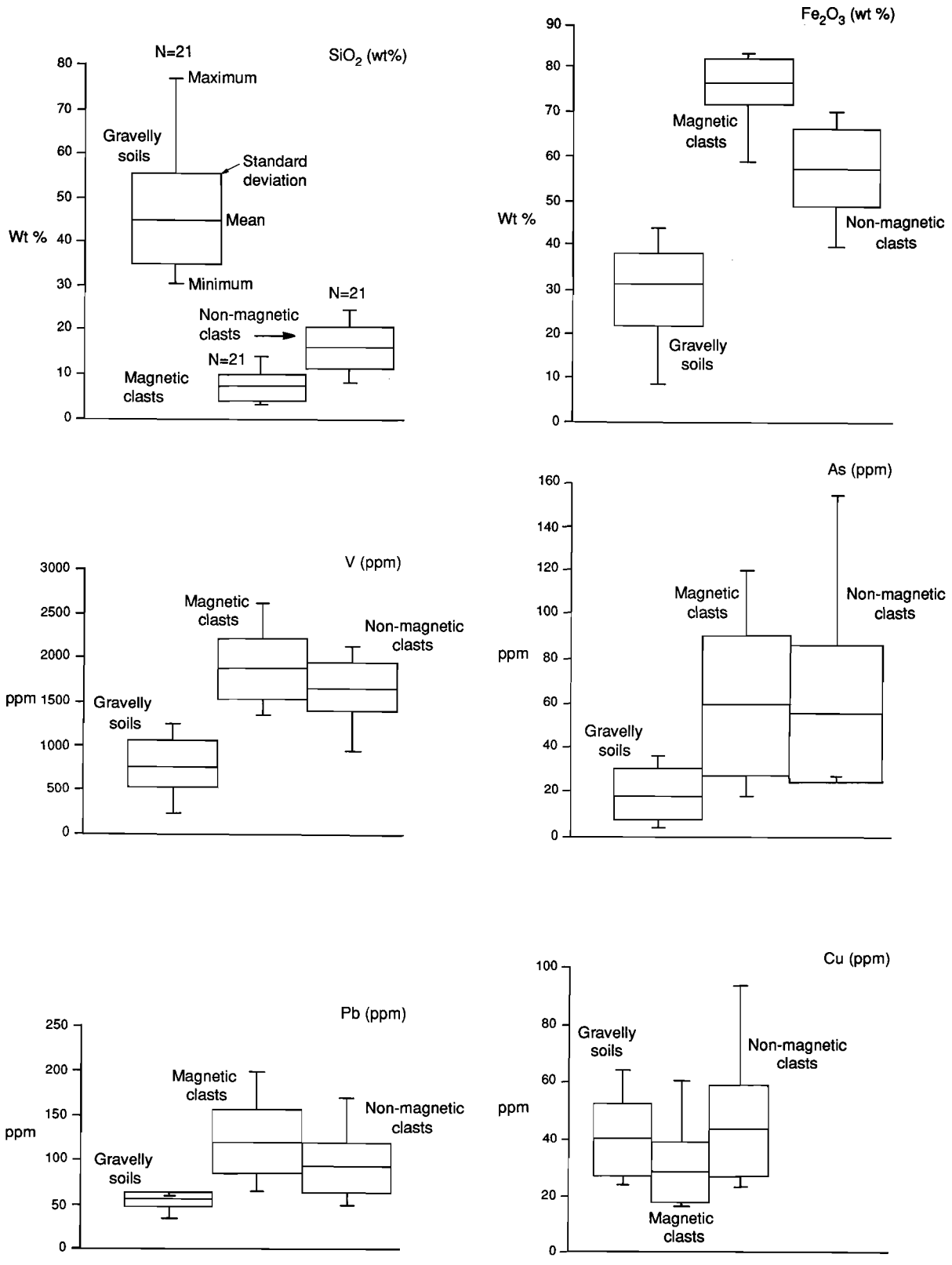

Fig. 24. Box plots showing distribution of SiO_2, Fe_2O_3, V, As, Pb, and Cu in magnetic and non-magnetic clasts separated from soils. Gravelly soils (complete) are included for comparison.

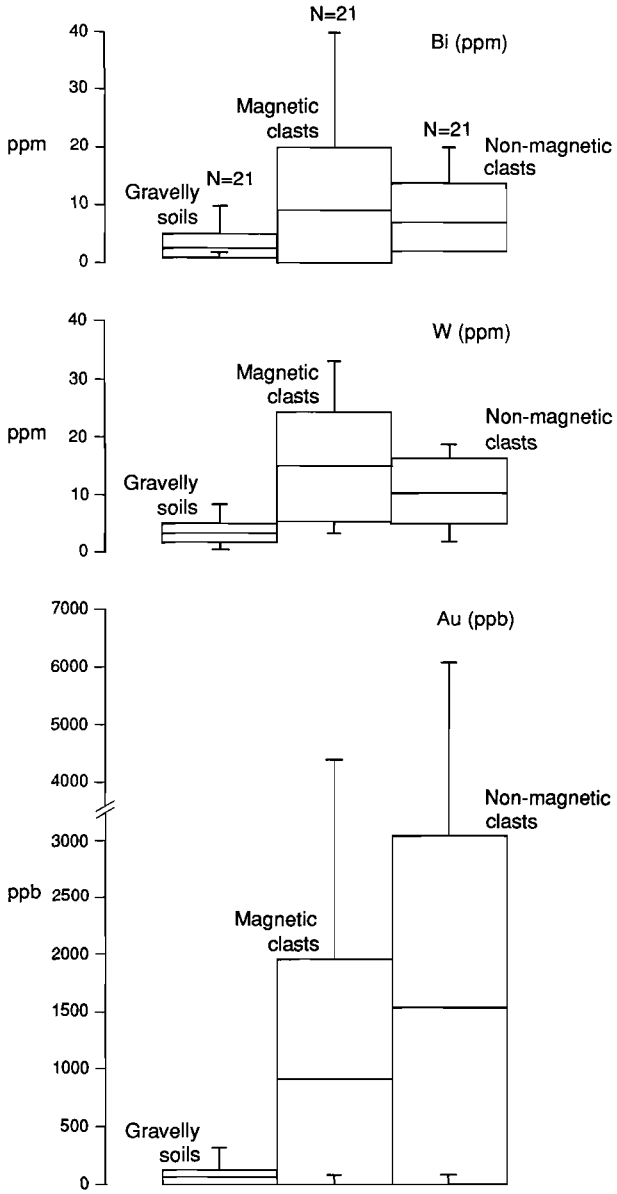

Fig. 25. Box plots showing distribution of Bi, W, and Au in magnetic and non-magnetic clasts separated from soils. Gravelly soils (complete) are included for comparison.

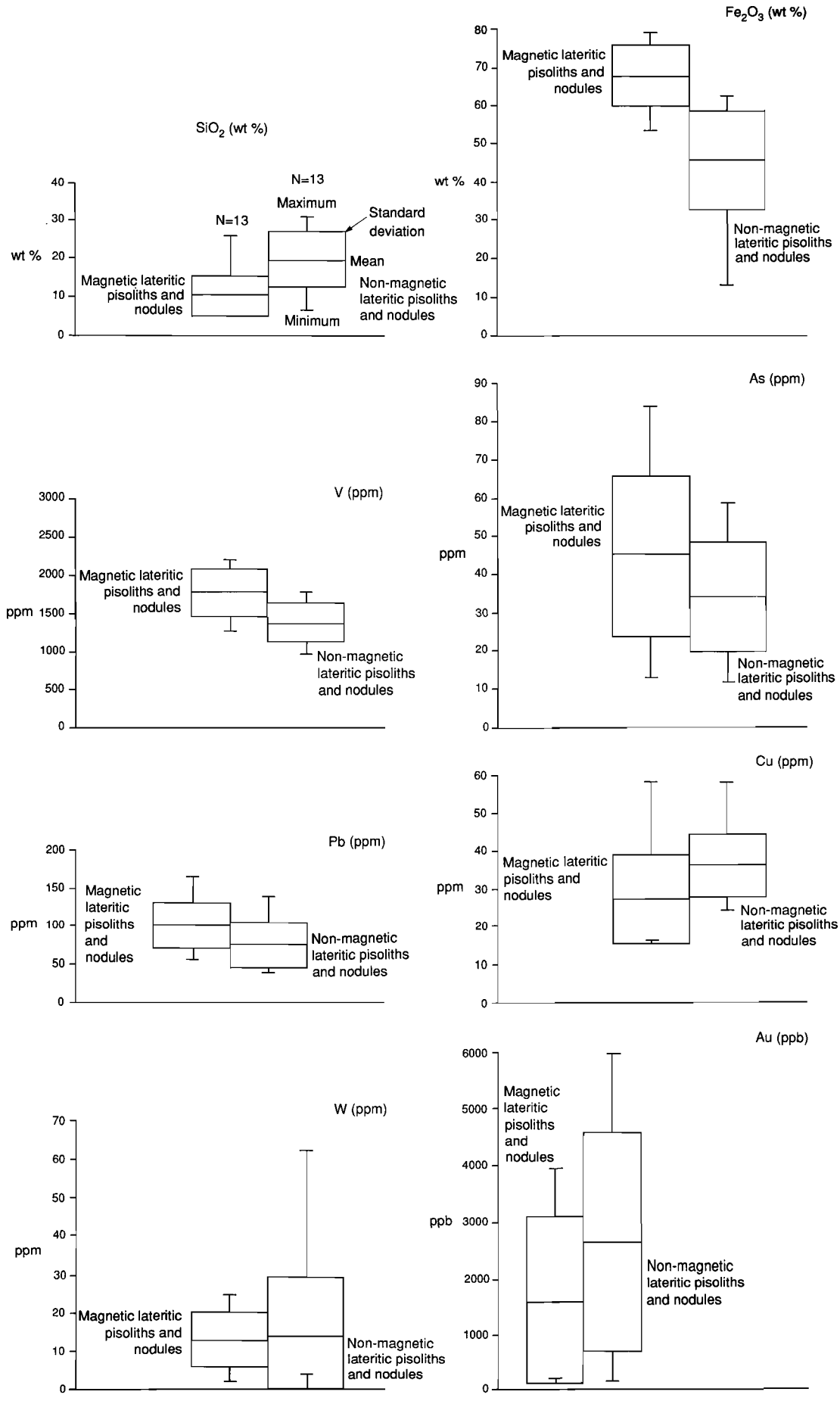

Fig. 26. Box plots showing distribution of SiO_2, Fe_2O_3, V, As, Pb, Cu, W, and Au in magnetic and non-magnetic pisoliths and nodules separated from lateritic residuum.

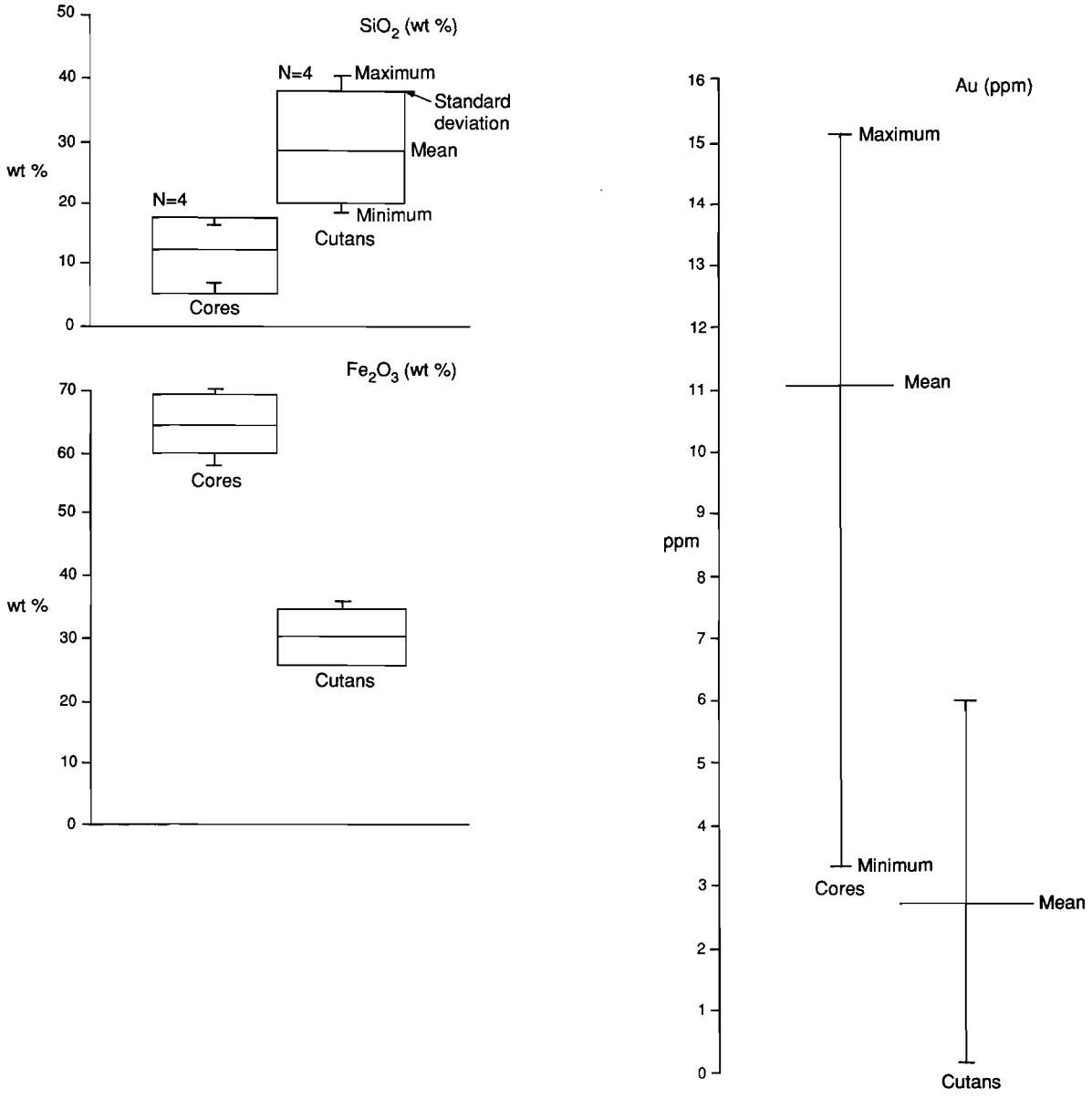

Fig. 27 Box plots showing distribution of SiO_2, Fe_2O_3, and Au in cores and cutans separated from loose pisoliths.

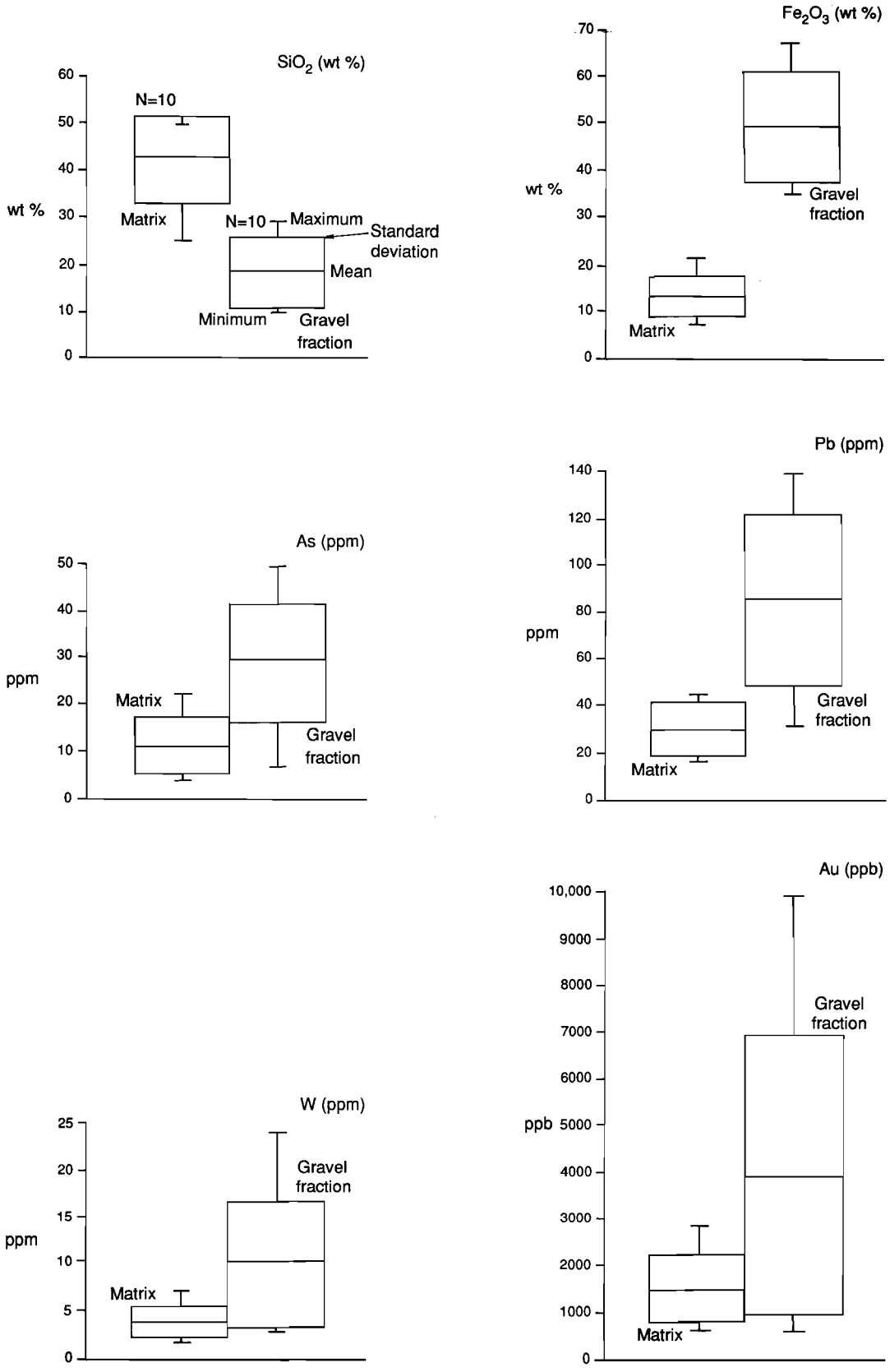

Fig. 28. Box plots showing distribution of SiO_2, Fe_2O_3, As, Pb, W, and Au in matrix and gravel fraction separated from hardpanized colluvium.

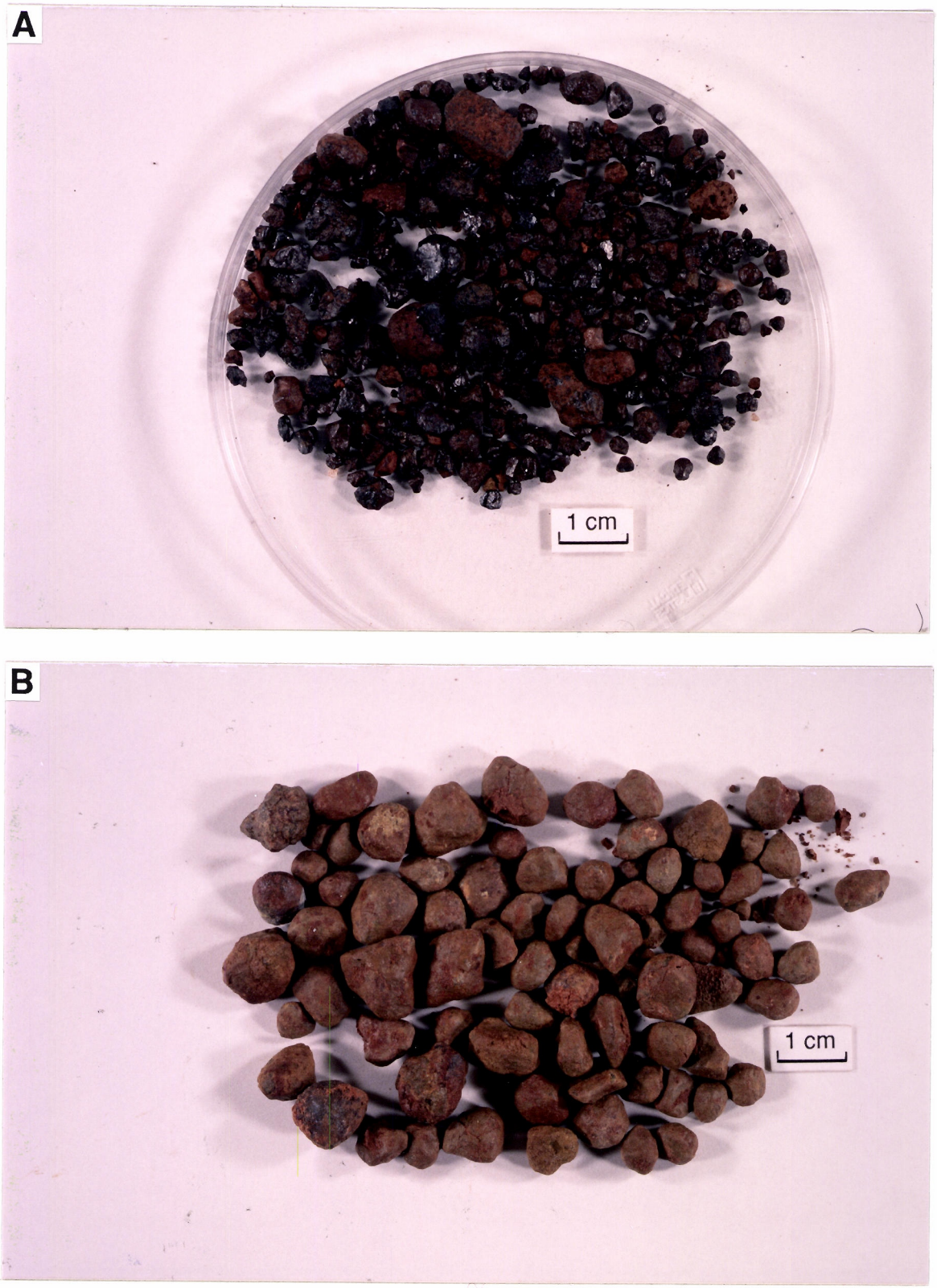

Fig.29A. Hand specimen of gravel fraction separated from acid red earth developed in colluvium. Note the low abundance of cutans, Location 1800N, 825E, Sample No.07-0253, S2 Pit.

Fig.29B. Hand specimen of lateritic nodules and pisoliths (LT103) separated from lateritic residuum. Pisoliths and nodules show 1-2 mm thick yellowish-brown cutans, typical of residual lateritic gravels, Location 2050N, 850E, Sample No.07-0266, S2 Pit.

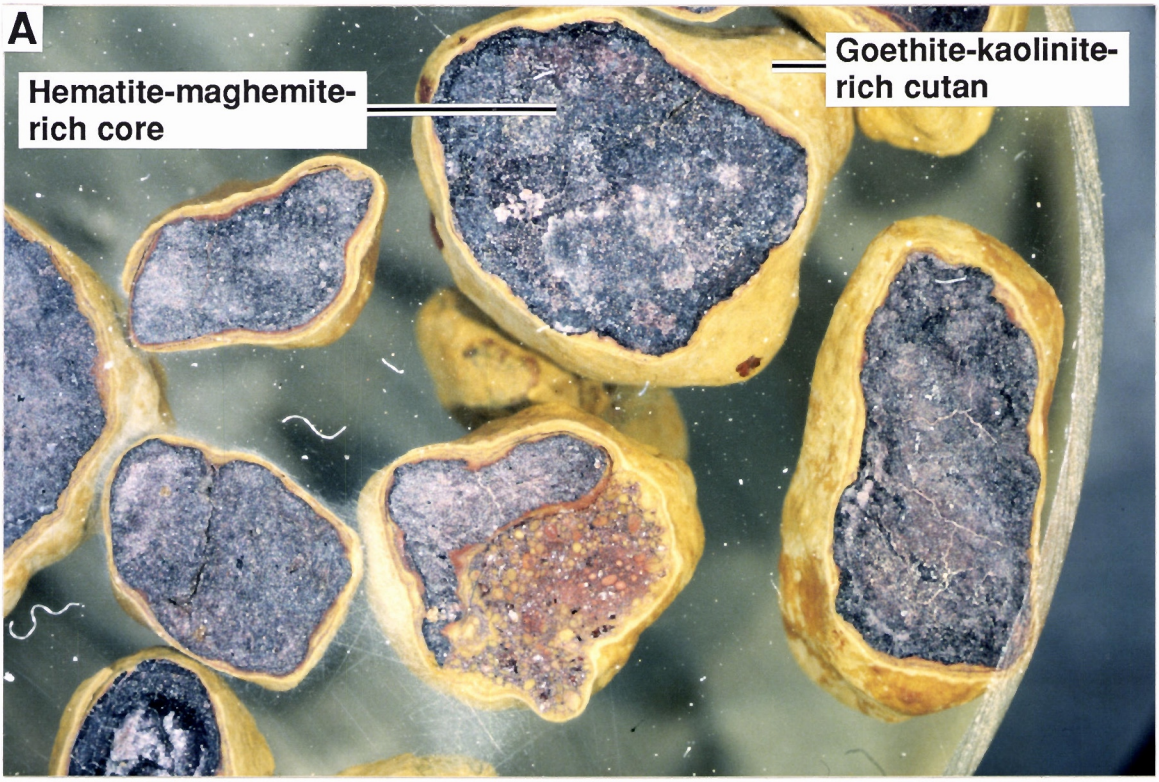

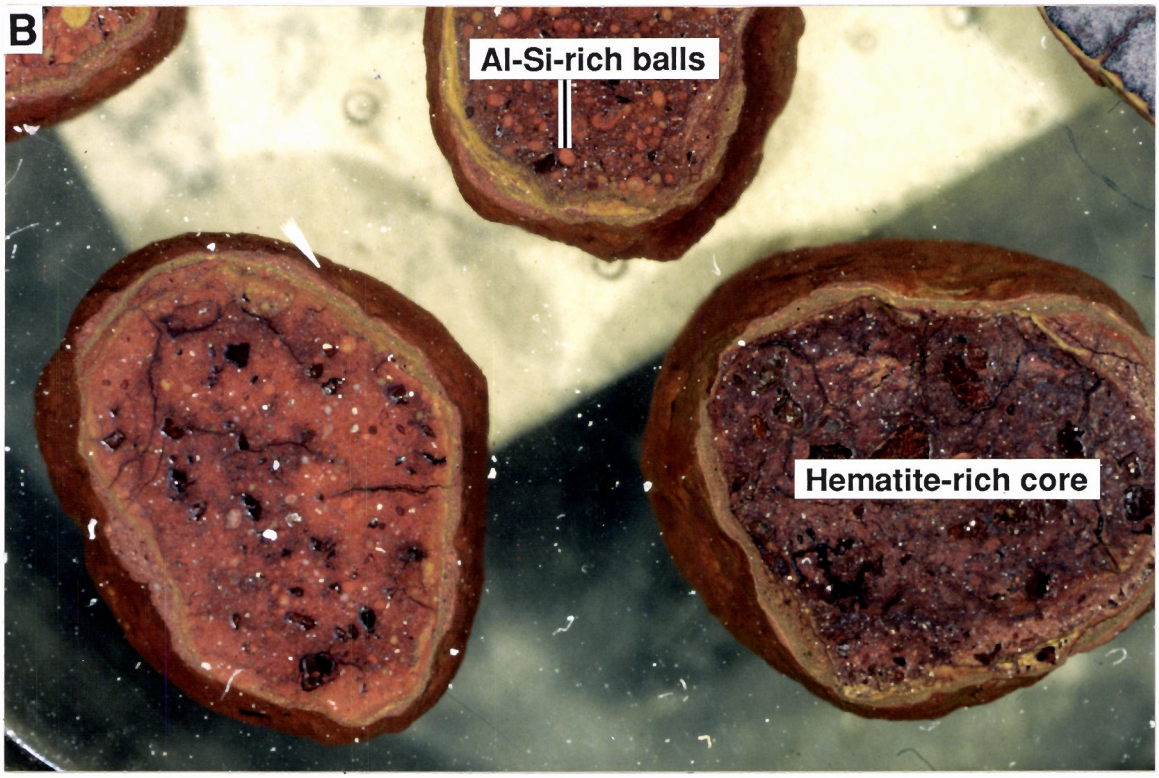

Fig.30A. Slice through magnetic nodules and pisoliths (LT103) from lateritic residuum, Location 1550N, 760E, Sample No.07-0792A, S1 Pit.

Fig.30B. Slice through non-magnetic pisoliths (LT102) from lateritic residuum, Location 1550N, 760E, Sample No.07-0792B, S1 Pit.

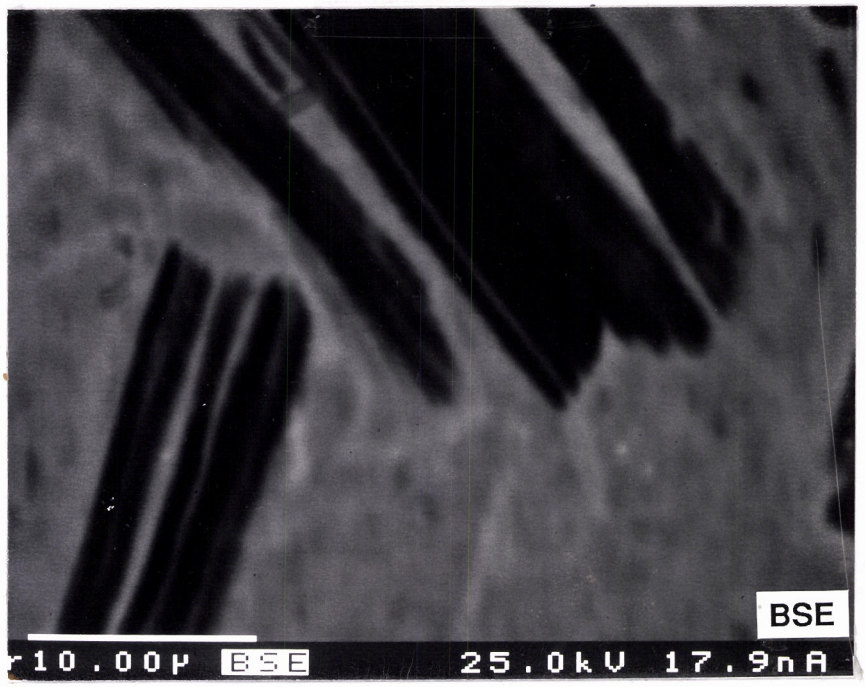

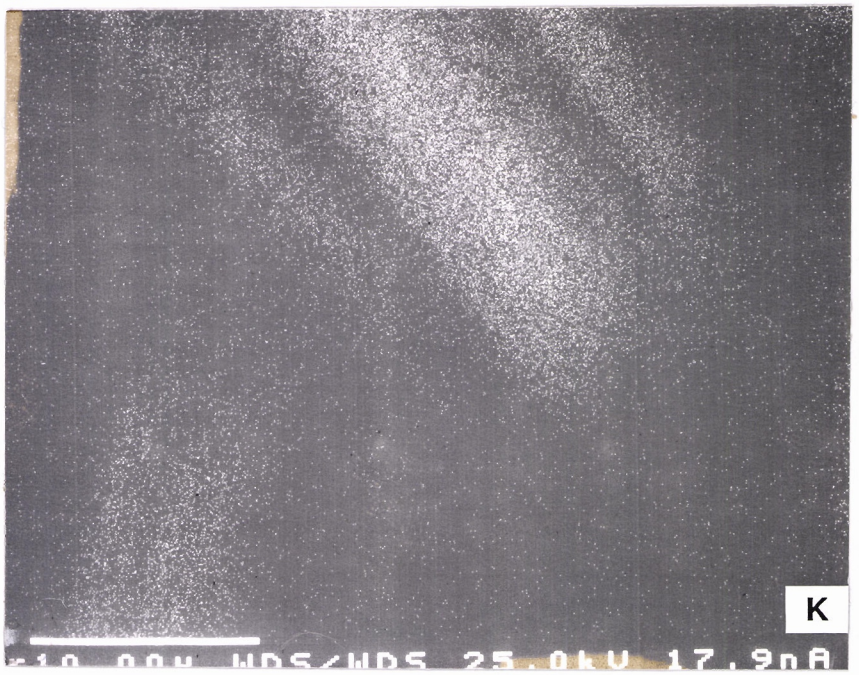

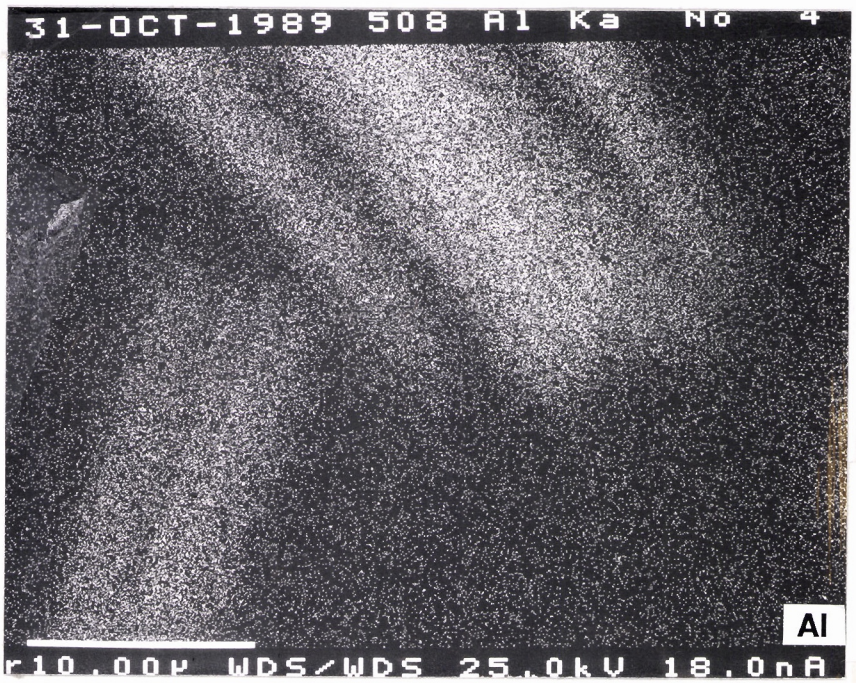

See caption next page

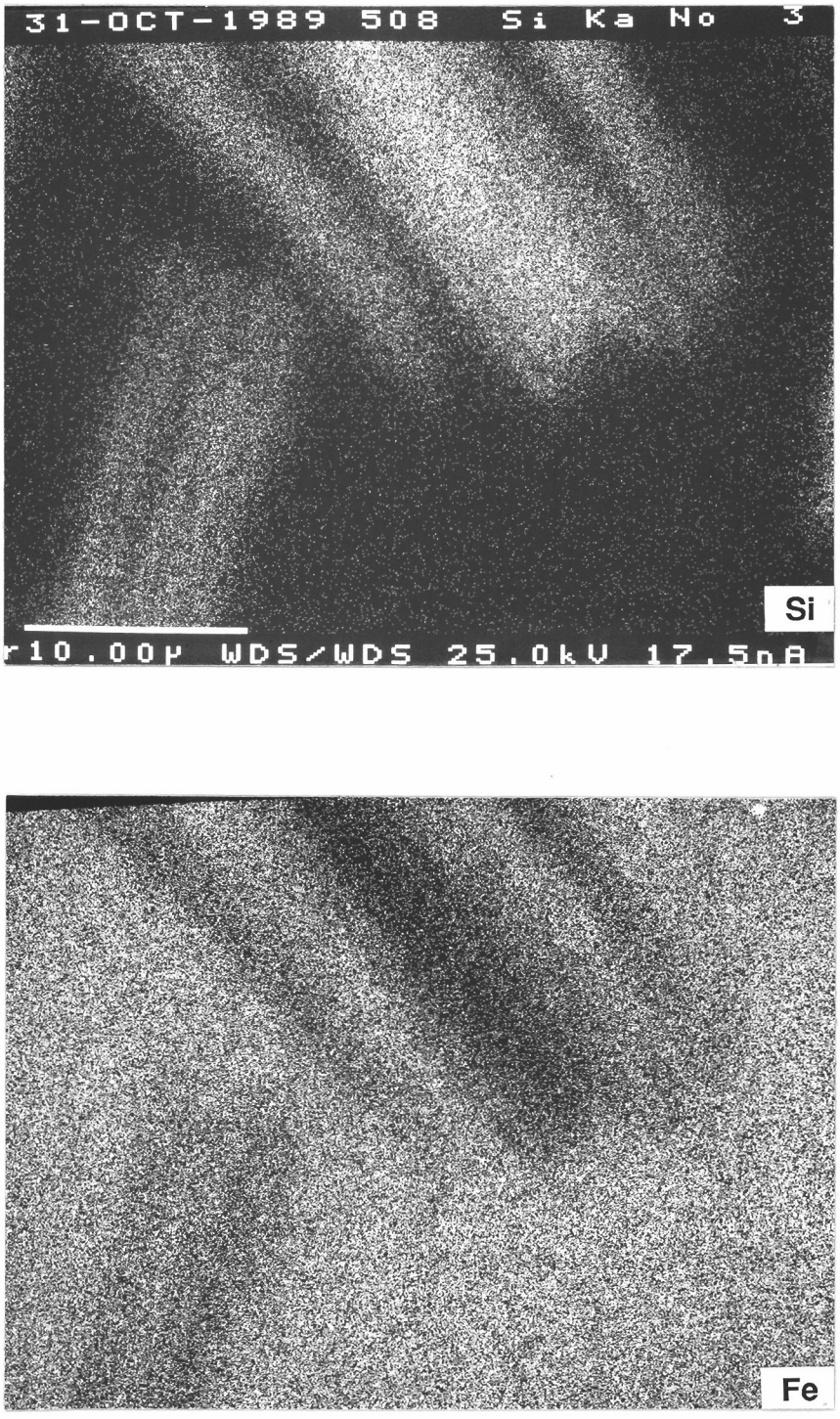

Fig.31. Electron microprobe back scattered electron image of part of a lateritic pisolith. X-ray images showing the distribution of K, Al, Si, and Fe, Location 1487N, 760E, Sample No.07-0510, S1 Pit.

7.4.2 MECHANICAL DISPERSION

Petrographic and SEM studies of polished sections of lateritic nodules and pisoliths have shown that much of the Sn occurs as a cassiterite (Fig. 32A). Cassiterite was also found to occur as inclusions in anatase/rutile grains. This suggests that Sn dispersed mechanically during laterite formation. Barium occurs primarily in the form of sulphate (Fig. 32B). Barite is resistant to weathering and can be retained in lateritic nodules as a residual primary mineral. Barium is also a constituent of feldspars and micas which, on weathering, release Ba into solution. The Ba reacts readily with sulphate, precipitating as barite. Barite was indeed also found to occur in the cutans of pisoliths. Barium therefore may not be a very useful element in geochemical exploration.

Titanium mainly occurs as anatase, rutile (Fig. 32C), and ilmenite. Anatase is the commonly occurring weathering product. Rutile and ilmenite are resistant to weathering and can be retained in lateritic pisoliths as residual primary minerals.

7.4.3 HYDROMORPHIC DISPERSION

A correlation matrix between the abundances of elements (Table 11) and electron microprobe analyses of Fe-oxide-rich and kaolinite-rich areas in lateritic pisoliths and nodules showed that As, Zn, Cu, Pb, Sb, Cr, V, and Mo, are intimately associated with hematite while Ni and Cu are associated with kaolinite and/or goethite.

Significant relationships are observed between mineralogical and geochemical variables. An Fe-oxide association is marked by a relationship between Fe, Cr, V, Pb, Sb, Mo, Ga, and Zr. Chromium, Pb, V, Sb, and Mo are also associated. These elements are correlated with hematite and maghemite, and are consequently more abundant in the magnetic gravel fraction. Nickel and Cu are strongly associated with kaolinite and goethite. Nickel is even more strongly correlated with kaolinite than with goethite. Consequently, these elements are more abundant in the non-magnetic gravel fraction and matrix of hardpanized colluvium. Electron microprobe analyses of many Fe-oxides rich areas have shown that As, Cr, and V may be associated with hematite and goethite (Table 11). In contrast, kaolinite-rich areas contained relatively-low concentrations of these elements. Electron microprobe analyses of goethite-rich phases have also shown the association of goethite with Cu (Table 12).

Manganese oxides are well known for scavenging trace elements as is expressed by the correlation of Mn with Zn. However, discrete Mn-oxide phases were not found. Electron microprobe analysis of goethite rich areas has shown the strong association of Zn with goethite (Table 11).

Strong correlations of Ti occur with Nb, V, Ga, Zn, and gibbsite. Petrogrpahic and SEM studies of polished specimens have shown that Ti mainly occurs as anatase and rutile. However, some Ti is also found to be bound within Fe-oxides, where Ti^{+3} substitutes for Fe^{+3} in goethite/hematite.

Gold correlates with Ag, Cu, kaolinite and goethite, these elements are more abundant in the non-magnetic gravel fraction.

The relative enrichment of various trace elements by Fe-oxides may be due to surface adsorption, co-precipitation with Fe-oxyhydroxides and oxides, and isomorphous substitution in the mineral. Iron in its octahedral position in the structure of Fe-oxides can be replaced by other metals. Aluminum is the best known example for this substitution, although other metals such as Mn, Co, Cr, Ni, and V, may also substitute for Fe. Arsenic, Sb, and Bi co-precipitate readily with Fe-oxides over a wide pH range and tend to be retained throughout the weathering process. For this reason they are very useful pathfinder elements. Organic matter can also be an important sink for minor elements, Filipek *et al.* (1981) having shown that organic materials can be more efficient scavengers of minor elements than Fe or Mn-oxides.

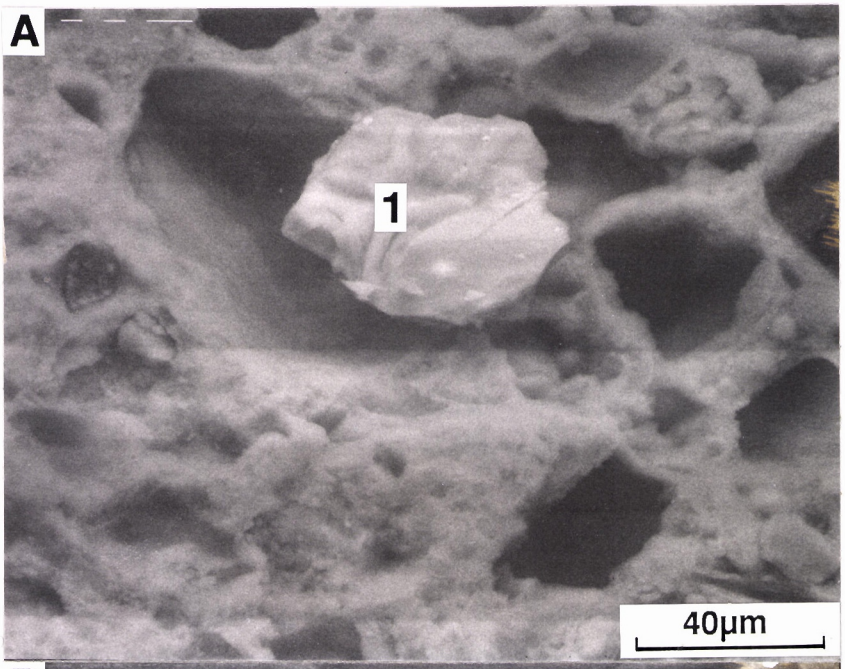

Fig.32A. Scanning electron micrograph of part of a lateritic nodule showing cassiterite grain (1) in goethite-rich matrix, Location 1950N, 900E, Sample No.07-0799, S2 Pit.

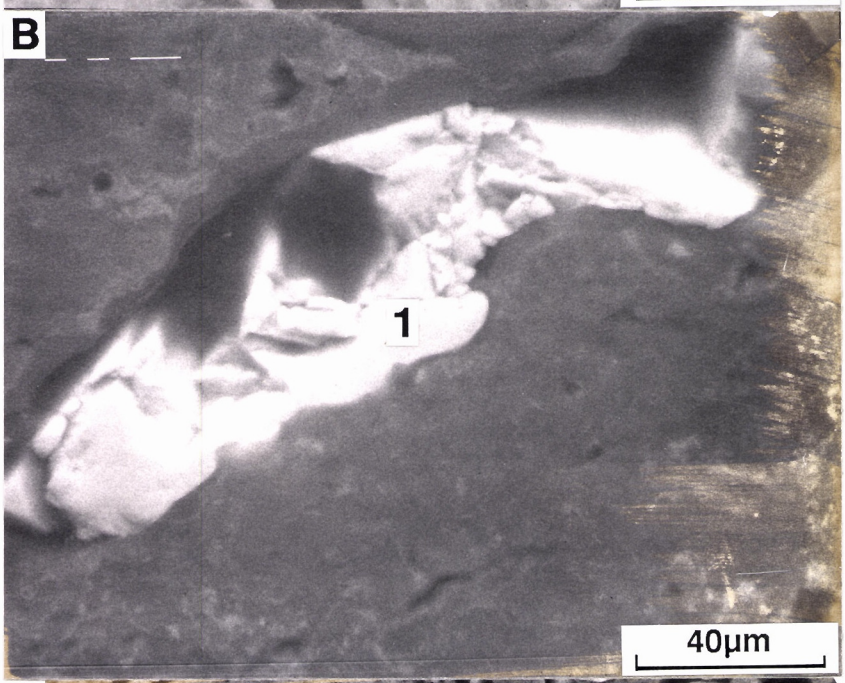

Fig.32B. Scanning electron micrograph of part of a lateritic nodule showing barite grain (1) in Fe-Al rich matrix, Location 1790N, 925E, Sample No.07-0323, S1 Pit.

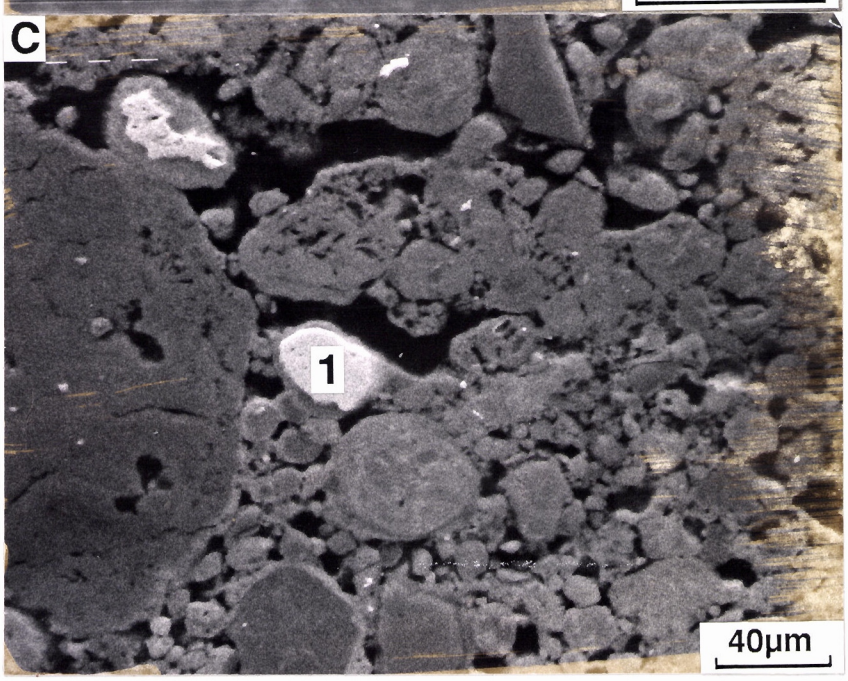

Fig.32C. Scanning electron micrograph of part of a lateritic nodule showing anatase/rutile grain (1) in Fe-rich matrix, Location 1950N, 900E, Sample No.07-0798B, S2 Pit.

Table 11. Correlation matrix for soils, hardpanized colluvium, calcrete and lateritic residuum.

	SiO2	Al2O3	Fe2O3	MgO	CaO	Na2O	K2O	TiO2	Ag	Mn	Cr	Cu	V	Pb	Zn	Ni	Co	As	Sb	Bi	Mo	W	Ga	Sn	Ba	Zr	Nb	Se	Be	Au	Hem	Goe	Mag	Kao	Gibb	Qtz
SiO2	1.00																																		
Al2O3	0.55	1.00																																	
Fe2O3	-0.81	-0.57	1.00																																
MgO	0.28	0.01	-0.63	1.00																															
CaO	0.08	-0.21	-0.53	0.77	1.00																														
Na2O	0.60	0.46	-0.70	0.51	0.35	1.00																													
K2O	0.64	0.16	-0.68	0.64	0.47	0.66	1.00																												
TiO2	-0.39	0.05	0.42	-0.36	-0.40	-0.13	-0.46	1.00																											
Ag	0.19	0.45	-0.20	-0.05	-0.11	0.20	-0.07	0.02	1.00																										
Mn	-0.36	-0.34	0.38	-0.08	-0.06	-0.22	0.05	-0.02	-0.17	1.00																									
Cr	-0.57	-0.33	0.75	-0.59	-0.50	-0.54	-0.63	0.40	0.03	0.01	1.00																								
Cu	0.40	0.51	-0.40	0.14	-0.04	0.42	0.29	-0.25	0.67	0.02	-0.29	1.00																							
V	-0.69	-0.43	0.87	-0.65	-0.56	-0.67	-0.72	0.54	-0.15	0.15	0.76	-0.38	1.00																						
Pb	-0.51	-0.37	0.70	-0.53	-0.43	-0.52	-0.55	0.31	-0.11	0.04	0.69	-0.30	0.64	1.00																					
Zn	-0.34	-0.45	0.41	-0.14	-0.09	-0.31	-0.04	-0.11	-0.09	0.59	0.15	-0.02	0.26	0.30	1.00																				
Ni	0.72	0.61	-0.49	-0.04	-0.20	0.35	0.32	-0.26	0.33	-0.15	-0.31	0.49	-0.42	-0.26	-0.11	1.00																			
Co	0.40	0.27	-0.30	0.09	0.03	0.32	0.39	-0.13	0.03	0.17	-0.29	0.24	-0.41	-0.32	-0.02	0.47	1.00																		
As	-0.35	-0.26	0.48	-0.36	-0.30	-0.48	-0.39	-0.10	-0.05	0.19	0.42	-0.04	0.49	0.36	0.29	-0.27	-0.35	1.00																	
Sb	-0.40	-0.31	0.56	-0.47	-0.38	-0.49	-0.49	0.25	0.06	-0.01	0.63	-0.22	0.64	0.79	0.33	-0.23	-0.37	0.45	1.00																
Bi	-0.27	-0.15	0.33	-0.26	-0.17	-0.35	-0.30	-0.01	-0.01	0.15	0.33	0.01	0.43	0.38	0.34	-0.06	-0.16	0.53	0.46	1.00															
Mo	-0.52	-0.25	0.60	-0.44	-0.37	-0.56	-0.49	0.18	-0.08	0.23	0.33	-0.16	0.48	0.53	0.42	-0.26	-0.11	0.32	0.46	0.43	1.00														
W	-0.36	-0.12	0.42	-0.33	-0.28	-0.40	-0.37	0.38	-0.02	0.01	0.34	-0.22	0.43	0.50	0.17	-0.23	-0.15	0.04	0.53	0.21	0.48	1.00													
Ga	-0.48	-0.12	0.57	-0.46	-0.44	-0.36	-0.47	0.51	-0.10	0.06	0.48	-0.23	0.60	0.45	0.12	-0.29	-0.12	0.07	0.27	0.20	0.56	0.47	1.00												
Sn	-0.06	0.25	0.02	-0.08	-0.17	0.09	-0.19	0.58	0.07	-0.02	0.07	0.03	0.06	0.01	-0.18	-0.07	0.12	-0.16	-0.10	-0.01	0.08	0.10	0.36	1.00											
Ba	0.46	0.20	-0.37	0.19	0.07	0.42	0.58	-0.16	0.06	0.05	-0.33	0.36	-0.39	-0.31	0.02	0.34	0.41	-0.30	-0.23	-0.14	-0.22	-0.19	-0.21	-0.14	1.00										
Zr	-0.37	-0.18	0.57	-0.51	-0.50	-0.37	-0.53	0.52	-0.04	0.15	0.56	-0.23	0.60	0.45	0.04	-0.21	-0.21	0.44	0.38	0.22	0.23	0.12	0.31	0.35	-0.30	1.00									
Nb	-0.19	0.18	0.18	-0.21	-0.30	-0.11	-0.29	0.59	-0.12	0.10	-0.08	-0.11	0.24	0.08	-0.01	-0.11	0.01	0.00	-0.04	0.09	0.38	0.30	0.47	0.63	-0.12	0.33	1.00								
Se	-0.27	-0.08	0.29	-0.29	-0.26	-0.39	-0.42	0.20	0.01	-0.03	0.27	-0.11	0.41	0.02	-0.02	-0.23	-0.21	0.28	0.07	0.17	0.22	0.17	0.22	0.04	-0.28	0.25	0.26	1.00							
Be	0.29	0.26	-0.17	-0.09	-0.18	0.17	0.15	-0.13	-0.01	-0.01	-0.26	0.26	-0.17	0.08	0.08	0.40	0.33	-0.11	0.01	0.00	0.16	0.05	0.01	-0.11	0.24	-0.22	0.10	-0.16	1.00						
Au	0.04	0.29	-0.09	-0.05	-0.09	0.18	-0.07	0.20	0.52	-0.19	0.06	0.38	0.04	-0.02	-0.17	0.03	-0.06	-0.14	0.01	0.00	-0.02	0.08	0.17	0.08	0.08	0.04	-0.04	0.04	0.06	1.00					
Hematite	-0.69	-0.44	0.88	-0.64	-0.53	-0.74	-0.70	0.33	-0.21	0.28	0.67	-0.39	0.82	0.63	0.31	-0.35	-0.31	0.48	0.53	0.30	0.58	0.38	0.49	0.02	-0.42	0.51	0.17	0.28	-0.18	-0.19	1.00				
Goethite	0.34	0.57	-0.32	-0.08	-0.15	0.08	-0.04	-0.07	0.40	-0.36	-0.13	0.49	-0.18	-0.16	-0.39	0.40	0.18	-0.04	-0.04	-0.02	0.01	0.00	-0.09	0.11	0.18	-0.16	0.03	0.10	0.22	0.26	-0.18	1.00			
Maghemite	-0.61	-0.61	0.70	-0.28	-0.22	-0.33	-0.30	0.32	-0.26	0.38	0.49	-0.40	0.55	0.46	0.43	-0.55	-0.24	0.26	0.35	0.24	0.33	0.22	0.40	-0.05	-0.20	0.40	0.11	0.17	-0.15	-0.05	0.37	-0.68	1.00		
Kaolinite	0.79	0.71	-0.64	0.09	-0.11	0.44	0.36	-0.33	0.32	-0.42	-0.37	0.49	-0.51	-0.34	-0.38	0.72	0.29	-0.19	-0.25	-0.22	-0.38	-0.23	-0.36	-0.05	0.29	-0.30	-0.21	-0.15	0.31	0.09	-0.48	0.58	-0.74	1.00	
Gibbsite	0.02	0.43	-0.17	0.09	-0.03	0.21	-0.07	0.49	0.37	-0.02	-0.15	0.20	-0.14	-0.26	-0.24	0.06	0.14	-0.23	-0.28	-0.04	-0.10	-0.01	0.04	0.57	-0.02	0.10	0.52	0.11	-0.02	0.21	-0.21	0.11	-0.10	-0.05	1.00
Quartz	0.81	0.30	-0.65	0.31	0.15	0.52	0.55	-0.22	0.03	-0.33	-0.42	0.22	-0.51	-0.40	-0.27	0.51	0.37	-0.33	-0.32	-0.16	-0.49	-0.30	-0.36	0.04	0.39	-0.22	-0.10	-0.20	0.19	-0.01	-0.59	0.19	-0.39	0.44	0.12	1.00

n = 116, p = 0.01, r = 0.25

Table 12. Electron microprobe analyses of various Fe-oxide-rich and clay-rich phases (average values).

Element	Kaolinite-rich areas (N=34)	Hematite-goethite-rich areas (N=19)	Bulk Composition
Sample No. 07-0319 - Mottled duricrust			
SiO_2(%)	43.15	7.73	50.27
Al_2O_3(%)	30.99	7.02	18.89
Fe_2O_3(%)	4.83	78.61	24.17
TiO_2(%)	0.80	0.65	2.13
Cr(ppm)	100	540	239
V(ppm)	800	5136	1850
As(ppm)	<60	600	103
Sample No. 07-0290 - Loose nodules			
	Goethite-rich areas (N=18)	Kaolinite-goethite-rich areas (N=13)	Bulk Composition
SiO_2(%)	7.20	26.31	26.52
Al_2O_3(%)	4.50	26.91	19.08
Fe_2O_3(%)	73.81	30.10	42.18
TiO_2(%)	0.12	0.06	0.65
Cr(ppm)	540	200	527
V(ppm)	1210	190	923
Cu(ppm)	940	170	300
Zn(ppm)	270	<50	28
Sample No. 07-300A - Loose pisoliths			
	Hematite-goethite-gibbsite-rich areas (N=27)	Kaolinite-gibbsite-rich areas (N=19)	Bulk Composition
SiO_2(%)	4.82	29.63	7.08
Al_2O_3(%)	22.14	44.85	19.27
Fe_2O_3(%)	68.80	6.85	63.92
TiO_2(%)	0.78	0.05	4.58
Zn(ppm)	830	<50	13

Hydromorphic dispersion probably has its maximum effect near the water table where the activity of the ore-forming elements is high and there is an ample supply of water. Some hydromorphic dispersion must also occur in the near-surface environment, since anlaysis of Fe-oxide-rich cutans around cores of pisoliths has shown them to contain anomalous Cu, Zn, and As.

7.5 Occurrence and Mineralogical Association of Gold

The determination of the location of Au in lateritic nodules/pisoliths, the matrix of hardpanized colluvium, and the calcareous fragments from calcretes was attempted by scanning electron microscopy of polished sections of many samples. The samples examined had concentrations exceeding 2 ppm. Gold grains were found in several samples of nodules/pisoliths. However, this was not the case for the hardpan matrix or the calcareous fragments where only two grains of Au were found.

Gold grains observed in the lateritic nodules/pisoliths occur as angular, subhedral to anhedral crystals largely in voids or cracks, which are either filled with kaolinite and goethite or empty (Fig. 33A). Some grains also occur on the surfaces of goethite-rich fragments. Less common are wires (Fig. 33B). The crystals range in size from 15-400 μm, most being between 20-100 μm. In one sample of loose pisoliths (07-0510), Au crystals occurred in the range of 200-400 μm.

Gold grains in the matrix of hardpanized colluvium also occur in silicified voids. These voids are generally lined with amorphous silica, poorly-crystalline kaolinite, and goethite. Gold grains were not detected in calcareous fragments using SEM. It is possible that Au in the hardpan matrix and calcareous fragments occurs as very fine particles or even as an adsorbed species, and hence would not be detected by SEM.

Under high magnification, some of the Au crystals show dissolution features and surface pitting. Both small and large voids are observed in the cores of nodules. Occassionally, these voids may be connected to each other, creating a bigger void which is filled with Au or highly-crystalline kaolinite and goethite. The cracks may have developed by a dissolution process or dehydration of goethite to form hematite.

Energy dispersive microprobe analysis shows that Ag in the Au grains is below the detection limit of the technique (~1%). Secondary Au is consistently described as being of high purity, and where assayed contains less than 0.6% Ag. High purity in secondary Au has previously been recognized as a criterion of secondary remobilization (Mann, 1984).

The close association of Au and Fe-oxides, morphology, and geochemistry (low Ag) of Au indicates that the Au analysed is dominantly secondary, having been remobilized and precipitated (Mann, 1984). During weathering, both the crystal morphology and composition will change as primary Au is dissolved and reprecipitated as secondary crystals. The physico-chemical conditions required for the dissolution of Au have been studied intensively (Boyle, 1979). The most common ionic species are Au^{+} and Au^{3+}. Ions in these oxidation states are unstable in solution. To remain in solution, the ions need appropriate ligands as well as suitable pH and Eh conditions. Possible ligand donor ions are OH^{-}, I^{-}, Br^{-}, Cl^{-}, SO_3^{2-}, $S_2O_3^{2-}$, and SO_4^{2-} (Boyle, 1979), some of these anions occur in percolating solutions under semi-arid conditions. In the semi-arid environments of Western Australia, Au is thought to have been remobilized and precipitated during saline groundwater conditions and reprecipitated by supergene processes (Mann, 1984; Gray, 1988). Processes operating during the formation of the lateritic nodules could also have contributed to the dissolution of Au particles. For example, the epigenetic replacement of kaolinite by hematite in the ferruginous zone involves the dissolution of kaolinite and the release of protons which may contribute to the dissolution of Au particles (Colin *et al.* 1989).

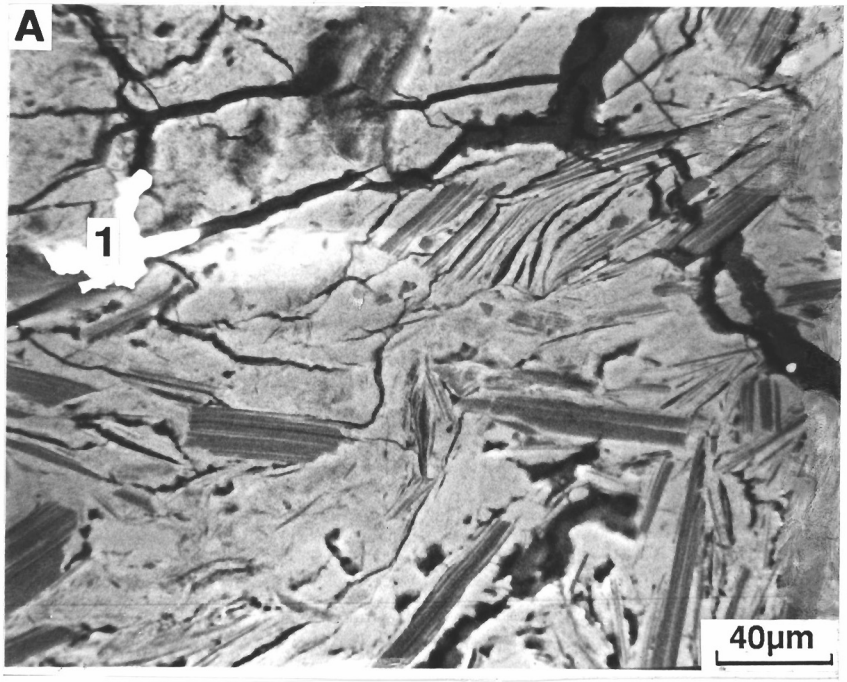

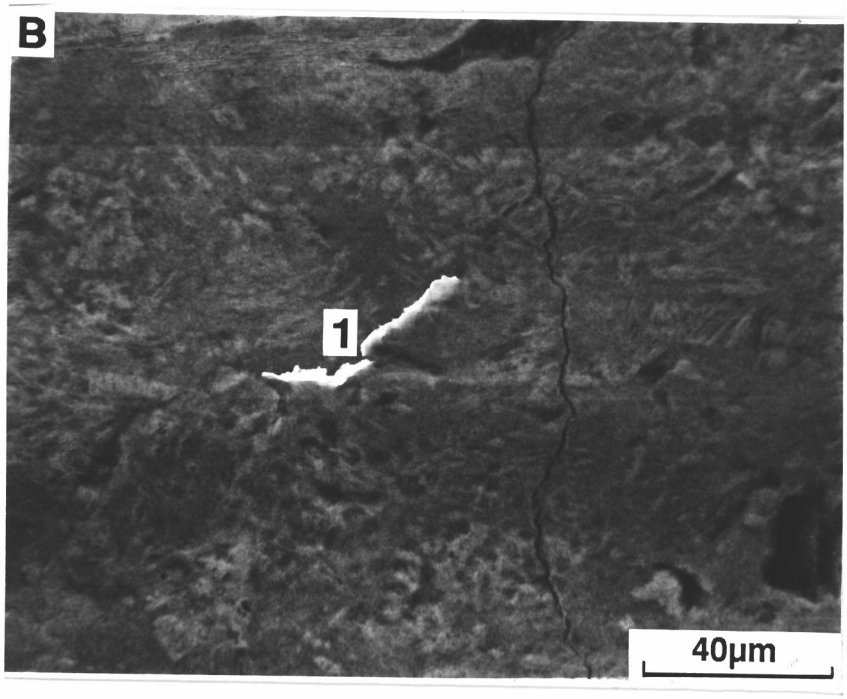

Fig.33A. Scanning electron micrograph of part of a lateritic pisolith showing an angular, anhedral crystal of Au (1) in a void. Matrix of pisolith shows geothite and kaolinite pseudomorphs after muscovite, Location 1510N, 775E, Sample No.07-0508, S1 Pit.

Fig.33B. Scanning electron micrograph of part of a lateritic pisolith showing wire-shaped crystal of Au (1) attached to the geothite-rich surface, Location 1510N, 775E, Sample No. 07-0508, S1 Pit.

7.6 Conclusions on the Siting and Bonding of Elements and Dispersion Processes

- The non-magnetic lateritic gravel fraction is the dominant fraction of both soils and laterite residuum. Magnetic lateritic clasts or nodules are generally smaller in size than the non-magnetic clasts or nodules. The external appearances of both the magnetic and non-magnetic gravel fractions are similar. However, they have different internal fabrics. The cores of magnetic clasts or nodules are black and massive, whereas those of non-magnetic clasts or nodules are yellowish brown and porous.

- There are significant differences in mineralogy between the two gravel fractions. Non-magnetic clasts or nodules contain higher amounts of goethite and kaolinite relative to magnetic clasts or nodules, while maghemite is present only in the magnetic clasts or nodules. Hematite is the dominant mineral of both the gravel fractions. Cutans are dominated by goethite. Gibbsite occurs only in small amounts which can be taken as an indicator of low leaching conditions during an arid climate.

- The matrix of hardpanized colluvium (red-brown hardpan) largely consists of kaolinite, quartz, hematite, and amorphous silica. The red colour of the hardpan is due to the presence of hematite which is a product of the current arid climate.

- Both the magnetic and non-magnetic gravel fractions are anomalous in chalcophile elements. However Fe, Cr, V, Pb, As, W, Sb, Bi, and Zn are enriched in magnetic nodules relative to the non-magnetic nodules. By contrast, Au, Al, Si, Cu, Ag, and Ni are relatively more abundant in the non-magnetic nodules.

- Several significant correlations occur between elements and minerals. From the correlations, the following affinity groups were recognized:

  Fe, Cr, V, Ga, Pb, As, Sb, Zr, hematite, maghemite;
  Al, Cu, Ni, Ag, Au, goethite, kaolinite.

- Zinc, As, Pb, Cr, V, and Sb dispersed hydromorphically and are strongly associated with Fe-oxides. Barium and Sn occurred as barite and cassiterite, respectively.

- Gold is much more abundant in the non-magnetic nodules relative to the magnetic nodules. The differences in the amounts of Au may be due to differences in the nature of the mineralogy of the two fractions.

- The non-magnetic lateritic nodules are a better sampling medium for Au exploration at the Mt. Gibson Au deposits. Non-magnetic clasts separated from soils developed in colluvium can also be used as a first pass sampling medium in regolith situations where the source and distance of transportation of the materials can be established.

- Cores of nodules contain higher amounts of Au than the cutans.

- The matrix of hardpanized colluvium (hardpan) is highly anomalous in Au and Ag which possibly reflects the original levels in the source material. However, introduction of Au in the later stages in the hardpan development may not be completely ruled out.

- Calcareous fragments separated from calcrete are anomalous in Au.

- Gold observed in the lateritic nodules occurs as irregular subhedral to anhedral crystals in cracks which are either filled with goethite and kaolinite or empty. Gold crystals also occur on the surfaces of goethite. These forms of Au, however, form a small proportion of the total Au.

8.0 OVERALL DISCUSSION AND CONCLUSIONS

8.1 Regolith Evolution and Distribution of Elements

8.1.1 LATERITIZATION PROCESSES

The regolith stratigraphy at the Mt. Gibson district comprises lags, soils, hardpanized colluvium, lateritic residuum, hardpanized lateritic residuum, calcrete, and silcrete. It contains components of the regolith stratigraphy seen elsewhere in the Yilgarn, for example in the Leonora and Kalgoorlie regions. At Mt. Gibson, both red-brown hardpans and pedogenic carbonates are extensively developed in both transported and residual materials. This is in contrast to the Lawlers and Bottle Creek areas where pedogenic carbonates are either absent or present only in minor amounts.

The lateritization and post-lateritization processes, probably related to the changes in climate, are responsible for the evolution of the variety of regolith types in the Mt. Gibson district. These processes, summarized in Fig. 34, are briefly described below.

8.1.1.1 Lateritic Residuum

The lateritization probably took place in response to tropical/sub-tropical weathering, at a then stable water table and was then accompanied by major leaching of the underlying material. Lateritic residuum, can be as thick as 6 metres and comprises several fabric types (pisolitic, nodular, or fragmental). Iron released by the weathering of ferromagnesian minerals circulates upwards in the groundwater, is oxidized at the redox interface and precipitates as Fe-oxides to form a ferruginous zone. Nodules are initiated by small scale migration and segregation of Fe as mottles. Higher up the profile, the mottles evolve into nodules and pisoliths. These pisolitic, nodular structures are common in the S, C, N, and Midway North Pits. The mode of formation of these nodules and pisoliths (lateritic residuum) differs somewhat from that of the Lawlers district where the lateritic residuum is primarily formed by the fragmentation of the ferruginous saprolite. Ferruginous saprolite forms a continuous blanket deposit in the Lawlers area and is formed by the infusion of Fe into clay-rich saprolite. The differences in regolith stratigraphy (presence or absence of ferruginous saprolite) and in the mechanism of formation of nodules/pisoliths between the two areas are probably due to the differences in the amount of Fe available for the formation of the regolith. The Lawlers district is dominated by a suite of mixtures of mafic and ultramafic lithologies. These contrast with the mafic volcanics and hyperbyssal rocks, felsic volcanics, and felsic-metasedimentary rocks of the greenstone sequence at Mt. Gibson.

Several hypotheses have been put forward for the mechanism of enrichment of Fe in the ferruginous zone. Several workers have advocated that laterites form in sediments that unconformably overlie either bedrock or saprolite. It has been established from this and other work that many classes of laterites are dominantly residual, and, to a degree, reflect the underlying lithologies and associated mineralization, although there may have been considerable modification. Primary Au mineralization at Mt. Gibson (S, C, N and Midway North Pits) is indicated by a broad Au anomaly in the lateritic residuum (Anand *et al.*, March 1989 and this report). Mineralization is also indicated by higher concentration of other ore-related elements, principally As, Pb, Ag, W, Sb, and Bi. These anomalies have wider, consistent haloes.

One of the principal characteristics of the lateritic weathering profile is the tendency for its chemical and mineralogical composition to be dominated by the three elements Si, Al, and Fe in the form of kaolinite, quartz, and Fe-oxides (hematite, goethite, and maghemite). The distribution of Au, As, Cu, Pb, Zn, Ag, and Bi is controlled wholly or in part by the distribution of hematite, goethite, and kaolinite. This is clearly shown by the differences in abundances of these elements in magnetic and non-magnetic fractions. Hematite is the major mineral in both the fractions and appears to have a strong affinity for As, Pb, Zn, Bi, Cr, and V. These elements are therefore abundant in both the fractions; however, it is the difference in the abundances of goethite between the two fractions which appears to determine the abundances of Au, Cu, and Ag.

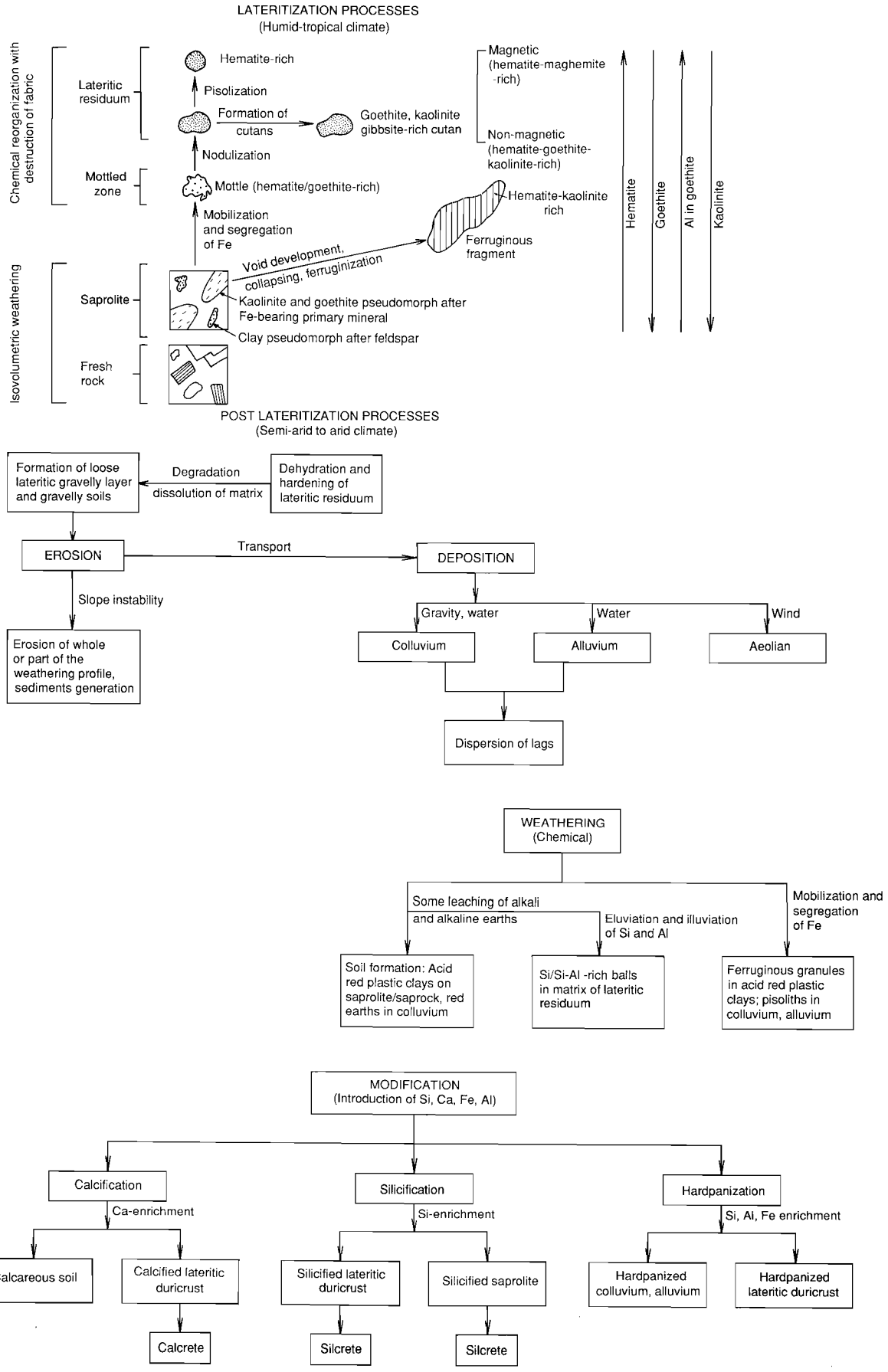

Fig. 34. Flow chart showing processes responsible for the evolution of the variety of regolith types in the Mt. Gibson district.

They are more abundant in the non-magnetic fraction and hence this is a better sampling medium for Au exploration at the Mt. Gibson Au deposits.

The presence of Au in the lateritic nodules and pisoliths is related to the humid-tropical conditions during the formation of the ferruginous zone. Most of the Au in the regolith is presumed to be secondary on the basis of its morphology and composition. Acid oxidizing environments are favourable for Au mobilization either as organic, thiosulphate, or chloride complexes, and reprecipitation as fine grained particles, with secondary Fe-oxides. Gold is in both hematite-rich cores and goethite-kaolinite-rich cutans. The level of abundance is, however, relatively low in cutans. The cutans are formed by the concentric concentrations of Al and Fe-rich solutions around a nucleus and therefore may not have a direct genetic link with the formation of material that comprises the nucleus. This suggests that Au enrichment in cores and in the cutans did not occur at the same time and indicates that Au has been mobile during several periods of regolith development.

Origin of magnetic and non-magnetic lateritic nodules and pisoliths

Nodules in the lateritic residuum are formed by migration and segregation of Fe. Minerals constituting the nodules and pisoliths are the same as those present in the corresponding matrix, but generally the kaolinite and quartz contents are smaller and the content of Fe-oxides is greater. Analyses of areas within the cores of nodules suggest replacement of kaolinite by hematite and goethite leading to the formation of Fe-rich nodules. Mobilization and concentration of Fe in nodules can be accomplished by three main processes: (i) movement in suspension of colloidal material; (ii) reduction of Fe^{3+} phases to soluble and mobile Fe^{2+} and migration of Fe^{2+} into the nodules where it precipitates as Fe^{3+} oxides; and (iii) formation of soluble Fe^{3+} complexes that migrate into the nodules (Coventry *et al,* 1983). Process (ii) appears to have operated in the formation of nodules and pisoliths at Mt. Gibson. The greater concentration of Fe minerals and presence of maghemite which contains minor amounts of Fe^{2+} (Taylor and Schwertmann, 1974) indicates that Fe may have been mobilized as Fe^{2+}. Migration of Fe is known to occur under a reduced state because of the differences in the oxido-reduction potential (Eh) that exists continuously within lateritic weathering profiles. Furthermore, in a reducing environment, concentration of ferrous ions other than Fe^{2+} are negligible. In this case, concentration of total ferrous ions of percolating or diffusing solutions can be considered as being that of the simple Fe^{2+} ion. The formation of hematite or goethite from these solutions is governed by a number of factors, among which soil temperature, water activity, organic matter, pH and Al concentration are the most important.

In nodules and pisoliths, hematite is more abundant than goethite. The presence of high amounts of hematite in nodules and pisoliths has been observed in several other studies (Taylor and Schwertmann, 1974; Anand and Gilkes, 1987a). Both goethite and hematite can form from ferrihydrite, but ferrihydrite is believed to be a necessary precursor for hematite (Schwertmann, 1988). Goethite may form by dissolution of ferrihydrite and subsequent reprecipitation, whereas hematite forms through an internal rearrangement of ferrihydrite. These propositions are not proven and hematite certainly also forms by dehydroxylation of goethite and by oxidation of magnetite (Anand and Gilkes, 1984; Wells *et al.*, 1989). Goethite can form directly from primary Fe-containing minerals, and from lepidocrocite. Observations made in synthesis experiments suggest that high values of pH, Ca and Mg in the pedoenvironment and a higher rate of Fe supply may favour formation of hematite over goethite during weathering of mafic rocks. This is consistent with the lower goethite/(goethite + hematite) ratio for lateritic pisoliths and nodules observed in this work.

Many hypotheses have been given for the formation of maghemite in soil (e.g. oxidation of magnetite, oxidation of green-rust at pH 7-8, transformation of other pedogenic oxides by heating at approximately 300-500°C in the presence of organic matter). The mechanism of maghemite formation proposed by Coventry *et al.,* (1983) is that a fluctuating water table concentrates Fe^{2+} in soil pores and subsequent oxidation leads to the formation of hematite and/or maghemite. Rapid oxidation of all Fe^{2+} in such situations could lead to the precipitation of ferrihydrite (precursor of hematite) whereas slower oxidation, which allows an interaction

between Fe^{3+} hydroxy species formed on oxidation and remaining Fe^{2+} hydroxy species in solution would yield maghemite. Although reducing conditions do not occur in the near surface horizons of lateritic profiles in the Mt. Gibson area at the present time this might have been possible in the past. Formation of maghemite due to heating by bushfires which occur frequently in uncleared forests may also be a mechanism and this origin is supported by the association of corundum and maghemite in laterites in the Darling Range, WA (Anand and Gilkes, 1987b).

Aluminium substitution in goethite in lateritic nodules and pisoliths is high (19 mole % - mean) which is consistent with the results of several other authors (Fitzpatrick and Schwertmann, 1982; Anand and Gilkes, 1987a) who have found generally high levels of Al substitution (20-35 mole %) in goethites from laterites and bauxites. The degree of Al substitution in the Mt. Gibson laterites is similar to the Lawlers laterites (18 mole % - mean), but differs markedly from the Darling Range lateritic bauxites (27 mole % - mean). These different levels of Al substitution in goethite between the three areas suggest different environments for their formation. High substitution reflects weathering in an environment with a high degree of Al availability which is then incorporated in the goethite structure. Goethites in the Mt. Gibson and Lawlers laterites contain relatively low Al substitution which is due to the relatively low degree of weathering as indicated by the low gibbsite content of laterites. In contrast, Darling Range lateritic bauxites are characterised by high gibbsite contents. Where goethite is associated with gibbsite (as in bauxites), its structural Al content tends to be the highest. Fitzpatrick and Schwertmann (1982) believed that both the presence of gibbsite and highly Al-substituted goethite characterize a pedogenic environment where the Al activity is high and where goethite competes with gibbsite for dissolved Al during crystal growth.

8.1.2 POST-LATERITIZATION PROCESSES

Post-lateritization processes in the Mt. Gibson district include the following:

- Dehydration and hardening of lateritic residuum;
- Erosion of whole or part of the weathering profile;
- Deposition of detritus generated from the erosion;
- Weathering of the exposed regolith; and
- Modification of the transported and residual regolith.

The above processes can be related with a general change to a drier climate for the inland parts of Yilgarn, a change which has probably taken place since the mid-Tertiary, the first arid period believed to have been late Miocene, with cycles of aridity continuing to the present. The arid to semi-arid climates, which still prevail, have resulted in modifications to the pre-existing profile due to the development of acid and highly-saline groundwaters, a general lowering of watertables and changes to, and decline of, chemical weathering. Vegetation changed with climate, resulting in slope instability. Truncation of the lateritic profile, in particular on the upper slope convexities, has resulted in burial of the lateritic profile on adjacent foot slopes and valley floors. Both complete and truncated profiles are buried beneath the valley sediments. Residual laterite is widespread under the sediments, and it is generally thicker in valley floors than on footslopes and crests. Sediments can be of mixed origin (granitic, mafic) and may contain abundant lateritic debris. In drilling programmes designed to detect buried geochemical haloes, it is important to distinguish colluvial units which contain abundant lateritic pisoliths and nodules from residual lateritic gravels.

8.1.2.1 Acid Red Earths

Acid red earths containing varying amounts of lateritic debris have developed in colluvium and these soils show very little or no profile development , i.e. A and B horizons. Gravelly acid red earths are anomalous in Au, As, Pb, Zn, Bi, and Ag; however, the soils without gravels are low in these elements. Furthermore, the separation of magnetic and non-magnetic clasts from these soils suggested that most of the Au, As, Pb, Zn, and Bi are associated with Fe-oxide rich clasts. Fine matrix comprising quartz, kaolinite, and hematite is poor in these elements. Hence clasts

separated from acid earths can be used as a first pass sampling medium in situations where the source and distance of transportation can be established.

8.1.2.2 Hardpanized Colluvium, Hardpanized Lateritic Residuum

Hardpanization processes (cementation by amorphous Si, Al, Fe) have not only affected colluvium and alluvium but also lateritic residuum at Mt. Gibson. Hardpanization is commonly developed within the upper several metres of the regolith. Generally in the Mt. Gibson district, the maximum depth of hardpan is about 10 m. A well-developed hardpan is not common in the erosional regimes. The process of hardpan formation appears to involve the infusion of Si dominantly with lesser Fe and Al by authigenic deposition. Carbonates are common in the hardpanized colluvium and are interpreted to have been deposited after the hardpan had formed. Hardpanization is relatively a recent process and is believed to be in equilibrium with the present arid climate. Hence, Fe-oxides formed in these materials (mainly hematite and some goethite) probably by the *in situ* breakdown of Fe-bearing silicates (such as amphiboles, biotite) and non-silicate grains (ilmenite and magnetite) by alkaline water. This weathering environment has also resulted in the formation of some smectite and illite.

Gold occurs in higher concentrations in both fine matrix (kaolinite, amorphous silica, hematite, goethite) and clasts of hardpanized colluvium at Mt. Gibson. This is in contrast to acid red earths in which much of the Au occurs in the clasts. The Au-enrichment in the hardpan matrix may reflect the original levels of Au in the materials derived from the erosion of the upper part of the weathering profile. Introduction of Au into the hardpan matrix at a much later stage is also a possibility.

8.1.2.3 Acid Red Plastic Clays, Calcareous Clays, Nodular Calcrete

Calcareous clays overlying acid red plastic clays are a characteristic of the erosional areas in the Mt. Gibson district. Acid plastic clays are strongly leached as indicated by the low base status and large amounts of kaolinite. This suggests that red clays are formed from the weatheing of leached saprolite. The levels of Au are quite low in acid red plastic clays. In contrast, calcareous clays contain large concentrations of Au. However, the magnitude of a Au anomaly in calcareous clays and nodular calcrete is much smaller than that in lateritic residuum. At Mt. Gibson, carbonates have displaced and/or replaced pre-existing regolith fabrics so that the Au which now occurs in carbonates may represent Au that was originally present in the original regolith. It is also possible that Au-enrichment in calcareous clays and nodular calcrete has taken place during the formation of carbonates. The origin of carbonates is uncertain. Some evidence suggests that powdery carbonates in calcareous clays from the erosional regime may have originated as an aeolian sediment. On the contrary, the needle-like fibre crystals of calcite in nodular calcrete (overlying lateritic residuum) from the depositional regime suggest that organisms have played a significant role in their formation. The source of Ca is probably Ca-bearing mafic rock fragments derived from upland erosional areas.

8.1.2.4 Ferruginous Granules In Acid Red Plastic Clays

Black, hematite-rich ferruginous granules that have developed in acid plastic clays must be distinguished from lateritic pisoliths. Their origins are different and they may have different geochemical characteristics. Furthermore, as a result of erosional/depositional dynamics, the present location of ferruginous granules can be out of sequence, for example in some buried situations, they may occur on top of the full laterite profile.

8.1.2.5 Calcareous Duricrust, Siliceous Duricrust

Though the lateritic nodules and pisoliths in lateritic duricrust are residual, there is also extensive chemical modification, including the precipitation of carbonates and silica. The matrix and nodules/pisoliths appear to have been replaced and/or displaced by carbonates and silica with consequent formation of calcareous and siliceous duricrusts. Evidence suggests that the process taken to completion would eventually result in the formation of calcrete and silcrete.

9.0 ACKNOWLEDGEMENTS

We wish to thank the management and staff of Mt. Gibson Gold Project and of the joint venture partners Forsayth (Gibson) Ltd and Reynolds Australia Mines Pty Ltd for their co-operation and hospitality without which this study would not have been possible. We also acknowledge the funding provided through AMIRA by the consortium of 24 sponsoring companies of the CSIRO/AMIRA Laterite Geochemistry Project.

Sample preparation was carried out by Ms Angela Janes under the supervision of Mr John Crabb. The XRD analyses were performed by Mr M.K.W. Hart. Polished sections were prepared by Mr A.G. Bowyer. Assistance on the SEM and Cameca microprobe was given by Messrs B.W. Robinson and G. Burkhalter.

Diagrams were drafted by Mr Colin Steel. Typing to a tight deadline was admirably carried out by Ms Jenny Porter. Thanks also go to Dr Bob Gilkes who provided critical comment on the manuscript. We should also like to thank Mr John Perdrix who assisted with checking the final document.

10.0 REFERENCES

Anand, R.R. and Gilkes, R.J., 1987a. Variations in the properties of iron oxides within individual specimens of lateritic duricrust. *Aust. J. Soil Res.*, **25**, 287-302.

Anand, R.R. and Gilkes, R.J., 1987b. The association of maghemite and corundum in Darling Range laterites, Western Australia. *Aust. J. Soil Res.*, **25**, 303-311.

Anand, R.R., Smith, R.E., Innes, J., Churchward, H.M., Perdrix, J.L. and Grunsky, E.C., August 1989. *Laterite types and associated ferruginous materials, Yilgarn Block, W.A. Terminology, Classification and Atlas.* CSIRO Division of Exploration Geoscience Restricted Report 60R (unpaginated).

Anand, R.R. and Gilkes, R.J., 1984. Mineralogical and chemical properties of weathered magnetite grains from lateritic saprolite. *J. Soil Sci.*, **35**, 559-567.

Anand, R.R., Smith, R.E., Innes, J. and Churchward, H.M., March 1989. Exploration Geochemistry about the Mt. Gibson gold deposits, Western Australia. CSIRO Division of Exploration Geoscience Restricted Report 20R, 93 pp.

Baxter, J.L. and Lipple, S.L., 1985. Perenjori, Western Australia. *Geol. Surv. West. Aust. 1:250 000 geol. Series Explan. Notes,* 32 pp.

Baxter, J.L., Lipple. S.L. and Marston, R.J., 1983. Kirkalocka, Western Australia. *Geol. Surv. West. Aust. 1:250 000 geol. Series Explan. Notes,* 24 pp.

Beard, J.S., 1976. *Vegetation Survey of Western Australia.* Vegmap Publications, 6 Fraser Road, Applecross, W.A.

Bettenay, E. and Mulcahy, M.J., 1972. Soil and landscape studies of Western Australia. *J. Geol. Soc. Aust.*, **18**, 359-369.

Bisdom, E.B.A., Stoops, G., Deluigne, J., Curmi, P. and Altemuller, H.J., 1982. Micromorphology of weathering biotite and its secondary products. *Pedologie*, **32**, 225-252.

Boyle, R.W., 1979. The geochemistry of gold and its deposits. *Geol. Surv. Can. Bull.*, **280**, 584pp.

Briot, Ph., 1978. Phénomènes de concentration de l'uranium dans les environments évaporitiques intracontinentaux: les calcrètes de l'Yilgarn australien. Essai de comparaison avec les calcrètes de Mauritanie et de Namibie. Thèse de doctorat de spécialité, Univ. of Paris Sud, 196 pp.

Colin, R., Lecomte, P. and Boulanges, B., 1989. Dissolution features of gold particles in a lateritic profile at Dundi Mobi, Gabon. *Geoderma,* **45**, 241-250.

Coventry, R.J., Taylor, R.M. and Fitzpatrick, R.W., 1983. Pedological significance of the gravels in some red and grey earths of central Queensland. *Aust. J. Soil Res.*, **21**, 219-240.

El-Ansary, M and Sale, M., 1990. Mt. Gibson gold deposits, In: F.E. Hughes (Ed.), *Geology of the Mineral Deposits of Australia and Papua New Guinea,* The Australian Institute of Mining and Metallurgy, Melbourne, pp.95-98.

Filipek, L.M., Chao, T.T. and Carpenter, R.H., 1981. Factors affecting the partioning of Cu, Zn and Pb in boulder coatings and stream sediments in the vicinity of a polymetallic sulphide deposit. *Chem. Geol.*, **33**, 45-64.

Fitzpatrick, R.W. and Schwertmann, U., 1982. Al substituted goethite - an indicator of pedogenic and other weathering environments in South Africa. *Geoderma,* **27** 335-347.

Garnet, D.L., Rea, W.J. and Fuge, R., 1982. Geochemical exploration techniques applicable to calcrete-covered areas. In: H.M. Glen (Edr), *Proc. 12th CMMI Congress, Johannesburg, S. Afr.* Inst. Min. Metall., pp. 945-955.

Guedria, A., 1981. Comportement des métaux (Pb, Zn) dans les sols encroûtés par le calcaire (Région de Bou Grine, Tunisie). Application à la prospection géochimique de ces métaux. Thèse de doctorat de spécialité, Univ. of Orléans, 135 pp.

Gray, D.G., 1988. The aqueous chemistry of gold in the weathering environment. CSIRO Division of Exploration Geoscience Restricted Report EG4R, 65 pp.

Hallberg, J.A., 1976. A petrochemical study of a portion of the western Yilgarn Block. *CSIRO Div. of Mineralogy Rept. FP 13,* 38 pp.

Hingston, F. and Gailitis, V., 1976. The geographical variation of salt precipitated over Western Australia. *Aust. J. Soil Res.,* **14**, 319-335.

Jutson, J.T., 1950. The physiography (geomorphology) of Western Australia. *Geol. Surv. West. Aust. Bull.,* **95**, (3rd ed.), 366 pp.

Klappa, C.F., 1979. Calcified filaments in Quaternary calcretes: organo-mineral interactions in the subaerial vadose environment. *J. Sediment. Petrol.,* **49**, 955-68.

Lintern, M.J., 1989. Study of the distribution of gold in soils at Mt. Hope, Western Australia. *CSIRO Division of Exploration Geoscience Restricted Report 24R,* 17 pp.

Lipple, S.L., Baxter, L.J. and Marston, R.J., 1983. Ninghan, Western Australia. *Geol. Surv. West. Aust. 1:250 000 geol. Series Explan. Notes,* 23 pp.

Mann, A.W., 1984. Mobility of gold and silver in lateritic weathering profile: some observations from Western Australia. *Econ. Geol.,* **79**, 38-49.

Muhling, P.C. and Low, G.H., 1973. Explanatory notes on the Yalgoo 1:250,000 geological sheet, Western Australia. *Geol. Surv. West. Aust. Record* 1973/6.

Muhling, P.C. and Low, G.H., 1977. Yalgoo, Western Australia. *Geol. Surv. W. Aust. 1:250,000 geol. Series Explan. Notes,* 36 pp.

Muller, J.P. and Bocquier, G., 1986. Dissolution of kaolinites and accumulations of iron oxides in lateritic-ferruginous nodules: mineralogical and microstructural transformations. *Geoderma,* **37**, 113-136.

Phillips, S.E., Milnes, A.R. and Foster, R.C., 1987. Calcified filaments: An example of biological influences in the formation of calcrete in South Australia. *Aust. J. Soil Res.,* **25**, 405-28.

Schulze, D.G., 1984. The influence of aluminium on iron oxides. VIII. Unit cell dimensions of Al-substituted goethites and estimation of Al from them. *Clays Clay Miner.,* **32**, 36-44.

Schwertmann, U., 1988. Occurrence and formation of iron oxides in various pedoenvironments. In: Stuck, J.W., Goodman, B.A. and Schwertmann, U. (Eds), *Iron in Soils and Clay Minerals,* D Reidel Publishing Company, Tokyo, pp.267-308

Smith, R.E., 1987. Patterns in lateritic geochemistry Mt. Gibson, Western Australia. Progress report of Geochemex Australia to Forsayth NL, December, 37 pp.

Stace, H.C.T., Hubble, G.D., Brewer, R., Northcote, K.H., Sleeman, J.R., Mulcahy, M.J. and Hallsworth, E.G., 1968. *A Handbook of Australian Soils*. Rellim Press: Glenside, S. Aust, 435 pp.

Taylor, R.M. and Schwertmann, U., 1974. Maghemite in soils and its origin. 1. Properties and observations in soil maghemites. *Clay Miner.*, **10**, 289-98.

Watkins, K.P. and Hickman, A.H., 1988a. Geology of the Murchison Province: Locality Guide. *Geol. Surv. West. Aust., Centennial Field Excursion Guidebook,* 22 pp.

Watkins, K.P. and Hickman, A.H., 1988b. Murchison Province: Stratigraphy, structure and mineralization. *Geol. Surv. West. Aust. Bull.*, **137**, Plate 2.

Wells, M.A., Gilkes, R.J. and Anand, R.R., 1989. The formation of corundum and aluminous hematite by the thermal deydroxylation of aluminous goethite. *Clay Miner,* **24,** 513-530.

APPENDICES
(I - III)

APPENDIX I

Chemical Composition of Regolith Units From Four Vertical Profiles, Midway North Pit

Sample Number	Sample Type	Sample Code	Depth Below Surface (cm)	Easting (local grid)	Northing (local grid)	SiO_2 %	Al_2O_3 %	Fe_2O_3 %	MgO %	CaO %	Na_2O %	K_2O %	TiO_2 %	LOI %	TOTAL
PROFILE 1															
07-1417	Soil	SU203	20-40	1930	6054	66.40	10.60	10.60	0.130	0.049	0.176	0.38	0.633	6.85	**95.82**
07-1416	Gravelly colluvium	CV105HP	120-160	1930	6054	38.90	19.40	29.30	0.389	0.234	0.36	0.992	11.07	11.07	**100.89**
07-1415	Nodular duricrust	LT204	300-380	1930	6054	26.40	21.40	43.10	0.176	0.101	0.201	<0.06	1.130	10.59	**103.10**
07-1414	Nodular duricrust	LT204	500-550	1930	6054	32.00	22.20	31.70	0.184	0.084	0.262	0.07	1.290	12.66	**100.45**
07-1413	Mottled zone	MZ	600	1930	6054	37.10	24.30	23.60	0.275	0.091	0.286	0.12	1.380	14.49	**101.64**
PROFILE 2															
07-1437	Soil	SU203	25-40	1860	6090	68.00	13.30	8.00	0.372	0.285	0.717	0.59	0.736	9.16	**101.16**
07-1438	Silty colluvium	CV102HP	110-200	1860	6090	57.90	18.70	10.10	0.602	0.340	0.340	0.78	0.846	12.45	**102.06**
07-1439	Hardpanized nodular duricrust	LT204HP	320-340	1860	6090	45.80	16.20	28.40	0.442	0.356	0.304	0.48	0.933	9.44	**102.36**
07-1440	Nodular duricrust	LT204	410-440	1860	6090	27.80	22.70	39.90	0.182	0.105	0.243	0.09	0.970	12.15	**104.14**
PROFILE 3															
07-1424	Calcareous clay	cc	90-160	2088	6054	22.90	7.60	6.10	12.300	17.900	0.874	0.61	0.414	33.18	**101.88**
07-1423	Acid plastic clay	apc	440-470	2088	6054	47.00	19.10	17.60	1.167	0.168	0.990	1.10	0.914	13.31	**101.35**
07-1422	Upper saprolite	usp	590-630	2088	6054	62.80	1.40	21.20	0.189	0.042	0.950	0.19	1.080	10.30	**98.15**
PROFILE 4															
07-1412	Soil	SU203	20-30	1905	6054N	63.40	13.50	10.30	0.196	0.135	0.092	0.52	0.733	8.13	**97.01**
07-1407	Silty colluvium	CV102HP	150-180	1905	6054N	57.70	17.60	13.50	0.581	0.225	0.223	0.73	0.845	11.40	**102.88**
07-1408	Gravelly colluvium	CV105HP	200-240	1905	6054N	37.90	14.40	36.20	0.271	0.154	0.190	0.26	0.998	7.96	**98.33**
07-1410	Hardpanized lateritic pisoliths/nodules	LT103HP	400-440	1905	6054N	35.80	18.60	35.20	0.307	0.122	0.344	0.16	1.060	10.35	**101.94**
07-1411	Lateritic pisoliths/nodules	LT103	530-560	1905	6054E	26.90	18.80	42.60	0.200	0.088	0.262	0.08	1.100	9.96	**99.99**

SU = Undifferentiated soils; CVHP = Hardpanized colluvium; LT = Lateritic residuum;
cc = Calcareous clay; apc = Acid plastic clay; usp = Upper saprolite

Appendix I (cont'd)

Sample Number	Mn ppm	Cr ppm	V ppm	Cu ppm	Pb ppm	Zn ppm	Ni ppm	Co ppm	As ppm	Sb ppm	Bi ppm	Mo ppm	Ag ppm	Sn ppm	Ge ppm	Ga ppm	W ppm
PROFILE 1																	
07-1417	92	253	186	16	16	13	10	5	6	<2	2	1	<0.1	3	<2	16	5
07-1416	305	608	508	58	48	36	90	14	46	6	6	2	1.1	2	<2	36	<4
07-1415	102	875	839	68	75	25	76	14	80	8	3	3	1.5	3	3	40	8
07-1414	70	758	629	48	46	22	58	8	48	4	6	<1	1.1	3	<2	34	4
07-1413	41	618	555	42	26	14	48	6	30	3	5	1	0.9	<2	<2	48	6
PROFILE 2																	
07-1437	164	206	143	28	19	35	40	10	6	2	4	2	<0.1	3	<2	20	<4
07-1438	653	249	179	48	22	44	90	20	8	<2	2	<1	<0.1	<2	<2	24	6
07-1439	708	790	519	48	52	32	72	16	32	7	2	2	0.5	2	<2	42	4
07-1440	209	1090	823	88	52	24	88	22	58	11	4	4	0.8	2	<2	42	4
PROFILE 3																	
07-1424	326	154	116	48	17	36	70	10	7	4	4	<1	0.2	<2	<2	12	<4
07-1423	624	387	339	90	58	60	60	54	26	<2	2	<1	0.8	2	<2	25	4
07-1422	95	573	228	86	43	38	28	8	13	<2	7	2	<0.1	3	3	12	<4
PROFILE 4																	
07-1412	584	252	187	34	26	36	55	16	6	<2	3	<1	0.1	<2	<2	20	<4
07-1407	325	327	244	44	26	36	58	10	13	<2	3	<1	0.5	2	<2	26	<4
07-1408	235	784	601	44	74	28	80	10	54	3	<2	3	1.1	<2	<2	38	4
07-1410	131	701	586	46	62	30	84	12	56	6	4	3	1.3	3	<2	40	<4
07-1411	130	815	740	64	76	26	76	12	80	8	<2	3	1.5	3	<2	48	8

Appendix I (cont'd)

Sample Number	Ba ppm	Zr ppm	Nb ppm	Se ppm	Be ppm	Au ppb
PROFILE 1						
07-1417	82	77	10	2	<1	60
07-1416	128	110	9	3	1	190
07-1415	102	108	10	3	<1	200
07-1414	32	70	10	<2	<1	400
07-1413	70	77	10	4	<1	120
PROFILE 2						
07-1437	119	101	10	3	1	41
07-1438	228	106	13	2	2	100
07-1439	170	105	10	<2	1	140
07-1440	184	107	4	7	1	150
PROFILE 3						
07-1424	106	43	4	<2	<1	88
07-1423	219	82	7	<2	1	28
07-1422	278	55	5	4	<1	16
PROFILE 4						
07-1412	111	96	11	3	1	74
07-1407	189	104	10	2	1	120
07-1408	140	135	11	3	1	230
07-1410	192	120	10	2	1	56
07-1411	64	117	10	<2	1	130

APPENDIX II

Chemical Composition of Lower Saprolite and Ferruginous Saprolite, Southern Wall Midway North Pit

Sample Number	Sample Type	SiO_2 %	Al_2O_3 %	Fe_2O_3 %	MgO %	CaO %	Na_2O %	K_2O %	TiO_2 %	LOI %	TOTAL	Mn ppm	Cr ppm	V ppm	Cu ppm	Pb ppm
07-1429	lsp	61.20	17.60	3.20	0.722	0.053	1.940	1.30	0.586	12.35	**98.95**	316	2230	268	86	66
07-1430	lsp	46.90	20.90	7.30	4.310	0.046	2.670	1.57	0.640	16.33	**100.67**	153	338	305	360	54
07-1431	lsp	68.50	17.20	0.40	0.318	0.039	1.480	0.70	0.329	8.86	**97.83**	<15	<20	60	22	26
07-1433	lsp	46.30	19.00	9.40	3.420	1.550	2.200	0.29	0.556	16.69	**99.41**	428	360	280	32	13
07-1432	Fe-sp	63.00	4.60	26.10	0.264	0.068	1.370	0.11	0.420	6.05	**101.98**	49	237	496	76	480
07-1435	Fe-sp	46.10	18.20	19.50	0.599	0.369	1.680	0.32	4.370	13.09	**104.23**	652	<20	712	10	40
07-1436	Fe-sp	47.60	19.10	16.20	0.458	0.088	0.945	0.40	4.440	13.05	**102.28**	585	<20	685	400	50

	Zn ppm	Ni ppm	Co ppm	As ppm	Sb ppm	Bi ppm	Mo ppm	Ag ppm	Sn ppm	Ge ppm	Ga ppm	W ppm	Ba ppm	Zr ppm	Nb ppm	Se ppm	Be ppm	Au ppb
07-1429	155	125	18	8	2	5	<1	0.1	<2	<2	20	6	145	37	2	<2	<2	1900
07-1430	630	170	58	10	5	2	<1	0.1	<2	3	18	4	100	38	2	<2	<2	1
07-1431	26	8	4	8	4	3	<1	0.1	2	<2	20	4	319	138	6	<2	<2	82
07-1433	470	380	75	4	2	2	<1	0.1	<2	<2	22	4	66	34	<2	2	2	57
07-1432	290	22	6	300	6	125	1	<0.1	5	3	18	8	18	17	2	6	6	1180
07-1435	135	155	50	7	3	<2	<1	<0.1	<2	<2	30	<4	176	51	15	<2	<2	3
07-1436	470	240	78	19	11	2	<1	<0.1	<2	<2	28	<4	54	77	16	<2	<2	2

lsp = Lower saprolite; Fe-sp = Ferruginous saprolite

APPENDIX III

Chemical and Mineral Compositions of Mt.Gibson Samples.

Sample Number	Sample Type	Box field	Component	AMG Coordinates		SiO2	Al2O3	Fe2O3	MgO	CaO	Na2O	K2O	TiO2	Mn	Cr	V	Cu	Pb	Zn
				Easting	Northing	wt %	wt %	wt %	wt %	wt %	wt %	wt %	wt %	ppm	ppm	ppm	ppm	ppm	ppm
07-0254A	CA204	CA	G	516065	6707376	11.30	6.23	66.80	0.328	4.750	0.067	0.067	1.920	308	832	1970	50	72	30
07-0254C	CA204	CA	CF	516065	6707376	18.20	7.72	4.73	2.100	34.000	0.123	0.259	0.298	108	110	129	30	9	14
07-0275A	CA204	CA	G	516252	6707471	15.00	25.50	37.18	0.560	4.309	0.136	<0.060	1.239	231	805	710	135	44	30
07-0275B	CA204	CA	CF	516252	6707471	23.30	9.97	4.80	1.691	28.959	0.187	0.317	0.399	305	140	108	38	18	31
07-0276A	CA204	CA	G	516252	6707471	28.30	27.58	28.03	0.429	0.869	0.441	0.069	0.862	79	746	645	110	35	12
07-0276B	CA204	CA	CF	516252	6707471	8.51	3.93	1.30	1.890	46.447	0.305	0.112	0.132	41	55	35	16	18	11
07-0504A	CA	CA	CF	515883	6707106	25.10	12.11	8.05	4.659	19.166	0.204	0.240	0.941	99	113	216	40	13	13
07-0504B	CA	CA	G	515883	6707106	18.50	23.99	39.32	0.403	1.441	0.146	<0.060	3.253	137	486	1110	50	40	10
07-0526A	CA	CA	G	516136	6706849	38.30	31.55	15.30	0.252	0.360	0.237	0.069	1.066	102	842	736	53	36	10
07-0526B	CA	CA	CF	516136	6706849	23.30	9.77	2.53	2.636	47.986	0.357	0.480	0.340	172	109	92	28	14	12
07-0331A	LT203	ccu	C	515939	6708370	16.20	14.41	58.34	0.146	0.104	0.156	<0.060	4.003	60	1170	1960	19	163	9
07-0331B	LT203	ccu	CU	515939	6708370	31.40	23.61	28.46	0.270	0.113	0.255	0.074	3.553	19	813	1380	32	119	8
07-0508A	LT102	ccu	C	515917	6707090	7.69	17.17	66.78	0.154	0.112	0.189	<0.060	2.619	152	801	1980	30	64	16
07-0508B	LT102	ccu	CU	515917	6707090	18.80	35.14	26.31	0.262	0.109	0.280	<0.060	3.903	31	409	1110	35	49	6
07-0510A	LT102	ccu	C	515902	6707067	9.01	10.54	69.93	0.143	0.097	0.148	<0.060	3.386	127	865	2190	22	69	12
07-0510B	LT102	ccu	CU	515902	6707067	25.90	24.56	30.03	0.221	0.101	0.274	<0.060	4.687	55	424	1230	40	56	8
07-0592A	LT102	ccu	C	515926	6708430	17.10	7.88	63.92	0.040	0.029	0.078	<0.060	2.969	73	1070	1850	22	85	12
07-0592B	LT102	ccu	CU	515926	6708430	40.20	14.89	36.18	0.300	0.040	0.110	<0.060	3.870	35	637	1360	36	71	6
07-0270B	CV105HP	hc	G	516001	6707628	23.00	17.40	44.10	0.299	1.410	0.252	0.138	1.390	185	665	1040	80	32	16
07-0270C	CV105HP	hc	M	516001	6707628	49.10	21.40	13.30	0.412	0.401	0.289	0.321	0.732	132	188	301	42	22	22
07-0299B	CV105CFHP	hc	M	516068	6709117	50.10	21.72	10.54	1.378	0.429	0.485	0.709	1.153	212	286	287	80	19	22
07-0299C	CV105CFHP	hc	G	516068	6709117	11.60	18.89	56.20	0.310	0.285	0.214	0.088	3.286	159	1290	1700	62	122	13
07-0537B	CV105CFHP	hc	G	516250	6709397	26.40	17.90	36.00	0.336	2.590	0.127	0.174	1.180	120	639	1190	74	110	10
07-0537C	CV105CFHP	hc	M	516250	6709397	49.40	17.00	7.89	0.723	6.180	0.189	0.380	0.469	250	141	220	48	19	16
07-0553B	CV105HP	hc	G	516557	6709454	28.10	21.40	36.50	0.171	0.224	0.087	0.088	1.370	103	610	944	50	86	13
07-0553C	CV105HP	hc	M	516557	6709454	49.30	19.10	16.00	0.000	0.672	0.239	0.242	0.895	165	285	390	46	44	18
07-0554B	CV105HP	hc	G	516557	6709454	28.80	20.80	35.30	0.218	0.548	0.135	0.104	1.170	66	518	697	60	72	13
07-0554C	CV105HP	hc	M	516557	6709454	38.40	21.60	21.40	0.367	2.190	0.155	0.152	1.120	126	352	424	50	44	18
07-0571A	CV105CFHP	hc	G	516471	6709847	17.70	12.60	62.30	0.181	0.263	0.086	0.154	1.780	318	743	1420	42	76	17
07-0571C	CV105CFHP	hc	M	516471	6709847	45.70	20.00	19.50	0.422	0.834	0.195	0.437	0.999	231	326	546	34	44	22
07-0576A	CV105CFHP	hc	G	516416	6708848	16.60	16.80	53.50	0.288	0.184	0.277	0.074	2.480	198	816	1900	70	140	18
07-0576C	CV105CFHP	hc	M	516416	6708848	42.20	25.60	13.20	0.779	0.614	0.498	0.269	0.991	164	226	483	62	36	16
07-0793A	CV105HP	hc	G	516901	6707107	10.50	20.20	50.60	0.521	2.470	0.171	0.133	2.180	545	347	1090	36	36	18
07-0793C	CV105HP	hc	M	516901	6707107	25.00	26.50	10.90	1.860	10.300	0.326	0.352	1.120	135	103	245	28	17	8
07-0800A	CV105HP	hc	G	517098	6709133	10.40	19.70	57.70	0.267	0.897	0.082	0.077	2.520	124	715	1750	56	66	18
07-0800C	CV105HP	hc	M	517098	6709133	35.40	17.20	9.30	1.580	12.400	0.224	0.446	0.717	129	149	285	86	18	18
07-0810A	CV105HP	hc	G	517046	6708203	13.70	11.70	66.80	0.220	0.136	0.208	0.071	1.970	213	762	1700	62	115	19
07-0810C	CV105HP	hc	M	517046	6708203	48.40	17.70	13.10	0.883	3.940	0.376	0.226	0.760	134	157	376	58	30	13
07-0266A	LT102	LT	MP	516006	6707628	8.32	7.69	77.00	0.062	0.170	0.030	<0.060	2.410	237	865	2180	22	105	34
07-0266B	LT102	LT	NMP	516006	6707628	25.70	20.80	41.10	0.068	0.054	0.031	<0.060	1.120	106	659	1400	36	60	18

APPENDIX III

Chemical and Mineral Composition of Mt Gibson Samples.

Sample Number	Ni ppm	Co ppm	As ppm	Sb ppm	Bi ppm	Mo ppm	Ag ppm	Sn ppm	Ga ppm	W ppm	Ba ppm	Zr ppm	Nb ppm	Se ppm	Be ppm	Au ppb	Hematite wt %	Goethite wt %	Maghemite wt %	Kaolinite wt %	Gibbsite wt %	Quartz wt %
07-0254A	14	4	27	6	15	7	<0.1	4	84	9	834	140	18	9	1	3891	35	18	17	3	0	10
07-0254C	12	4	4	<1	<2	<1	<0.1	2	20	1	161	46	8	2	<1	763	0	4	0	12	0	10
07-0275A	30	6	53	5	8	7	7.5	7	40	5	101	147	6	7	<1	15145	17	24	0	20	25	5
07-0275B	22	0	8	<1	<2	<1	<0.1	3	15	2	88	60	5	<2	<1	1803	0	4	0	15	0	5
07-0276A	25	0	56	5	<2	2	5.0	6	35	3	152	136	4	7	<1	9725	14	18	0	58	0	3
07-0276B	<4	<4	2	<1	<2	<1	<0.1	<2	<4	1	54	21	<3	<2	<1	322	0	0	0	5	0	3
07-0504A	16	<4	8	<1	<2	1	0.1	7	20	2	78	67	12	3	<1	1177	0	10	0	25	5	15
07-0504B	18	4	25	2	6	7	0.8	25	80	12	134	203	32	6	<1	3431	24	22	0	15	20	12
07-0526A	45	0	27	2	13	<1	2.0	5	55	3	23	103	8	3	1	1920	8	9	0	45	14	18
07-0526B	18	8	4	<1	9	<1	<0.1	<2	10	1	171	67	4	<2	<1	590	0	12	0	15	0	20
07-0331A	16	0	24	11	<2	<1	0.9	0	0	18	196	295	0	0	<1	15163	30	10	20	20	0	10
07-0331B	26	0	18	7	<2	<1	1.0	15	90	10	38	288	22	<2	<1	257	22	12	0	45	0	12
07-0508A	14	<4	17	3	9	7	0.3	7	160	9	24	175	12	<2	<1	14035	35	5	30	5	5	5
07-0508B	30	0	11	2	5	<1	1.0	10	40	9	17	120	35	6	<1	6084	20	10	0	20	20	10
07-0510A	8	4	19	2	2	11	0.2	15	230	15	22	211	27	10	<1	12049	40	5	30	0	0	8
07-0510B	26	8	17	2	5	6	<0.1	25	80	15	21	345	45	7	1	773	25	10	0	25	25	15
07-0592A	9	0	14	4	<2	<1	0.7	5	80	13	13	154	15	10	<1	3333	32	15	20	12	12	15
07-0592B	38	6	9	3	8	4	2.9	15	65	15	55	206	26	6	1	3754	28	12	0	30	30	25
07-0270B	32	4	35	3	7	4	0.8	6	44	11	68	164	11	8	1	1938	30	20	0	35	0	12
07-0270C	46	16	13	1	<2	<1	0.2	4	36	3	806	99	11	<2	2	1148	3	12	0	45	0	25
07-0299B	38	8	5	1	<2	<1	0.9	<2	35	4	931	92	7	<2	1	2042	3	9	0	45	0	20
07-0299C	18	4	12	6	9	6	1.3	6	120	17	457	132	12	<2	<1	4833	30	10	20	30	0	4
07-0537B	24	4	40	5	10	6	1.5	4	90	6	175	175	17	5	1	9941	20	20	0	30	0	15
07-0537C	30	8	7	1	<2	<1	0.1	6	34	4	174	66	8	2	1	2866	3	8	0	35	0	20
07-0553B	30	4	37	6	3	10	0.9	2	60	13	407	138	13	4	2	3359	22	18	0	30	0	10
07-0553C	40	8	14	3	<2	4	0.7	3	40	7	431	95	11	<2	1	2027	10	20	0	40	0	25
07-0554B	30	4	33	5	4	7	1.1	<2	60	10	484	140	11	<2	1	983	22	18	0	40	0	10
07-0554C	36	8	22	4	4	4	0.9	3	40	6	212	117	12	2	1	719	10	15	0	45	0	10
07-0571A	32	6	29	4	<2	6	1.2	4	76	4	100	164	12	2	1	3048	35	10	20	20	0	0
07-0571C	38	6	14	2	2	3	0.6	5	46	2	396	114	13	<2	1	1955	14	8	0	45	0	15
07-0576A	30	6	21	4	7	5	0.9	9	100	3	61	123	18	4	2	7799	30	10	20	20	5	6
07-0576C	44	10	6	1	<2	<1	0.4	5	50	2	54	80	11	2	2	1177	0	15	0	50	0	15
07-0793A	14	6	49	2	9	8	0.1	10	64	9	104	188	26	9	1	629	32	5	20	15	15	3
07-0793C	16	4	19	<1	2	<1	<0.1	3	30	3	84	98	13	<2	1	673	4	8	0	30	15	10
07-0800A	20	<4	7	4	5	5	1.5	8	125	24	321	116	18	5	<1	1558	30	10	20	20	12	3
07-0800C	34	6	4	1	<2	<1	0.7	4	34	4	191	65	9	<2	1	1875	0	10	0	35	0	20
07-0810A	26	4	25	4	6	6	0.2	3	74	3	232	185	15	<2	2	5568	35	10	25	25	5	5
07-0810C	26	8	9	<1	<2	<1	0.3	3	36	3	110	97	10	2	1	1242	5	10	0	35	2	25
07-0266A	14	<4	86	6	10	10	0.1	5	90	14	13	177	18	10	1	845	50	5	25	10	0	5
07-0266B	28	4	59	2	8	5	0.5	2	64	6	25	145	12	14	1	4744	30	15	0	40	0	8

APPENDIX III

Chemical and Mineral Compositions of Mt.Gibson Samples.

Sample Number	Sample Type	Box field	Component	AMG Coordinates		SiO2	Al2O3	Fe2O3	MgO	CaO	Na2O	K2O	TiO2	Mn	Cr	V	Cu	Pb	Zn
				Easting	Northing	wt %	wt %	wt %	wt %	wt %	wt %	wt %	wt %	ppm	ppm	ppm	ppm	ppm	ppm
07-0295A	LT104	LT	MN	516216	6709048	6.34	9.60	79.22	0.041	0.027	0.032	<0.060	2.285	172	1570	1800	16	117	17
07-0295B	LT104	LT	NMN	516216	6709048	15.00	15.28	60.63	0.058	0.028	0.027	<0.060	1.801	196	1240	1670	40	85	18
07-0300A	LT102	LT	MP	516068	6709117	7.08	19.27	63.92	0.093	0.087	0.069	<0.060	4.587	144	1430	1860	32	115	13
07-0300C	LT102	LT	NMP	516068	6709117	6.40	22.86	62.63	0.080	0.074	0.061	<0.060	3.019	133	1460	1780	36	103	11
07-0328B	LT212	LT	MN	515950	6708404	13.40	10.69	70.78	0.080	0.066	0.077	<0.060	1.646	101	1050	1390	18	113	14
07-0328A	LT212	LT	NMN	515950	6708404	21.30	14.72	51.62	0.096	0.059	0.090	<0.060	1.216	103	707	1060	24	79	11
07-0329A	LT212	LT	MN	515950	6708404	25.90	10.43	53.48	0.083	0.111	0.129	<0.060	2.002	63	1220	1890	29	139	11
07-0329C	LT212	LT	NMN	515950	6708404	31.40	23.23	33.18	0.098	0.081	0.151	<0.060	1.885	19	803	1370	32	92	11
07-0534A	LT104	LT	MN	516321	6709420	8.98	10.30	72.70	0.043	0.039	0.032	<0.060	1.620	141	991	1670	20	94	19
07-0534B	LT104	LT	NMN	516321	6709420	21.50	18.40	49.30	0.062	0.043	0.029	<0.060	1.120	129	741	1300	40	140	14
07-0548A	LT104	LT	MN	516473	6709296	10.60	15.10	66.80	0.041	0.033	0.027	<0.060	1.420	108	867	1280	24	165	17
07-0548B	LT104	LT	NMN	516473	6709296	24.40	21.00	43.00	0.062	0.031	0.026	<0.060	1.120	108	657	978	36	110	16
07-0577A	LT104	LT	MN	516416	6708848	10.80	20.97	53.91	0.161	0.111	0.177	<0.060	3.319	144	908	1650	42	86	12
07-0577B	LT104	LT	NMN	516416	6708848	16.70	20.40	49.05	0.202	0.108	0.213	0.066	2.068	92	841	1040	40	53	19
07-0792A	LT102	LT	MP	516901	6707107	7.47	15.30	61.60	0.348	2.170	0.063	0.076	2.070	475	431	1300	58	54	26
07-0792B	LT102	LT	NMP	516901	6707107	11.30	20.50	47.50	0.533	3.510	0.075	0.076	2.080	474	396	1200	58	38	16
07-0794A	LT102	LT	MP	516890	6707087	6.11	17.00	66.50	0.164	0.329	0.090	<0.060	3.220	133	546	1700	24	72	15
07-0794B	LT102	LT	NMP	516891	6707087	14.50	20.00	50.40	0.283	1.040	0.122	<0.060	2.700	99	448	1450	28	58	13
07-0798A	LT104	LT	MN	517050	6707503	10.40	9.54	72.50	0.079	0.024	0.014	<0.060	1.840	127	1070	2150	24	86	22
07-0798B	LT104	LT	NMN	517050	6707503	27.40	21.40	38.80	0.079	0.024	0.013	<0.060	1.240	48	729	1540	36	50	16
07-0799A	LT104	LT	MN	517050	6707503	9.65	8.57	74.70	0.073	0.020	0.023	<0.060	1.730	124	1080	2170	17	88	14
07-0799B	LT104	LT	NMN	517050	6707503	26.30	18.80	13.30	0.079	0.019	0.026	<0.060	1.380	50	671	1550	30	54	11
07-0805A	LT104	LT	MN	517138	6709122	8.81	11.90	71.00	0.064	0.033	0.009	<0.060	1.380	138	1070	1790	22	76	16
07-0805B	LT104	LT	NMN	517138	6709122	16.70	17.40	56.50	0.075	0.020	0.011	<0.060	1.250	147	845	1610	30	50	14
07-0253A	SU203	soils	MG	516065	6707376	12.50	7.59	75.50	0.088	0.112	0.063	0.107	1.600	370	945	1610	42	82	24
07-0253B	SU203	soils	NMG	516065	6707376	24.10	15.09	56.06	0.093	0.099	0.055	0.086	1.243	207	831	1460	42	60	8
07-0261A	SU202	soils	MG	516206	6707632	6.42	7.10	82.80	0.048	0.046	0.040	<0.060	2.035	214	1690	2220	17	110	16
07-0261B	SU202	soils	NMG	516206	6707632	12.20	11.56	69.35	0.055	0.081	0.030	<0.060	2.118	171	1320	2150	23	89	13
07-0265A	SU202	soils	MG	516009	6707628	4.02	6.84	80.79	0.078	0.064	0.073	<0.060	2.585	243	1100	2030	21	91	21
07-0265B	SU202	soils	NMG	516009	6707628	17.30	14.64	63.06	0.053	0.043	0.032	<0.060	1.968	179	928	1780	30	64	10
07-0296A	SU202	soils	MG	516216	6709048	5.36	8.62	80.60	0.043	0.055	0.040	<0.060	1.070	221	1110	1850	26	115	22
07-0296B	SU202	soils	NMG	516216	6709048	13.50	14.60	63.80	0.051	0.057	0.037	<0.060	1.770	228	1070	1930	48	105	26
07-0301A	SU203	soils	MG	516068	6709117	6.35	12.00	75.30	0.068	0.129	0.051	<0.060	2.150	313	1020	1880	38	115	30
07-0301B	SU203	soils	NMG	516068	6709117	14.40	16.40	59.30	0.086	0.438	0.050	<0.060	1.980	292	835	1822	60	105	26
07-0337A	SU203	soils	MG	516023	6708327	8.74	7.80	79.94	0.070	0.057	0.044	<0.060	2.035	258	961	1690	26	132	21
07-0337B	SU203	soils	NMG	516023	6708327	14.90	13.28	64.78	0.073	0.059	0.063	<0.060	1.835	174	824	1680	31	91	14
07-0502A	SU203	soils	MG	515883	6707106	7.65	11.77	71.21	0.103	0.129	0.036	<0.060	2.519	427	731	1470	26	66	32
07-0502B	SU203	soils	NMG	515883	6707106	15.30	18.06	57.91	0.103	0.118	0.043	<0.060	2.268	376	572	1450	52	57	22
07-0511A	SU203	soils	MG	515916	6707050	6.43	9.73	77.80	0.066	0.131	0.116	<0.060	2.320	204	600	1990	22	100	22
07-0511B	SU203	soils	NMG	515916	6707050	13.80	15.10	62.50	0.123	0.123	0.055	<0.060	2.020	133	550	1830	32	86	16

APPENDIX III

Chemical and Mineral Composition of Mt Gibson Samples.

Sample Number	Ni ppm	Co ppm	As ppm	Sb ppm	Bi ppm	Mo ppm	Ag ppm	Sn ppm	Ga ppm	W ppm	Ba ppm	Zr ppm	Nb ppm	Se ppm	Be ppm	Au ppb	Hematite wt %	Goethite wt %	Maghemite wt %	Kaolinite wt %	Gibbsite wt %	Quartz wt %
07-0295A	10	6	45	6	10	7	0.7	9	90	18	<5	223	7	7	<1	1404	45	5	35	0	0	10
07-0295B	28	8	30	4	7	6	1.6	4	65	11	12	194	8	6	<1	1179	55	10	0	25	0	2
07-0300A	18	4	13	7	14	7	0.6	15	130	25	112	138	23	6	<1	3398	30	12	25	10	20	3
07-0300C	20	10	12	5	8	5	0.2	15	150	18	65	131	11	4	1	4656	40	23	0	30	5	3
07-0328B	18	6	38	4	<2	7	<0.1	4	65	3	52	186	8	5	<1	380	40	5	25	20	0	5
07-0328A	34	6	28	3	2	6	<0.1	<2	55	4	114	147	8	3	<1	690	45	10	0	30	0	10
07-0329A	23	0	30	12	<2	<1	0.6	6	80	2	32	245	8	8	<1	180	30	10	20	18	0	20
07-0329C	36	6	27	10	17	5	1.5	8	60	10	128	137	7	6	<1	1209	22	15	0	40	0	12
07-0534A	16	<4	48	9	14	8	0.5	2	74	23	13	164	13	4	<1	3954	40	12	25	15	0	2
07-0534B	24	4	39	6	14	12	0.6	5	150	63	14	132	24	7	1	4772	40	15	0	30	0	10
07-0548A	16	4	64	9	4	10	0.4	7	88	20	20	175	17	3	1	300	35	15	20	20	0	3
07-0548B	32	6	47	5	4	6	0.5	3	70	13	21	157	17	5	1	877	25	20	0	40	0	7
07-0577A	26	6	30	4	3	4	2.0	4	120	9	39	249	15	8	1	3500	30	12	15	20	12	5
07-0577B	26	12	23	3	<2	4	0.5	5	65	4	150	99	13	5	1	140	40	16	0	25	8	15
07-0792A	20	8	55	3	9	7	0.4	6	88	14	232	188	22	8	1	3869	30	0	25	10	15	2
07-0792B	20	8	53	2	8	6	0.8	8	52	9	233	188	24	8	1	2035	30	20	0	15	15	5
07-0794A	10	<4	22	3	4	11	0.4	6	150	15	37	128	26	9	1	1209	40	10	25	8	10	3
07-0794B	18	<4	24	3	4	8	0.5	5	78	8	55	121	20	6	1	1264	40	15	0	20	12	5
07-0798A	26	<4	68	5	16	10	0.1	<2	74	10	12	197	16	19	<1	811	38	10	30	15	0	5
07-0798B	22	<4	46	4	11	5	0.5	5	70	10	11	157	13	13	1	5975	30	15	0	40	0	10
07-0799A	10	<4	63	4	13	8	<0.1	3	66	5	9	187	16	13	<1	284	45	10	25	10	0	5
07-0799B	24	<4	39	6	9	4	0.3	4	72	4	8	146	12	12	1	2855	35	15	0	30	0	15
07-0805A	18	<4	28	4	5	7	<0.1	3	60	12	<5	153	11	10	<1	705	40	10	25	18	0	0
07-0805B	30	4	19	3	3	4	0.5	<2	60	24	<5	133	12	9	<1	4149	45	13	0	25	0	5
07-0253A	14	10	38	4	9	6	<0.1	8	55	7	63	211	9	4	<1	245	35	0	40	10	5	10
07-0253B	30	6	42	4	12	5	0.1	6	50	6	123	172	5	7	<1	520	45	12	0	30	0	10
07-0261A	10	0	118	9	<2	<1	<0.1	3	70	7	7	292	9	10	<1	317	45	0	40	5	0	5
07-0261B	16	0	114	8	<2	1	0.2	8	80	11	9	252	11	<2	<1	349	65	11	0	15	0	5
07-0265A	13	0	90	5	<2	<1	<0.1	<2	80	15	15	191	12	9	<1	587	45	0	35	8	0	5
07-0265B	18	4	88	4	6	6	<0.1	3	55	11	10	173	12	6	<1	584	50	15	0	25	0	5
07-0296A	18	<4	49	7	9	9	0.3	2	86	15	17	195	16	5	1	818	50	0	35	0	0	7
07-0296B	30	4	44	7	12	8	1.0	7	76	15	19	187	12	<2	1	1544	55	12	0	20	0	5
07-0301A	28	4	30	6	5	9	0.2	7	105	18	30	175	12	2	1	871	40	10	25	10	0	10
07-0301B	32	4	28	6	12	6	1.2	<2	70	18	70	169	15	7	1	670	45	15	0	25	0	10
07-0337A	15	0	18	2	<2	<1	0.3	6	85	4	9	227	11	4	<1	104	40	0	40	5	0	6
07-0337B	20	0	33	4	<2	<1	0.6	9	70	7	13	186	14	3	<1	233	55	5	0	30	0	5
07-0502A	22	6	41	4	7	9	<0.1	10	95	7	56	268	25	5	<1	355	30	5	40	7	2	5
07-0502B	28	6	38	3	3	6	0.7	8	55	9	56	179	20	5	<1	1255	50	17	0	25	2	5
07-0511A	18	4	38	4	9	11	<0.1	6	115	15	45	140	22	2	1	870	45	5	35	5	0	0
07-0511B	24	4	31	4	5	8	0.1	5	92	9	184	145	18	5	1	898	58	15	0	15	0	10

APPENDIX III

Chemical and Mineral Compositions of Mt.Gibson Samples.

Sample Number	Sample Type	Box field	Component	AMG Coordinates		SiO2	Al2O3	Fe2O3	MgO	CaO	Na2O	K2O	TiO2	Mn	Cr	V	Cu	Pb	Zn
				Easting	Northing	wt %	wt %	wt %	wt %	wt %	wt %	wt %	wt %	ppm	ppm	ppm	ppm	ppm	ppm
07-0516A	SU202	soils	MG	515991	6707028	7.57	9.26	77.50	0.055	0.062	0.025	<0.060	1.970	283	576	1600	32	110	30
07-0516B	SU202	soils	NMG	515991	6707028	14.20	13.60	64.60	0.051	0.051	0.022	<0.060	1.210	180	461	1290	60	84	22
07-0528A	SU203	soils	MG	516136	6706849	7.63	8.31	81.65	0.093	0.221	0.047	<0.060	1.553	283	1060	1380	24	126	34
07-0528B	SU203	soils	NMG	516136	6706849	9.61	11.50	70.50	0.066	0.074	0.047	<0.060	1.308	283	1080	1490	36	114	20
07-0533A	SU203	soils	MG	516321	6709420	6.10	7.61	80.40	0.043	0.051	0.027	<0.060	2.470	180	1080	2360	22	135	28
07-0533B	SU203	soils	NMG	516321	6709420	13.60	13.60	65.00	0.062	0.067	0.046	<0.060	1.700	175	818	2130	36	120	20
07-0536A	SU203	soils	MG	516250	6709397	7.17	7.44	78.30	0.051	0.078	0.040	<0.060	3.170	227	807	2640	26	86	26
07-0536B	SU203	soils	NMG	516250	6709397	24.50	19.60	43.00	0.099	0.129	0.067	<0.060	1.900	76	715	2030	46	50	14
07-0541A	SU203	soils	MG	516248	6709322	6.39	10.40	77.10	0.060	0.118	0.035	<0.060	3.100	285	726	1940	22	130	24
07-0541B	SU203	soils	NMG	516248	6709322	18.90	18.70	51.70	0.072	0.102	0.036	<0.060	1.800	133	575	1480	58	98	15
07-0550A	SU202	soils	MG	516473	6709296	9.86	10.90	71.80	0.060	0.081	0.042	<0.060	1.880	139	1100	1460	38	200	20
07-0550B	SU202	soils	NMG	516473	6709296	23.60	22.20	39.60	0.082	0.089	0.060	0.062	1.530	54	696	972	42	105	9
07-0555A	SU203	soils	MG	516557	6709454	6.12	8.82	79.30	0.051	0.064	0.030	<0.060	2.550	232	1150	1910	24	170	56
07-0555B	SU203	soils	NMG	516557	6709454	12.20	13.80	66.50	0.060	0.065	0.031	<0.060	1.900	184	1010	1700	38	170	19
07-0557A	SU202	soils	MG	516285	6709611	5.73	8.05	81.20	0.041	0.052	0.035	<0.060	1.700	237	975	1820	19	185	22
07-0557B	SU202	soils	NMG	516285	6709611	17.30	17.30	56.90	0.060	0.044	0.030	<0.060	1.230	194	730	1550	34	150	22
07-0570A	SU203	soils	MG	516471	6709847	5.09	8.59	81.20	0.043	0.067	0.038	<0.060	2.430	342	848	1780	17	96	22
07-0570B	SU203	soils	NMG	516471	6709847	16.60	17.50	56.90	0.078	0.064	0.036	<0.060	1.660	208	776	1620	32	80	15
07-0595A	SU203	soils	MG	516244	6707152	12.50	9.81	71.40	0.132	0.222	0.057	0.081	1.110	294	903	2020	46	160	38
07-0595B	SU203	soils	NMG	516244	6707152	22.40	20.70	43.00	0.193	0.197	0.104	<0.060	0.842	78	668	1510	94	82	13
07-0614A	SU202	soils	MG	516233	6707772	6.86	8.71	78.80	0.041	0.059	0.029	<0.060	2.300	258	748	1850	24	96	22
07-0614B	SU202	soils	NMG	516233	6707722	14.80	15.30	62.20	0.049	0.049	0.032	<0.060	1.610	201	701	1680	26	76	14
07-0795A	SU202	soils	MG	517293	6707178	9.34	8.45	77.30	0.057	0.078	0.037	<0.060	1.260	230	1180	2360	26	145	28
07-0795B	SU202	soils	NMG	517293	6707178	25.20	21.00	43.30	0.047	0.043	0.021	<0.060	1.040	80	827	1680	42	94	19
07-0797A	SU202	soils	MG	517050	6707503	10.30	8.35	75.40	0.087	0.046	0.024	0.062	1.700	240	842	2060	28	78	24
07-0797B	SU202	soils	NMG	517050	6707503	20.00	15.80	54.90	0.076	0.035	0.012	0.061	1.600	166	720	2050	42	62	26

Component Codes:

G= Gravel fraction; CF= Calcareous fragment; M= Matrix;
C= Cores; CU =Cutans;
NMN = Non-magnetic lateritic nodules; MN = Magnetic lateritic nodules;
NMP = Non-magnetic lateritic pisoliths; MP = Magnetic lateritic pisoliths;
NMG = Non-magnetic gravel fraction; MG = Magnetic gravel fraction.

Box fields are codes for the major regolith units.

APPENDIX III

Chemical and Mineral Composition of Mt Gibson Samples.

Sample Number	Ni ppm	Co ppm	As ppm	Sb ppm	Bi ppm	Mo ppm	Ag ppm	Sn ppm	Ga ppm	W ppm	Ba ppm	Zr ppm	Nb ppm	Se ppm	Be ppm	Au ppb	Hematite wt %	Goethite wt %	Maghemite wt %	Kaolinite wt %	Gibbsite wt %	Quartz wt %
07-0516A	22	4	49	5	9	9	<0.1	5	72	10	17	205	19	5	1	333	50	0	30	10	0	4
07-0516B	24	<4	45	4	4	8	0.3	4	52	8	18	182	13	7	1	640	58	9	0	25	0	5
07-0528A	20	6	42	4	14	9	0.2	8	110	6	20	185	16	<2	1	126	45	0	40	8	0	5
07-0528B	26	<4	53	5	14	9	<0.1	6	80	2	27	182	4	4	<1	30	65	12	0	15	0	5
07-0533A	10	4	58	12	13	10	0.3	4	120	32	9	180	18	11	<1	947	50	5	30	8	0	3
07-0533B	20	<4	48	9	9	11	1.0	6	120	19	20	152	24	3	<1	1178	55	15	0	20	0	5
07-0536A	14	<4	39	14	12	5	1.0	2	54	33	20	142	11	5	1	3633	45	8	30	10	0	3
07-0536B	32	6	33	7	11	5	1.6	<2	72	17	51	138	11	4	2	6128	25	19	0	35	0	10
07-0541A	12	<4	28	9	8	7	0.1	6	90	34	19	156	13	9	1	904	45	5	30	10	0	5
07-0541B	34	<4	33	8	7	7	1.4	2	90	19	138	153	13	5	1	2694	35	22	0	30	0	5
07-0550A	16	<4	52	11	11	15	0.4	6	96	24	13	165	16	7	2	4647	40	13	26	10	0	5
07-0550B	18	<4	44	7	4	11	1.0	6	72	16	19	168	14	5	2	4868	20	20	0	45	0	5
07-0555A	14	<4	52	14	8	16	0.3	6	105	32	14	137	18	3	1	381	54	0	30	5	0	5
07-0555B	24	4	52	12	11	12	0.8	3	78	18	14	135	15	4	1	537	55	15	0	20	0	5
07-0557A	12	<4	48	10	8	7	<0.1	8	80	23	12	135	12	2	1	765	56	0	30	10	0	3
07-0557B	30	6	33	7	6	4	0.9	3	68	18	10	127	11	6	1	1512	45	16	0	35	0	3
07-0570A	12	<4	34	6	2	9	0.3	2	110	9	17	141	17	3	1	947	52	0	35	2	0	2
07-0570B	24	6	32	6	5	7	0.9	5	94	7	20	145	14	5	1	2051	45	14	0	28	0	5
07-0595A	26	<4	126	11	40	7	<0.1	2	68	6	93	228	12	<2	1	1964	45	0	30	10	0	8
07-0595B	20	<4	154	5	20	5	1.1	6	52	3	79	145	13	6	1	2090	25	30	0	40	0	10
07-0614A	12	<4	68	6	7	10	<0.1	9	68	12	6	192	19	8	<1	144	50	11	22	5	0	5
07-0614B	14	<4	59	5	4	9	0.3	2	66	8	12	184	12	<2	<1	100	50	18	0	25	0	0
07-0795A	16	<4	113	13	30	11	0.5	5	82	11	18	250	15	3	<1	616	45	5	30	5	0	8
07-0795B	32	<4	83	6	14	7	0.7	3	80	4	15	167	14	5	1	1524	32	14	0	35	0	12
07-0797A	10	<4	103	5	9	8	0.0	<2	72	9	21	185	15	8	<1	363	40	0	40	10	0	8
07-0797B	20	<4	70	4	10	5	0.4	5	78	3	14	173	14	10	<1	3052	45	13	0	35	0	8